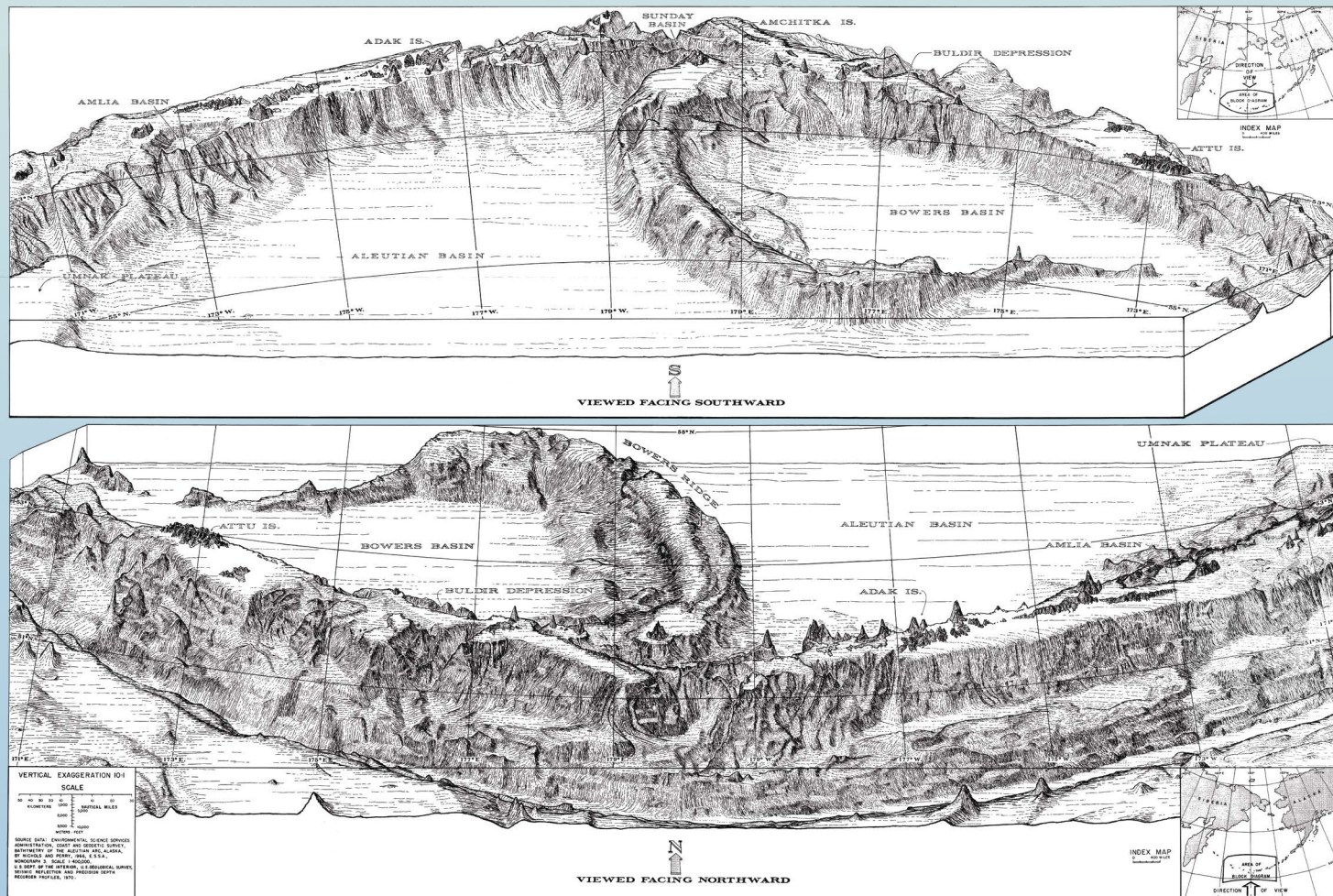


Marine Minerals in Alaska—A Review of Coastal and Deep-Ocean Regions



Professional Paper 1870

Cover. Physiographic diagrams of the central Aleutian arc viewed from the north and from the south. From Marlow and others (1973), figure 1. Used with permission of Geological Society of America, from Tectonic History of the Central Aleutian Arc, Geological Society of America Bulletin, Marlow and others, v. 84, no. 5, 1973; permission conveyed through Copyright Clearance Center, Inc.

Marine Minerals in Alaska—A Review of Coastal and Deep-Ocean Regions

By Amy Gartman, Kira Mizell, and Douglas C. Kreiner

Professional Paper 1870

U.S. Department of the Interior
U.S. Geological Survey

U.S. Geological Survey, Reston, Virginia: 2022

For more information on the USGS—the Federal source for science about the Earth, its natural and living resources, natural hazards, and the environment—visit <https://www.usgs.gov> or call 1–888–ASK–USGS.

For an overview of USGS information products, including maps, imagery, and publications, visit <https://store.usgs.gov>.

Any use of trade, firm, or product names is for descriptive purposes only and does not imply endorsement by the U.S. Government.

Although this information product, for the most part, is in the public domain, it also may contain copyrighted materials as noted in the text. Permission to reproduce copyrighted items must be secured from the copyright owner.

Suggested citation:

Gartman, A., Mizell, K., and Kreiner, D.C., 2022, Marine minerals in Alaska—A review of coastal and deep-ocean regions: U.S. Geological Survey Professional Paper 1870, 46 p., <https://doi.org/10.3133/pp1870>.

ISSN 1044-9612 (print)

ISSN 2330-7102 (online)

Acknowledgments

We are grateful to Manda Au and Denise Payan of the U.S. Geological Survey (USGS) and Noemi Ortega Dominguez and Luis Oliva of the University of California, Santa Cruz, for their significant contributions to the data compilation and rescue for this study. We additionally thank Manda Au for geographic information system (GIS) support. The USGS library staff has been invaluable in providing access to obscure texts. We also thank James R. Hein and Jamey Jones of the USGS for their reviews.

We acknowledge funding from the USGS Coastal and Marine Hazards and Resources Program through the USGS Pacific Coastal and Marine Science Center, and from the USGS Minerals Resources Program through the USGS Alaska Science Center and thank them for supporting this cross mission area work. This study was funded in part by the U.S. Department of the Interior, Bureau of Ocean Energy Management through Interagency Agreement M19PG00021 with the USGS.

Contents

Acknowledgments	iii
Marine Minerals in Alaska—A Review of Coastal and Deep-Ocean Regions	1
Abstract	1
Introduction.....	1
Ferromanganese Crusts.....	5
Gulf of Alaska Seamounts	8
Oceanographic and Geologic Setting	8
Marine Mineral Occurrences	10
Chukchi Borderland.....	11
Oceanographic and Geologic Setting	11
Marine Mineral Occurrences	13
Abyssal Plain Nodules	14
Canada Basin.....	15
Oceanographic and Geologic Setting	15
Marine Mineral Occurrences	16
Hydrothermal Minerals.....	17
Aleutian Arc	18
Oceanographic and Geologic Setting	18
Marine Mineral Occurrences.....	21
Coastal Marine Minerals.....	23
Seward Peninsula.....	23
Oceanographic and Geologic Setting	23
Marine Mineral Occurrences	25
Goodnews Bay	25
Oceanographic and Geologic Setting	25
Marine Mineral Occurrences	25
Bristol Bay and Alaska Peninsula	27
Oceanographic and Geologic Setting	27
Marine Mineral Occurrences	28
Southern and Southeastern Alaska.....	28
Oceanographic and Geologic Setting	28
Marine Mineral Occurrences	32
Summary.....	34
References Cited.....	34

Figures

1. Map of Alaska and surrounding bodies of water showing major marine regions of interest.....	2
2. Map of Alaska showing sample locations reviewed for this compilation	3
3. Global map of major marine regions that are prospective, and of economic interest, for ferromanganese crusts and manganese nodules.....	5
4. Map of the Gulf of Alaska seamounts region.....	6
5. Map of Patton Seamount, Gulf of Alaska.....	7
6. Map of the Chukchi Borderland region in the Arctic Ocean.....	9
7. Map of the Canada Basin region	15
8. Map of the Aleutian Arc, Alaska, showing active volcanoes along the arc and back arc.....	19
9. Map of the Bering Sea and Aleutian back arc, as well as part of the Alaska Peninsula	20
10. Map of the Ingenstrem Depression, Aleutian Arc, Alaska	22
11. Map of Seward Peninsula, including Norton Sound and Saint Lawrence Island, Alaska, and the Chukotka Peninsula in Russia.....	24
12. Map of the Bering Sea region including Kuskokwim Bay, Goodnews Bay, Chagvan Bay, Nushagak Bay, Kvichak Bay, and Bristol Bay, Alaska	26
13. Map of the Alaska Peninsula, with the Bering Sea to the north and the Pacific Ocean to the south.....	27
14. Map of Unga Island and some surrounding islands, off the southern coast of the Alaska Peninsula.....	29
15. Map of Prince William Sound and Cook Inlet, Alaska.....	30
16. Map of Icy and Yakutat Bays, southeastern Alaska	31
17. Map of southeast Alaska.....	33

Tables

1. Marine mineral resources as of 2021.....	4
2. Chemical composition of ferromanganese minerals from Alaska regions of the U.S. Exclusive Economic Zone, compared to crusts from the prime crust zone in the Northwest Pacific Ocean	10

Conversion Factors

U.S. customary units to International System of Units

Multiply	By	To obtain
Length		
mile (mi)	1.609	kilometer (km)
mile, nautical (nmi)	1.852	kilometer (km)
Mass		
ounce, troy	31.10	gram (g)

International System of Units to U.S. customary units

Multiply	By	To obtain
Length		
centimeter (cm)	0.3937	inch (in.)
millimeter (mm)	0.03937	inch (in.)
meter (m)	3.281	foot (ft)
kilometer (km)	0.6214	mile (mi)
kilometer (km)	0.5400	mile, nautical (nmi)
Area		
square meter (m ²)	0.0002471	acre
square kilometer (km ²)	247.1	acre
square meter (m ²)	10.76	square foot (ft ²)
square kilometer (km ²)	0.3861	square mile (mi ²)
Volume		
liter (L)	0.2642	gallon (gal)
Mass		
gram (g)	0.03215	ounce, troy
kilogram (kg)	2.205	pound avoirdupois (lb)
metric ton (t)	1.102	ton, short [2,000 lb]
metric ton (t)	0.9842	ton, long [2,240 lb]

Temperature in degrees Celsius (°C) may be converted to degrees Fahrenheit (°F) as follows:

$$^{\circ}\text{F} = (1.8 \times ^{\circ}\text{C}) + 32.$$

Supplemental Information

Wet metric ton (wmt) is defined as a metric ton of solids plus water per unit of total volume, irrespective of the degree of saturation. Typically used in ore pricing.

Concentrations of chemical constituents in water are given in micromoles per liter (μmol/L).

Abbreviations

AGDB3	Alaska Geochemical Database, ver. 3.0
CIM	Canadian Institute of Mining, Metallurgy and Petroleum
CCZ	Clarion-Clipperton Zone
DSDP	Deep Sea Drilling Project
EEZ	Exclusive Economic Zone
IMLGS	Index to Marine and Lacustrine Geological Samples (NOAA)
IODP	Integrated Ocean Drilling Program (now International Ocean Discovery Program)
ISA	International Seabed Authority
JOGMEC	Japanese Oil, Gas and Metals National Corporation
NOAA	National Oceanic and Atmospheric Administration
NORI	Nauru Ocean Resources, Inc.
ODP	Ocean Drilling Program
OCS	Outer Continental Shelf
OMZ	oxygen minimum zone
PAW	Peninsular–Alexander Wrangellia superterrane
PCZ	prime crust zone
PGE	platinum-group elements
PMS	polymetallic sulfide deposits
REE	rare earth elements
REY	rare earth elements and yttrium
ROV	remotely operated vehicle
RV	research vessel
SMS	seafloor massive sulfide deposits
TOML	Tonga Offshore Mining Limited
U.N.	United Nations
USCG	United States Coast Guard
USGS	U.S. Geological Survey
VMS	volcanogenic massive sulfide deposits

Elements

Aluminum	Al	Neodymium	Nd
Antimony	Sb	Nickel	Ni
Argon	Ar	Niobium	Nb
Arsenic	As	Osmium	Os
Barium	Ba	Oxygen	O
Beryllium	Be	Palladium	Pd
Bismuth	Bi	Phosphorous	P
Cadmium	Cd	Platinum	Pt
Calcium	Ca	Potassium	K
Carbon	C	Praseodymium	Pr
Cerium	Ce	Rhodium	Rh
Cesium	Cs	Rubidium	Rb
Chlorine	Cl	Ruthenium	Ru
Chromium	Cr	Samarium	Sm
Cobalt	Co	Scandium	Sc
Copper	Cu	Selenium	Se
Dysprosium	Dy	Silicon	Si
Erbium	Er	Silver	Ag
Europium	Eu	Sodium	Na
Gadolinium	Gd	Strontium	Sr
Gallium	Ga	Sulfur	S
Germanium	Ge	Tantalum	Ta
Gold	Au	Tellurium	Te
Hafnium	Hf	Terbium	Tb
Holmium	Ho	Thallium	Tl
Indium	In	Thorium	Th
Iridium	Ir	Thulium	Tm
Iron	Fe	Tin	Sn
Lanthanum	La	Titanium	Ti
Lead	Pb	Tungsten	W
Lithium	Li	Uranium	U
Lutetium	Lu	Vanadium	V
Magnesium	Mg	Ytterbium	Yb
Manganese	Mn	Yttrium	Y
Mercury	Hg	Zinc	Zn
Molybdenum	Mo	Zirconium	Zr

Marine Minerals in Alaska—A Review of Coastal and Deep-Ocean Regions

By Amy Gartman, Kira Mizell, and Douglas C. Kreiner

Abstract

Minerals occurring in marine environments span the globe and encompass a broad range of mineral categories, forming within varied geologic and oceanographic settings. They occur in coastal regions, either from the continuation or mechanical reworking of terrestrial mineralization, as well as in the deep ocean, from diagenetic, hydrogenetic, and hydrothermal processes. The oceans cover most of the Earth's surface and as a result, any inventory of global resources is incomplete without the inclusion of marine minerals. This study by the U.S. Geological Survey reviews current knowledge regarding deep-ocean and coastal marine minerals within the marine areas surrounding Alaska, including the Alaska Outer Continental Shelf (OCS). For the purposes of this study, we have divided these areas in to eight regions: (1) Gulf of Alaska seamounts, (2) Chukchi Borderland, (3) Canada Basin, (4) Aleutian Arc, (5) Seward Peninsula, (6) Goodnews Bay, (7) Bristol Bay and Alaska Peninsula, and (8) southern and southeastern Alaska. The Alaska OCS encompasses several areas broadly conducive to marine mineral formation, including extensional basins resulting from an active subduction zone where massive sulfide deposits may form, deep abyssal plains with conditions that may lead to manganese nodule formation, seamounts that can provide substrate for the growth of ferromanganese crusts, and erosional settings and submerged continental crust where placer deposits are found. For deep-ocean hydrothermal minerals and manganese nodules, the Alaska OCS contains prospective regions, including the Canada Basin and the Aleutian Arc; however, no such minerals have yet been identified. We explore the probability that these minerals occur based on reviews of existing geologic and oceanographic data within the relevant sections. In regions far from shore data are limited. Deep-ocean ferromanganese crusts are known to occur in two regions: (1) the Gulf of Alaska seamounts and (2) the Chukchi Borderland in the Arctic Ocean. Limited sampling has occurred in both regions, and along the Chukchi Borderland the sampling was outside of the OCS and the U.S. Exclusive Economic Zone. Data relevant to coastal minerals is more extensive, and in some places fairly systematic sampling was conducted. Several nearshore placer deposits have been exploited for decades; however, the potential for nearshore extension of terrestrial

ore deposits is less well considered. This contribution considers the state of knowledge regarding marine mineral occurrences within the Alaska regions and identifies the data gaps in order to help inform future marine mineral related research efforts around Alaska.

Introduction

Interest in Arctic-region science generally, and Arctic commodities specifically, has increased over the past decade as the Earth warms and the associated decrease in sea ice has resulted in improved accessibility to the Arctic Ocean, including the continental shelf and seafloor (Douglas, 2010). The surge in Arctic resource interest has led to an international compilation of minerals in the Arctic (Goldfarb and others, 2016) and potential new petroleum fields (for example, Bird and others, 2008), as well as the first study considering deep-ocean minerals in the Arctic as a potential resource (Hein and others, 2017). In this review by the U.S. Geological Survey (USGS), which covers literature from the mid 20th century until the present, we expand on Arctic mineral resource knowledge to consider a variety of marine-mineral types throughout the Alaska Outer Continental Shelf (OCS), which includes regions of the Arctic and North Pacific Oceans, and the continental shelf (figs. 1, 2). We review non-aggregate minerals that originate in ocean basins via hydrogenetic, diagenetic, and hydrothermal processes, referred to as deep-ocean minerals, as well as minerals that originate terrestrially and extend or have weathered into nearshore marine regions. We specifically focus on marine environments that are known to have the potential to host elements or minerals considered critical (Fortier and others, 2018, p. 1) in which “critical minerals,” as defined in the Energy Act of 2020 (30 USC 1606), are minerals, elements, substances, and materials that (i) are essential to the economic or national security of the United States, (ii) the supply chain of which is vulnerable to disruption, and (iii) serve an essential function in the manufacturing of a product, the absence of which would have significant consequences for our economy or our national security.”

Marine minerals can be broadly divided into two categories: (1) coastal minerals, which have been utilized for centuries, and (2) deep-ocean minerals, of which no mining has occurred anywhere on Earth to date. There are

2 Marine Minerals in Alaska—A Review of Coastal and Deep-Ocean Regions



Figure 1. Map of Alaska and surrounding bodies of water showing major marine regions of interest.

three categories of deep-ocean minerals generating the most interest internationally and defined by the International Seabed Authority (ISA) (ISBA/18/A/11; ISBA/16/A/12/Rev.1; ISBA/19/C/17) as currently eligible for exploration contracts in The Area, which is defined in the United Nations (U.N.) Convention on the Law of the Sea as the seabed and ocean floor and subsoil thereof, beyond the limits of national jurisdiction. These minerals are as follows: (1) manganese nodules (also called polymetallic nodules), (2) ferromanganese crusts (also called cobalt-rich crusts), and (3) seafloor massive sulfide (SMS) deposits (also called polymetallic sulfides). In this section, we use names that describe these minerals as geologic occurrences, rather than the resource-focused names defined by the ISA. The descriptor used here, ferromanganese rather than cobalt-rich, refers to the dominant composition of the mineral rather than the commodity expected to be

extracted, which may be a minor compositional component. The terms “crust” and “nodule” describe mineral morphology and do not, on their own, indicate mineral composition. Further categories of marine minerals attracting some amount of interest from a critical minerals perspective include phosphorite deposits, metalliferous sediments, and rare earth element (REE) rich muds; additionally, magmatic-hydrothermal deposits likely also occur deep below the seafloor (for example, Rona, 2008). These additional types are not extensively investigated here owing to lack of clear prospective regions in the Alaska OCS (REE-rich muds and phosphorites) or lack of data regarding any subsurface magmatic-hydrothermal deposits.

The trace-element enrichments, including critical elements, of marine minerals vary based on the location and mechanism of formation. The composition of ferromanganese

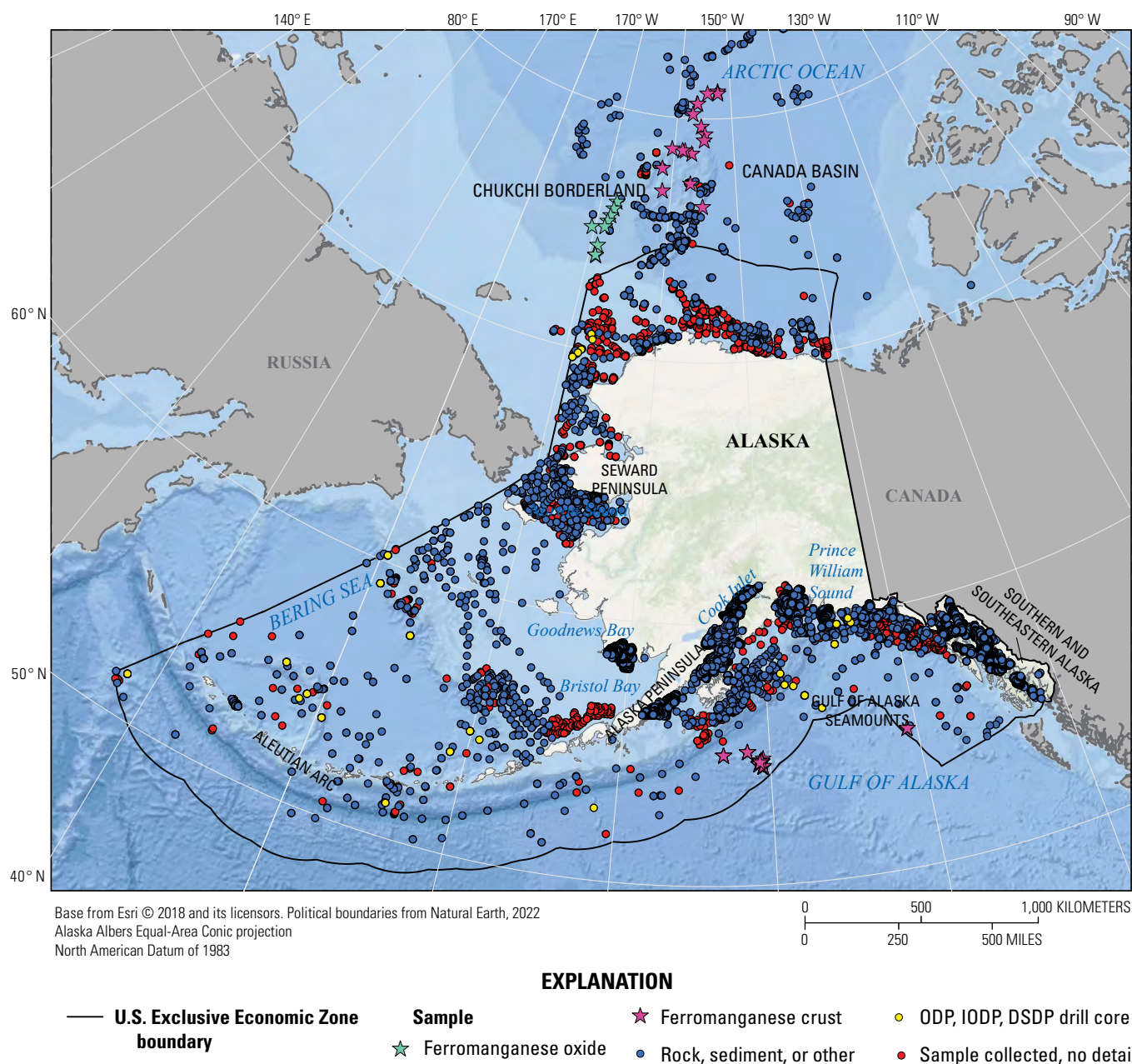


Figure 2. Map of Alaska showing sample locations reviewed for this compilation, labeled with any relevant mineral designations. “Ferromanganese oxide” refers to ferromanganese oxide samples where the morphology is not described well enough to be designated as a ferromanganese crust or nodule. Samples shown are from the Index to Marine and Lacustrine Geological Samples (IMLGS) (Curators of Marine and Lacustrine Geologic Sample Consortium, 1977) and other publications, with references included in the detailed regional figures. Data from the Alaska Geochemical Database, ver. 3.0 (AGDB3) (Granitto and others, 2019), are shown in regional maps (figs. 4, 5, 7, and 8–17). ODP, Ocean Drilling Program; IODP, Integrated Ocean Drilling Program; DSDP, Deep Sea Drilling Project.

minerals (ferromanganese crusts and manganese nodules) varies depending on broad regional factors such as the oxygen content of the surrounding water mass, primary productivity, rate of accumulation, and source of elements, whether diagenetic, hydrogenetic, or hydrothermal. For sulfide minerals, the host rock, contribution of magmatic fluids and (or) sediments, oxidation, and recrystallization influence their composition. The elements driving interest in possible

extraction are particular to the mineral type and region. Ferromanganese crusts are broadly considered to be of interest for Co, Mn, Ni, Cu, rare earth elements and yttrium (REY), and possibly Te, Sc, and Pt. Manganese nodules are considered broadly of interest for Mn, Ni, Co, Cu, and possibly Ti, REY, and Li. The relative concentration of each of these elements varies based on the processes of formation, and the elements of interest are predominantly based on the composition

of Pacific Ocean ferromanganese minerals, with lesser consideration of Atlantic and Indian Ocean minerals. Sulfide mineral occurrences are highly heterogenous in composition and are considered of interest for Cu, Zn, Au and Ag. Other elements including As, Be, Bi, Cd, Co, Cr, Ga, Ge, Hg, In, Mn, Mo, Ni, Se, Sn, Te, and platinum-group elements (PGE) have also been extracted from volcanogenic massive sulfide (VMS) deposits, which are terrestrial analogues of SMS deposit systems (Shanks and others, 2012). The logistics and economic feasibility of extracting any of these elements would need to be evaluated on a case-by-case basis. Although the rare and critical metal enrichments of the three major categories of deep-ocean minerals mentioned above have led to interest in marine minerals as resources in certain regions, and the three main marine mineral categories are ubiquitous as occurrences throughout the global ocean, most ferromanganese and hydrothermal minerals have not been sampled to a level that merits characterization as “deposits.” Extensive sampling during a campaign of multiple expeditions is required to achieve exchange-compliant resource assessments; this has been completed for a small but increasing number of marine mineral deposits. Currently, there are practices outlined in National Instrument (NI) 43–101, developed by the Canadian Institute of Mining, Metallurgy and Petroleum (CIM), which provides guidance on reporting and disclosure of mineral properties (CIM, 2011). Examples are shown in table 1, with locations indicated in figure 3. These examples include three SMS deposits, two occurring in the Bismarck Sea and one in the Okinawa Trough; two regions of the Clarion-Clipperton Zone (CCZ); and one unique hydrothermal brine sediment in the Red Sea. For crusts, there have been no exchange-compliant assessments to date, with relevant factors discussed in Hein and others (2009). Currently, interest in the resource potential of these minerals is ongoing internationally and prototype systems for seafloor collection are being tested and remain in the research and development stage for all deep-ocean mineral categories.

Although no mining of deep-ocean minerals has occurred globally to date, mining of coastal minerals has occurred for centuries. For example, a significant amount of global tin currently originates from offshore placers in Southeast Asia (Kamilli and others, 2017). In comparison to the lack of data relevant to the deep ocean, much more data are available regarding minerals in the Alaska region that originate from terrestrial deposits that either extend into the marine realm on continental shelves and slopes or are transported into the coastal zone through weathering processes, such as those that result in placer deposits. Nearshore minerals may form by different processes and occur predominately in shallow coastal zones and constitute an important class of marine critical mineral resources for Alaska. Mining of nearshore and placer mineral deposits is occurring across the globe, predominantly for gold, tin, titanium, and diamonds, as well as other heavy minerals (Baker and others, 2016; Hein and others, 2021; Kamilli and others, 2017). This extraction is often referred to as offshore mining and may use technology analogous to marine aggregate mining. These deposits occur at depths of less than 200 meters (m). In addition to offshore placers, which are most commonly discussed, there are terrestrial deposits extending onto the continental shelf within bedrock (Hannington and others, 2017). As examples, gold is extracted from the bottom of the Bohai Sea in China (Zhao and others, 2012) and barite has been produced from Castle Island in Alaska (summarized in the USGS Mineral Resources Online Spatial Data at https://mrdata.usgs.gov/ardf/show-ardf.php?ardf_num=PE026). In Alaska, gold is one of the principal offshore placer commodities. There are currently active mining claims and recreational mining allowed for gold placers offshore of Nome, Alaska, in the State waters of Norton Sound in the Bering Sea, and a lease sale was held in 2020 for 11 additional tracts there (<http://dnr.alaska.gov/mlw/mining/nome/>).

In this study we review regions prospective for deep-ocean minerals in the Alaska OCS, where “prospective” indicates

Table 1. Marine mineral resources as of 2021.

[For manganese nodule deposits, we use exchange compliant National Instrument (NI) 43–101 assessments (CIM, 2011); for seafloor massive sulfide (SMS) deposits we use those based on systematic drilling. The Solwara, Papua New Guinea, and Atlantis II Deep, Red Sea, sites are prepared by qualified persons and shared as NI 43–101 technical reports, whereas the Hakurei, Japan, site report is by the Japanese Oil, Gas and Metals National Corporation (JOGMEC). The SMS and Atlantis II Deep deposit tonnages are for dry material, whereas the Mn nodule values are wet metric tons. References are Lipton and others (2018) for the Solwara projects; Urabe and others (2015) for Hakurei site; McGarry and others (2014) for Atlantis II Deep; Lipton and others (2021) for Nauru Ocean Resources, Inc. (NORI) areas in the Clarion-Clipperton Zone (CCZ); and Lipton and others (2016) for the Tonga Offshore Mining Limited (TOML) area in the CCZ. See fig. 3 for locations of sites. Co, cobalt; Cu, copper; Mn, manganese; Ni, nickel; Pb, lead; Zn, zinc; Au, gold; Ag, silver; %, percent; g/t, grams per ton; Mt, million metric tons; –, no data.]

Site	Co (%)	Cu (%)	Mn (%)	Ni (%)	Pb (%)	Zn (%)	Au (g/t)	Ag (g/t)	Ore (Mt) (inferred)	Deposit type
Solwara 1	–	8.1	–	–	–	0.9	6.4	34	1.5	SMS
Solwara 12	–	7.3	–	–	–	3.6	3.6	56	0.23	SMS
Hakurei, Izena Caldera	–	0.4	–	–	2.74	7.14	3.62	237	3.74	SMS
Atlantis II Deep, Red Sea	–	0.46	2.69	–	–	2.03	–	41.14	80.88	Hydrothermal sediments/ brine
NORI Areas CCZ	0.18	1.08	29.2	1.30	–	–	–	–	909	Mn nodule
TOML Area CCZ	0.20	1.14	29.05	1.29	–	–	–	–	685.3	Mn nodule

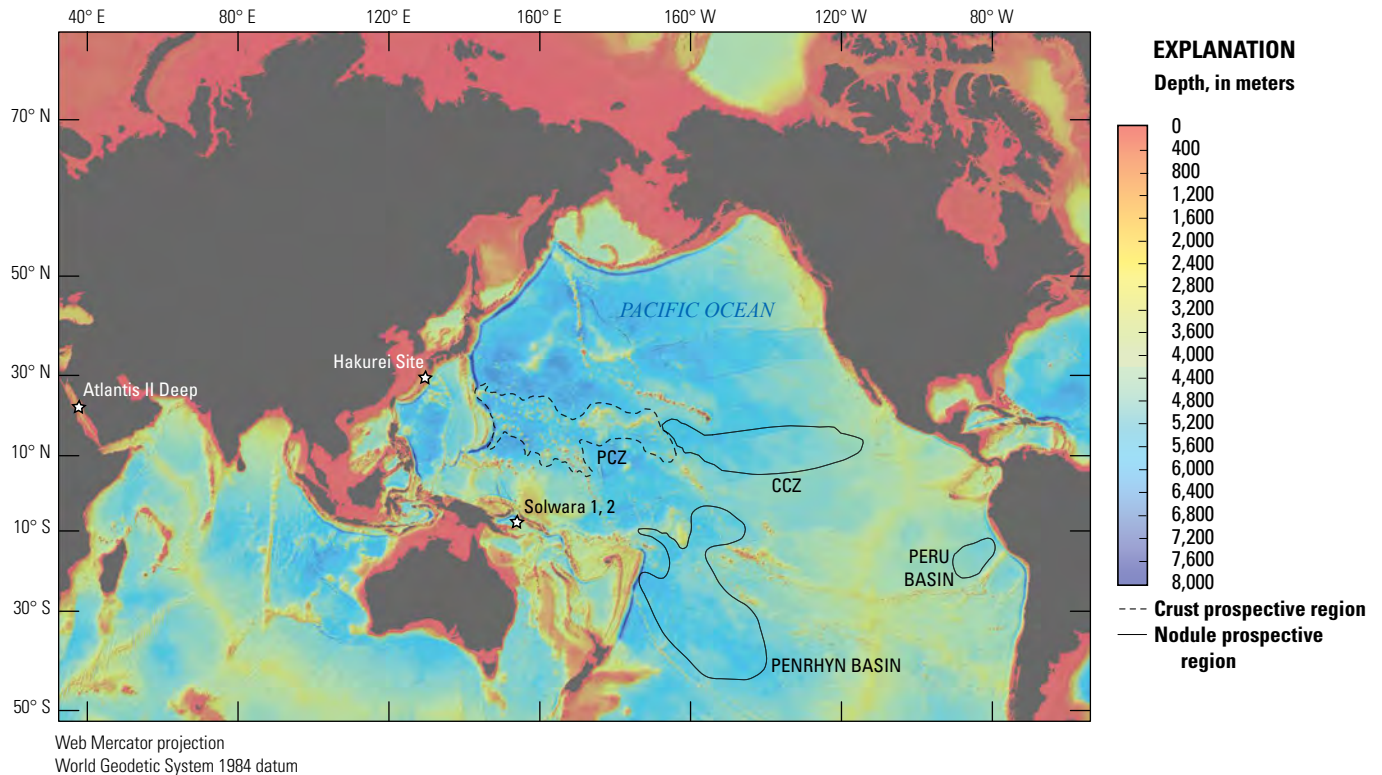


Figure 3. Global map of major marine regions that are prospective, and of economic interest, for ferromanganese crusts (prime crust zone [PCZ]) and manganese nodules (Clarion-Clipperton Zone [CCZ], Peru Basin, and Penrhyn Basin). Locations where marine mineral resource assessments have been conducted as of March 2021 are labeled with stars and are also listed in [table 1](#). The Nauru Ocean Resources, Inc. (NORI) and Tonga Offshore Mining Limited (TOML) area assessments in the CCZ include small subregions scattered throughout the CCZ.

that a region is consistent with the geologic and oceanographic criteria required to potentially host marine minerals. This does not mean that a region hosts marine minerals and does not indicate that the marine minerals occurring in that region will be economically viable. Regions not meeting the criteria for prospective designation are not reviewed here. As detailed in each section, the Arctic Ocean and areas of the Pacific Ocean falling within the Alaska OCS are unique and vary in significant ways from marine deposits that occur elsewhere. We take this unique setting into consideration in developing prospective region boundaries which are further informed by geologic samples that constrain the predicted distribution of deep-ocean minerals in the Alaska OCS.

Sparse geologic sampling limits knowledge of marine minerals in the Alaska region, especially in deep water regions. Environmental and biological parameters are also sparsely sampled, leading to concerns about the effect of extraction at poorly studied locations (Danovaro and others, 2020). Many factors are involved in the evaluation of marine minerals as a source of elements for societal needs, and the abundance of rare and critical elements in marine mineral deposits is only one of these factors. In reviewing each region, we also briefly discuss the regional environment, including the geologic and oceanographic setting of each region as an

important part of evaluating the state of knowledge of marine minerals in the Alaska OCS.

Ferromanganese Crusts

Ferromanganese crusts are chemical sedimentary rocks that form by the precipitation of iron and manganese oxide colloids onto the ubiquitous exposed rock surfaces of seamounts, ridges, and guyots in the deep ocean. The accretionary growth mechanism of ferromanganese crusts takes place over millions of years and therefore these thick, metal-rich crusts mostly occur in open ocean settings on seamounts, ridges, and guyots where sedimentation rates remain relatively low, or ocean current speeds are high enough to keep rock surfaces clear of other sedimentary debris (Hein and others, 2000). The best-known region for such open-ocean crusts is a subregion of the Northwest Pacific Ocean known as the prime crust zone (PCZ) ([fig. 3](#)), where many old mid-plate volcanic edifices have accumulated ferromanganese crusts for nearly 70 million years (m.y.) (Nielsen and others, 2009). The PCZ currently contains four exploration contracts issued by the ISA (<https://www.isa.org.jm/index.php/exploration-contracts/cobalt-rich-ferromanganese>). Ferromanganese crusts can also form in regions within and near continental margins

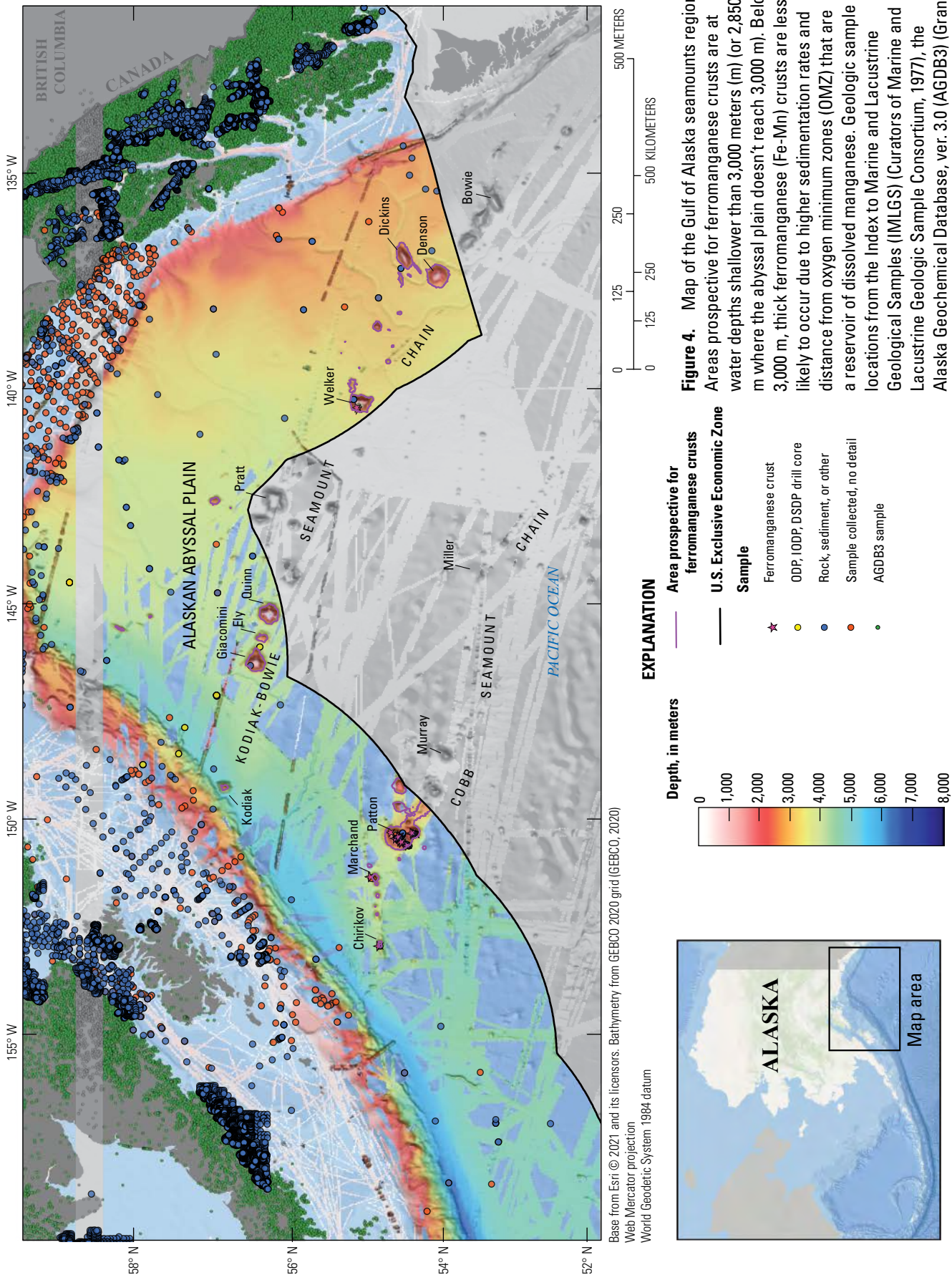


Figure 4. Map of the Gulf of Alaska seamounts region. Areas prospective for ferromanganese crusts are at water depths shallower than 3,000 meters (m) (or 2,850 m where the abyssal plain doesn't reach 3,000 m). Below 3,000 m, thick ferromanganese (Fe-Mn) crusts are less likely to occur due to higher sedimentation rates and distance from oxygen minimum zones (OMZ) that are a reservoir of dissolved manganese. Geologic sample locations from the Index to Marine and Lacustrine Geological Samples (IMLGS) (Curators of Marine and Lacustrine Geologic Sample Consortium, 1977), the Alaska Geochemical Database, ver. 3.0 (AGDB3) (Granitto and others, 2019), and a published dataset from Koski (1988). ODP, Ocean Drilling Program; IODP, Integrated Ocean Drilling Program; DSDP, Deep Sea Drilling Project.

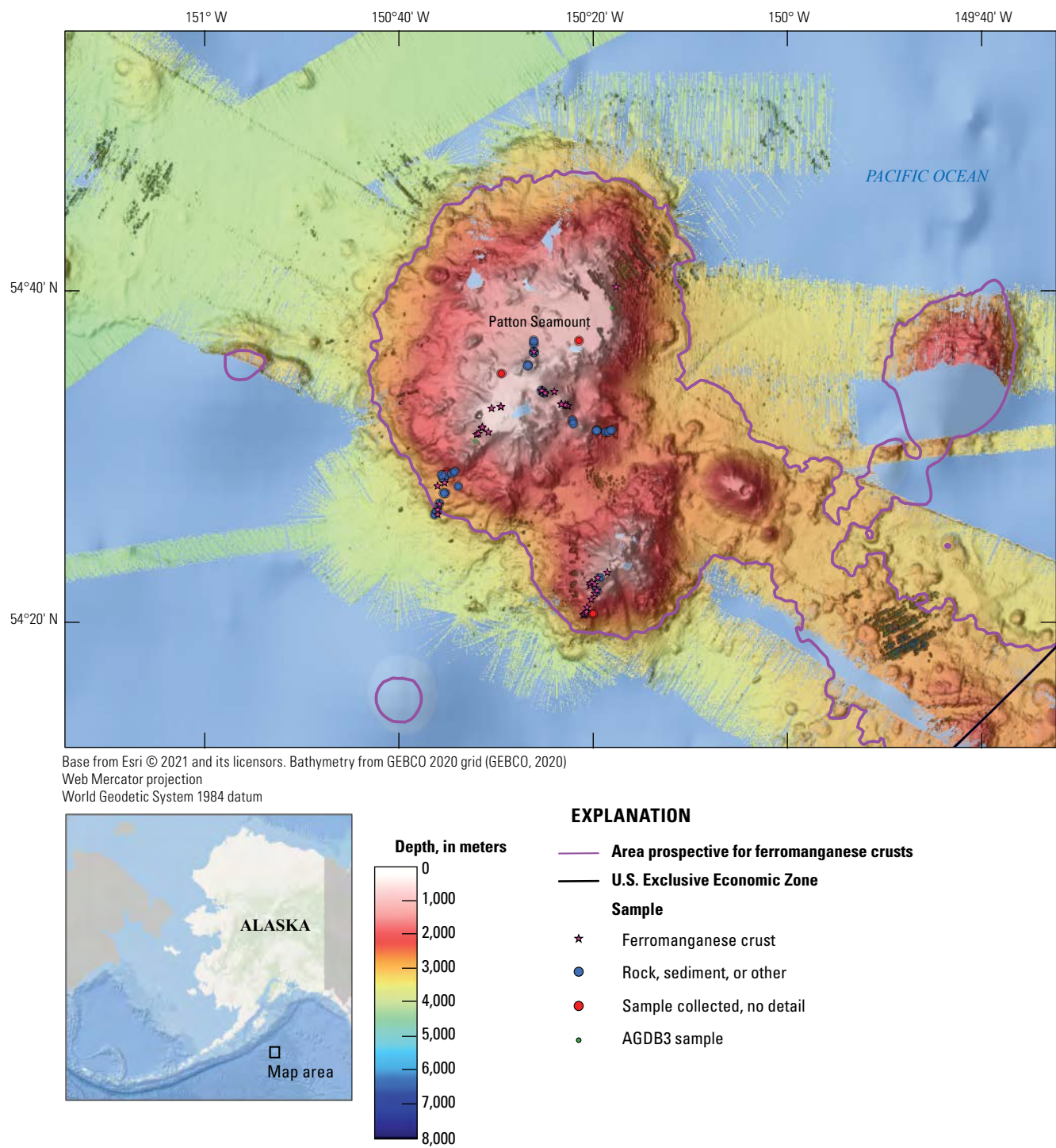


Figure 5. Map of Patton Seamount, Gulf of Alaska. Geologic sample locations from the Index to Marine and Lacustrine Geological Samples (IMLGS) (Curators of Marine and Lacustrine Geologic Sample Consortium, 1977), the Alaska Geochemical Database, ver. 3.0 (AGDB3) (Granitto and others, 2019), and a published dataset from Koski (1988), including depth-based transects of ferromanganese crusts.

(for example, on continental shelves, slopes, banks, and plateaus) where sedimentation rates are higher, which is the case for both prospective regions for ferromanganese crusts in the Alaska OCS: Gulf of Alaska Seamounts (figs. 4, 5) and the Chukchi Borderland (fig. 6). However, the compositions of crusts in and close to continental margins are generally less enriched in metals of economic interest (for example, Co, Ni) than open-ocean crusts and therefore typically considered less economically prospective (Conrad and others, 2017; Hein and others, 2016). This different composition is generally due to faster growth rates and greater inputs of iron (Conrad and others, 2017).

Ferromanganese crusts occur at a wide range of depths (700–7,000 m) (Mizell and Hein, 2020) and therefore are exposed to different seawater masses depending on the depth where each crust forms. Ferromanganese crusts are hydrogenetic precipitates, which mean that seawater is the source for all metals. As a result, the particular concentrations of dissolved oxygen, iron, manganese, trace metals, and organic matter in these different seawater masses surrounding each occurrence has a large influence on crust composition. Regarding these oceanographic factors in the Alaska OCS, the Gulf of Alaska occurs within a high biological productivity region in the North Pacific Ocean, and therefore Gulf of Alaska crusts may resemble crusts in the Pacific Ocean that occur in the highly biologically productive areas along the California margin and along the equator. In contrast, the Chukchi Borderland is located within the Arctic Ocean, which is known for its unique seawater masses influenced by extensive river inputs, a strong halocline, and extensive inputs from the broad continental shelf; thus, ferromanganese crusts in this region have a distinct composition compared to crusts from the other ocean basins.

Gulf of Alaska Seamounts

Oceanographic and Geologic Setting

The Gulf of Alaska seamount region (fig. 4) encompasses a group of volcanic edifices scattered south and west of Alaska extending from the Explorer–Juan de Fuca Ridge offshore Washington and British Columbia, Canada, at its southeastern extent to the Aleutian Islands in the northwest. This approximately 2,000-kilometer (km)-wide region contains more than 100 distinct seamounts taller than 1,000 m, and many of the seamounts within the gulf remain unnamed (Chaytor and others, 2007). Approximately half of the larger seamounts and ridges fall under U.S. jurisdiction, including the named Dickins, Denson, Welker, Quinn, Ely, Giacomini, Kodiak, Patton, Chirikov, and Marchand Seamounts (fig. 4).

The Gulf of Alaska seamount region occurs as two seamount chains, Kodiak–Bowie and Cobb (fig. 4), that are parallel to one another and aligned with the northwest direction of the movement of the Pacific Plate (Morgan, 1972; Chaytor and others, 2007). Isotopic age dating and seamount morphological studies overall support that the seamount

chains were formed through hotspot volcanism, originating from two separate hotspots at the southeast end of the chains (Desonie and Duncan, 1990; Turner and others, 1980; Chaytor and others, 2007). Among the two chains, the Gulf of Alaska seamounts range in age from about 0.7 mega-annum (Ma) in the younger, southeastern margin to ~26 Ma in the older, northwestern margin (Turner and others, 1973, 1980; Keller and others, 1997). Some out-of-sequence ages suggest the occurrence of either late rejuvenated volcanism, the additional influence of ridge generated volcanism (Desonie and Duncan, 1990), or perhaps a shift in the Juan de Fuca Ridge (Dalrymple and others, 1987). While all of the Gulf of Alaska seamounts are far younger than the ancient Jurassic seamounts of the Northwest Pacific Ocean (Hein and others, 2000), some are tens of millions of years in age and therefore may have accumulated relatively thick ferromanganese crusts on the exposed flanks and summits given typical crust growth rates of 1–6 millimeters per million years (mm/m.y.) (Hein and others, 2000). The periodic late-stage volcanism along the Gulf of Alaska seamounts mentioned above may also have generated distinct hydrothermal ferromanganese oxide deposits or altered previously formed hydrogenetic ferromanganese crusts by changing local seawater chemistry or increasing growth rates for ferromanganese stratigraphic layers.

The major summits in the Gulf of Alaska seamounts within the U.S. Exclusive Economic Zone (EEZ) summarized by Chaytor and others (2007) range from 2,129 m (Ely Seamount) to 160 m (Patton Seamount) water depth, with a median summit depth of approximately 760 m and a median base depth of 3,900 m. Only two major water masses occur in the Gulf of Alaska: (1) the upper 2,000 m, which is well-mixed due to wind-driven surface currents and associated gyres (Musgrave and others, 1992), and (2) the lower 2,000–4,000 m, which is Pacific Ocean deep water that is well-mixed and delivered to the North Pacific Ocean by thermohaline circulation (Knauss, 1962; Worthington, 1981; Talley and others, 2011). In the Western Pacific Ocean, ferromanganese crusts that are particularly enriched in manganese, cobalt, nickel, and other valuable and critical metals tend to accrete at depths near the local oxygen minimum zone (OMZ) (Mizell and others, 2020). The modern OMZ in the Gulf of Alaska, in general, has a vertical range between 670 and 1,060 m depth for most seasons (Paulmier and Ruiz-Pino, 2009) that is zonally consistent across the Gulf of Alaska. However, near the seamounts the OMZ can be more extensive, reaching depths of ~1,700 m (Baco, 2007). Therefore, large swaths of seamount area are available, from their summits to their bases, for the growth of crusts within less oxygenated conditions.

The Gulf of Alaska contains three large sediment fans that surround the seamounts, and these regions exhibit relatively high sedimentation rates (Chaytor and others, 2007). For example, drill cores showed estimated sedimentation rates of ~15 meters per million years (m/m.y.) in the abyssal plain near Patton Seamount over the last 18 m.y. (Weeks and others, 1995) and ~24 m/m.y. in the central Alaskan abyssal plain (Ness, 1972). Acoustic profiles indicate that most sediment

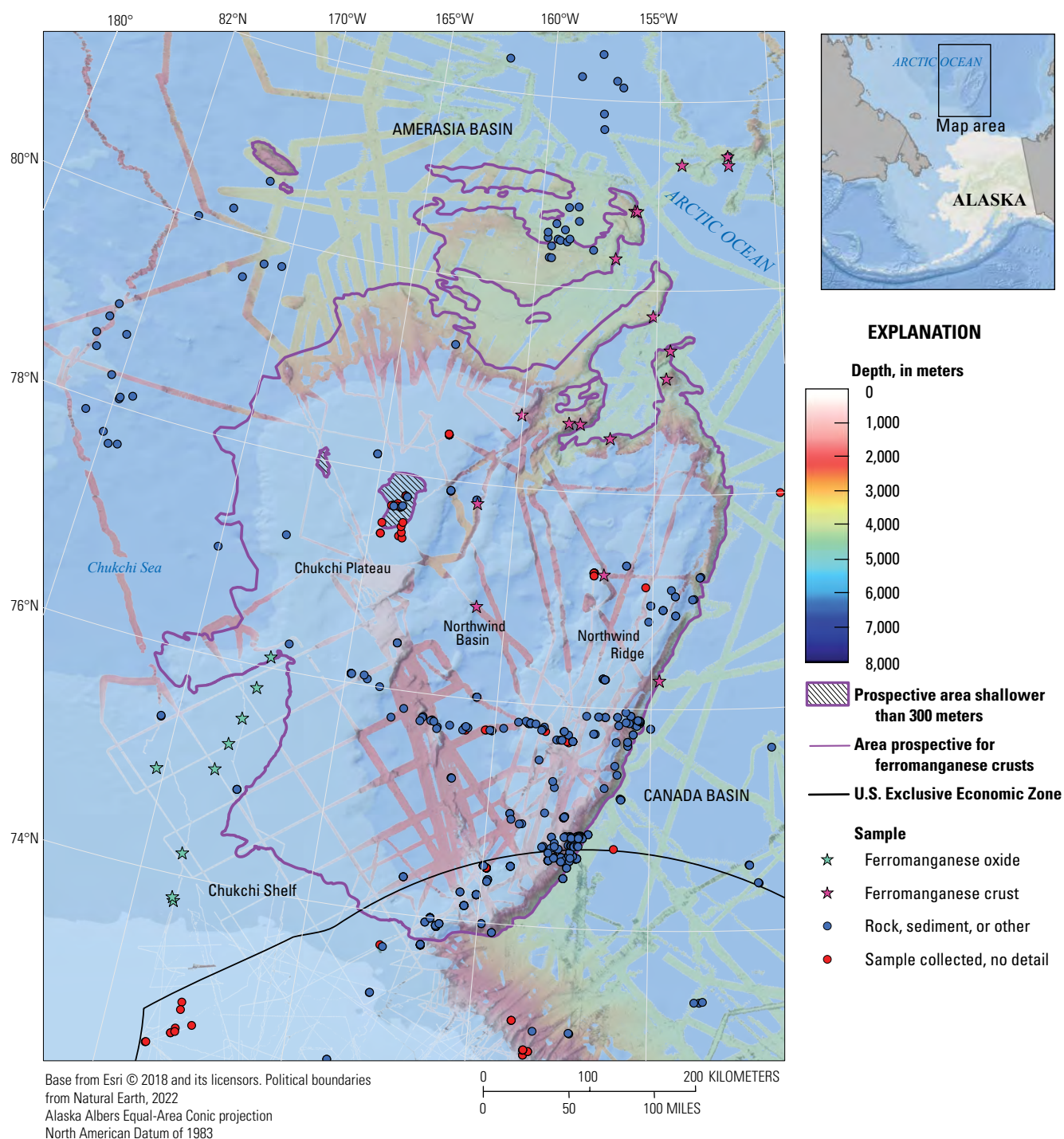


Figure 6. Map of the Chukchi Borderland region in the Arctic Ocean. “Ferromanganese oxide” refers to ferromanganese oxide samples where the morphology is not described well enough to be designated as a ferromanganese crust or nodule. Regions prospective for ferromanganese crusts are between water depths of 300 and 2,800 meters (m), except on the eastern flank of the Northwind Ridge where prospective depths extend down to 3,800 m, owing to steep slopes that prevent sediment accumulation. Geologic sample locations from the Index to Marine and Lacustrine Geological Samples (IMLGS) (Curators of Marine and Lacustrine Geologic Sample Consortium, 1977) and published datasets from Hein and others (2017), Cui and others (2020), and Wei and others (2019).

dispersed in the Gulf of Alaska abyssal plains was transported via turbidity currents from continental sources (Hamilton, 1967) and therefore may not disturb ferromanganese crusts growing at shallower depths along the summits and flanks of the seamounts. However, some of this sediment may reach the Gulf of Alaska seamounts and, in combination with the biological particle flux, either damper ferromanganese crust growth or increase growth rates. This biologically productive and high sedimentation environment would be similar to the conditions affecting crusts along the California continental margin (Conrad and others, 2017) and would result in distinct element compositions relative to well-studied crusts in regions with low sedimentation in the Northwest Pacific Ocean.

Seamounts are important benthic habitats and generally host a variety of deep-sea fauna (de Forges and others, 2000; Baco, 2007). The Gulf of Alaska seamounts host several marine fisheries, including sablefish (Maloney, 2004). In 2005, sixteen of the seamounts within the Gulf of Alaska and the U.S. EEZ were designated as Habitat Areas of Particular Concern by the North Pacific Fishery Management Council (2005) and are encompassed in the Alaska Seamount Habitat Protection Areas (50 CFR table 22 to part 679). Remotely operated vehicle (ROV)-based exploration surveys of five prominent Gulf of Alaska seamounts also revealed over 40 species of deep-water corals and abundant associated invertebrates inhabiting the seamounts (Baco, 2007). Deep-water coral abundance and diversity was lowest within the OMZ region for these seamounts (~1,700-m water depth; Baco, 2007), which coincides with the oceanographic conditions predicted to promote the formation of the thickest and most manganese-rich ferromanganese crusts.

Marine Mineral Occurrences

A single oceanographic expedition (S6-79) aboard the research vessel (RV) *S.P. Lee* was funded by the USGS in 1979, with the goal of studying ferromanganese crusts from Gulf of Alaska seamounts. During the 1979 expedition, ferromanganese crusts were recovered from five dredges on four seamounts: Welker, Patton, Miller, and Murray; the first two are located within the U.S. EEZ (fig. 4). Recovered ferromanganese crust thicknesses range from 1 to 48 mm with an average thickness of 30 mm, and the thickest crusts were collected on Welker and Patton Seamounts. Koski (1988) published detailed descriptions of 13 ferromanganese crusts recovered from this cruise. Sample morphologies are typically massive, laminated, and layered structures common to ferromanganese crusts, but also include a sample that is interlayered ferromanganese with phosphorite, and another that is irregular ferromanganese crust fragments within breccias of volcanic rock. The latter two samples were recovered from Patton Seamount. On average, bulk ferromanganese crusts from the Gulf of Alaska seamounts have higher concentrations of Mn and Ni than the average composition of crusts from the PCZ in the Northwest Pacific Ocean, while Fe and Zn concentrations are similar, and Co and

Cu concentrations are lower (table 2; Koski, 1988). Although the number of samples recovered and described from the 1979 USGS expedition is small, the sampling covered a broad area of the Gulf of Alaska seamount province. The characteristics of these ferromanganese crusts are similar enough to expect that crusts of this general nature will occur on other slopes of the same seamounts as well as other Gulf of Alaska seamounts in the U.S. EEZ, and their composition is comparable to ferromanganese crust in other regions of the Pacific Ocean.

Table 2. Chemical composition of ferromanganese minerals from Alaska regions of the U.S. Exclusive Economic Zone (EEZ), compared to crusts from the prime crust zone (PCZ) in the Northwest Pacific Ocean.

[Chukchi Borderland data from Hein and others (2017) for combined bulk and layer crust samples and nodules; Gulf of Alaska data from Koski (1988) for thick (10–50 millimeter [mm]) crusts only; Pacific Ocean prime crust zone (PCZ) data from Mizell and others, (2022). –, no data; wt. pct., weight percent; ppm, parts per million; ppb, parts per billion; REY, rare earth and yttrium (Y) elements.]

Element (symbol)	Chukchi Borderland	Gulf of Alaska	PCZ
(wt. pct.)			
Fe	19.9	23.3	16.9
Mn	7.67	12.7	22.8
Si	11.1	–	4.05
Al	6.32	–	1.01
Ca	1.18	–	4.03
Mg	1.66	–	1.10
Na	1.61	–	1.64
K	1.14	–	0.55
Ti	0.36	–	1.16
P	0.54	–	0.96
(ppm)			
Ag	<0.27	–	0.10
As	559	–	393
Ba	451	–	1,934
Be	5.8	–	6.1
Bi	3.9	–	43
Cd	3.5	–	3.6
Cl	>12,694	–	9,100
Co	1,452	4,300	6,662
Cr	43	–	28
Cs	3	–	3.7
Cu	643	520	976
Ga	13	–	18
Ge	0.69	–	–
Hf	10	–	9.4
(ppb)			
Hg	<54	–	9.3

Table 2. Chemical composition of ferromanganese minerals from Alaska regions of the U.S. Exclusive Economic Zone (EEZ), compared to crusts from the prime crust zone (PCZ) in the Northwest Pacific Ocean.—Continued.

Element (symbol)	Chukchi Borderland	Gulf of Alaska	PCZ
	(ppm)		
In	0.33	—	0.60
Li	89	—	2.9
Mo	209	—	461
Nb	39	—	52
Ni	2,289	4,000	4,209
Pb	233	—	1,641
Rb	47	—	17
S	2,693	—	2,600
Sb	48	—	39
Sc	47	—	6.6
Se	<0.64	—	15
Sn	8.4	—	10
Sr	476	—	1,510
Ta	0.85	—	2.4
Te	16	—	60
Th	62	29.2	11
Tl	83	—	155
U	11	15.9	12
V	936	—	641
W	49	—	89
Zn	341	660	668
Zr	428	—	548
La	150	259	339
Ce	849	1,801	1,322
Pr	42.2	—	61
Nd	170	263	258
Sm	42.6	59.3	52
Eu	10.8	13.1	12.5
Gd	47	61	56
Tb	7.81	9.15	8.8
Dy	44.6	54	60
Y	192	—	221
Ho	9	—	10.9
Er	24.2	—	30.9
Tm	3.74	4.74	4.6
Yb	22.7	28.3	29
Lu	3.57	4.40	4.30
Sum REY	1,619	—	2,469

The majority of modern sampling in the Gulf of Alaska seamounts has been focused on biological sampling using ROVs, with little physical sampling of Gulf of Alaska seamount geology. However, a review of some seafloor photographs and footage may help to confirm which regions exhibit ferromanganese crusts. For example, several seafloor photographs of Patton Seamount show surfaces that appear typical of ferromanganese crusts formed on basalt and coating various cobbles (Raymore, 1982).

Several additional studies have been carried out on the Gulf of Alaska seamounts to determine either the history of volcanism or the biological communities living in, on, and around the crusts. Volcanology cruises collect samples via dredge, and areas of the seamount with ferromanganese crust are often favored since the crust can be used to validate the freshness of the volcanic samples. The National Oceanic and Atmospheric Administration (NOAA) funded several volcanology research cruises to the Gulf of Alaska (RV *Atlantis* AT7–15, AT7–16, RV *Atlantis II* AT3–36, and AT11–15) (see <https://ngdc.noaa.gov/geosamples/index.jsp> and <http://4dgeo.who.edu/om-bin/eic2html.pl?f=/webdata/OM/Alvin/MDF/OM.Alvin.AT11-15.txt&t=/webdata/OM/Alvin/HTMLTemplate/alvin.v1.TEMPLATE>). These cruises recovered many rock samples via dredge with thin (<1 centimeter [cm]) ferromanganese crusts from Patton (fig. 5), Denson, Welker, Pratt, Murray, Marchand, Chirikov, and Warwick Seamounts (fig. 4). The dredges from all of these seamounts, except Chirikov Seamount, also recovered at least one sample with a thicker ferromanganese crust (1–6 cm). As another example, Dalrymple and others (1987) recorded that many of the 37 volcanic samples from 11 dredge locations in the Gulf of Alaska seamounts used for their age-dating study contained thick ferromanganese crusts. However, they published no further information regarding the crust characteristics, and several other cruises of this nature to the Gulf of Alaska seamounts have also neglected to mention or describe crusts.

Chukchi Borderland

Oceanographic and Geologic Setting

The Chukchi Borderland is a 600 by 700 km continental block located in the Arctic Ocean northwest of Alaska extending from the Chukchi Sea north to the Amerasia Basin (fig. 6; Arrigoni, 2008; Brumley and others, 2015; O'Brien and others, 2016). The majority of the Chukchi Borderland lies outside of the U.S. EEZ; however, the Chukchi Borderland is within the region mapped as part of the U.S. Extended Continental Shelf Project (<https://www.state.gov/u-s-extended-continental-shelf-project/>). In terms of its formation, the Chukchi Borderland has plate boundaries along its margins, and the geology of the region and the characterization of

these boundaries is complex, somewhat controversial, and has resulted in the development of multiple models to explain its origin (summarized by Ilhan and Coakley, 2018). Most formation models include the Chukchi Borderland rotating away from Canada and Alaska during the opening of the Amerasia Basin (for example, Carey, 1958), including several episodes of rotation throughout its history and in both clockwise and counterclockwise directions (for example, Grantz and others, 2011; Halgedahl and Jarrard, 1987; Hutchinson and others, 2017).

The Chukchi Borderland is composed of the Chukchi Plateau and Northwind Ridge, two north-south trending elevated features that lie on either side of the Northwind Basin (fig. 6). These three features are delineated by normal faults (Grantz and others, 1979, 1998, 1990). The Chukchi Plateau is approximately 25 km wide and has large swaths of fairly smooth summit areas that range from very shallow depths of 300 to 500 m (Jakobsson and others, 2000). The north and west edges of the Chukchi Plateau have moderately graded slopes whereas the eastern edges have steeper flanks, especially in the northeast surrounding a ~5-km-wide and ~25-km-long oval-shaped valley (Jakobsson and others, 2000). The Northwind Ridge is generally deeper and more rugged than the Chukchi Plateau, with summit depths along the ridge of approximately 1,000 m. It is bounded to the east by a very steep escarpment that gives way to the Canada Basin (Arrigoni, 2008). The varied depths and slopes of the Chukchi Borderland provide a wide range of environments for ferromanganese crust formation, and the thickness and growth history of crusts in each of these setting vary accordingly.

Piston cores collected on the flanks of Northwind Ridge reveal stratigraphic units that range from Paleozoic to Late Jurassic (Arrigoni, 2008). Sedimentation rates estimated from seismic data for the Chukchi Plateau have varied from 2 centimeters per thousand years (cm/k.y.) through the Oligocene, to 1 cm/k.y. through the Miocene, to 5 cm/k.y. from the end of the Miocene to present; sediment thickness decreases from the south to the north (Hegewald and Jokat, 2013). These ages and sedimentation rates indicate sufficient time and conditions to allow for the growth of thick ferromanganese crusts on hard rock surfaces, especially toward the north, as distance from the heavily sedimented Chukchi Shelf increases. Another unique feature of the Chukchi Plateau, compared with other regions with the potential for ferromanganese crust growth, is the record of glacial grounding and associated erosion. Jakobsson and others (2005) found that there are at least two recent episodes of ice grounding and seafloor erosion at depths up to 760 m between 191 and 71 thousand years before present (ka), and the extent of ice grounding on the Chukchi plateau was corroborated by Dove and others (2014). These large-scale ice grounding events may have completely or partially removed friable ferromanganese crusts from their rock surfaces or may have broken crusts up into smaller nodule-like fragments. These events may have caused disruption to the uniformity of ferromanganese crust occurrences within the glacial path as

well as possible redistribution of ferromanganese crust debris. Thus, the record of ice grounding should be considered when determining the regions that are prospective for crusts in the Chukchi Borderland.

The mixing of numerous unique water masses that bathe the Chukchi Borderland, and the Arctic Ocean in general, influence the chemical composition of ferromanganese crusts in this region. The Chukchi Sea and adjacent Amerasia Basin receive seawater from both the Atlantic and Pacific Oceans. Pacific Ocean seawater enters through the Bering Strait (fig. 1), which opened at about 5.4 Ma (Gladenkov and others, 2002). Atlantic Ocean seawater initially enters the Eurasia Basin of the Arctic Ocean through the Fram Strait between Greenland and Svalbard, Norway, which was opened to deepwater circulation at approximately 17 Ma (Jakobsson and others, 2007). Atlantic Ocean seawater then flows through a deep sill in the Lomonosov Ridge into the Amerasia Basin (Björk and others, 2007; Timmermans and others, 2005). In addition to deep water ventilation from the Pacific Ocean, the Atlantic Oceans, the Amerasia Basin, and the Arctic Ocean, the Chukchi Borderland also receives high volumes of freshwater in the form of river runoff (Jakobsson, 2002; van der Loeff and others, 2012) as well as brines produced by freezing along the extensive continental shelf. The combination of brine and freshwater creates a well-defined halocline capable of transporting shelf waters that may have unique metal enrichments offshore and to the deep basins where ferromanganese crusts are forming (Jones and others, 1995).

The Arctic Ocean in general is considered well oxygenated, and individual seas exhibit changes in oxygen concentration with water depth based on water mass distribution and biological productivity. The Chukchi Sea is biologically productive during times of sea ice retreat (Hill and Cota, 2005), which is linked to increased transport of nutrient-rich Pacific Ocean water delivered through the Bering Strait (Coachman and Aagaard, 1988). The combination of Pacific Ocean water contribution, high biological productivity, and extensive shelf area creates a region of lowest oxygen (~270 micromoles per liter [$\mu\text{mol/L}$]) in the Chukchi Borderland from 150 to 350 m depth (fig. 6) (Aguilar-Islas and others, 2013; Kondo and others, 2016). This lowest-oxygen zone near the Chukchi Borderland has as high or higher seawater oxygen concentrations than the maximum oxygen concentration in the open Pacific Ocean where thick ferromanganese crusts form. Oxygen minimum zones (especially below 100 $\mu\text{mol/L}$) are typically a source of dissolved manganese and other metals enriched in ferromanganese crusts in other oceans (Mizell and others, 2020), so the lack of a strong oxygen minimum, and higher oxygen concentrations throughout the water column in the Chukchi Sea, may cause decreased manganese and therefore manganese-associated element (Co, Ni, Mo) concentrations in crusts from the Chukchi Plateau and Northwind Ridge. Both dissolved and labile particulate iron and manganese in halocline waters are high near the Chukchi Shelf but are removed from seawater as the distance from the shelf

increases, with iron more rapidly removed than manganese (Aguilar-Islas and others, 2013; Kondo and others, 2016). This gradient illustrates that iron and manganese contents in Arctic Ocean seawater are highly influenced by scavenging processes along the shelf and that crusts growing farther north and farther from the shelf in the Chukchi Borderland may have slower growth rates and (or) different metal contents than those closer to the shelf. In addition to influencing dissolved metal concentrations and oxidation conditions in the upper-mid water column, the high biological productivity causes increased sedimentation and flux of organic matter to the deep Arctic Ocean (Brown and others, 2015), which can increase benthic productivity and create less oxygenated conditions that may slow crust formation and influence crust composition in deeper waters.

Marine Mineral Occurrences

Ferromanganese crust deposits in the Arctic Ocean were not studied prior to the late 2000s predominantly owing to extensive ice-cover that made sample collection difficult. Ferromanganese crusts from the Chukchi Borderland were first reported by Brumley and others (2015) and were first comprehensively studied by Hein and others (2017). The ferromanganese crusts reported in these two studies were collected via dredge sampling during cruises in 2008 (HLY0805), 2009 (HLY0905), and 2012 (HLY1202) on U.S. Coast Guard (USCG) cutter *Healy* as part of the U.S. Extended Continental Shelf Project. Of the 17 dredge locations taken during *Healy* cruises, 16 returned ferromanganese crusts, and crusts from 9 of these dredges were studied in detail by Hein and others (2017). A total of 50 ferromanganese samples from *Healy* cruises were recovered from three regions: the steep northern flanks of the Chukchi Plateau and Northwind Ridge, scattered seamounts at the far north edge of the Borderland, as well as a single dredge from the eastern edge of Northwind Ridge (Hein and others, 2017). Dredge water depths for all ferromanganese crust samples ranged from 1,605 to 3,851 m, which leaves most of the shallower summits of Northwind Ridge and all of the extremely shallow upper portions of the Chukchi Plateau unsampled. Interestingly, seven nodule samples were also collected during *Healy* dredge operations that are compositionally similar to the ferromanganese crusts. The 9th Chinese National Arctic Research Expedition in 2018 also returned ferromanganese oxides that were described as mixed nodules and crusts from benthic trawling stations on the southern Chukchi Plateau, but the composition was not reported (Wei and others, 2019). From these collections and observations, it appears that ferromanganese mineralization in the Chukchi Borderland likely occurs as concomitant crusts and nodules, although the abundance and distribution of nodules here may not be comparable to abyssal plain settings. The ferromanganese crusts from Hein and others (2017) range in thickness from 6 to 86 mm, with an average thickness of 43 mm, and are more concentrated in Fe and

especially Sc, As, Hg, Li, Th, and V and contain more detrital material than is typical of ferromanganese crusts in the Pacific Ocean (table 2). The enrichment of As and V is likely due to the high amount of Fe oxide, whereas Li is likely enriched in detrital material included in the crust, and Sc is shown to be associated with both the Fe-oxide phase and detritus (Hein and others, 2017). The low Mn concentrations cause lower Co and Ni concentrations; these three elements are typically considered metals of economic interest in ferromanganese crusts. The compositions determined for this limited sampling of ferromanganese crusts from the Chukchi Borderland indicated that crusts here might not have the same economic potential, in terms of metal content, as crusts elsewhere in the global oceans, unless markets for more rare and critical metals such as Sc evolve. Further sampling in a broader range of depths and slope angles may help determine overall crust extent in the region and whether similarly thick crusts with more economically favorable composition like higher manganese, cobalt, and nickel concentrations and less detrital material occur.

The majority of additional reports of ferromanganese-oxide mineral occurrences in this region are from cruises to the Chukchi Sea, just south of the Chukchi Borderland, and are identified as nodules or have compositional similarities with shallow-water shelf nodules. Early and preliminary studies of ferromanganese nodules in the Chukchi Sea were reported by scientists from the Soviet Union in the 1980s (Kalinenko and Pavlidis, 1982; Pavlidis, 1982; Shnyukov and others, 1987). This type of shallow-water shelf nodule is also abundant on the expansive Kara Sea Shelf in Russian Arctic waters and nodules from both the Chukchi and Kara Seas typically form by diagenetic process (Kuhn and others, 2017), in contrast to crusts which form by a hydrogenetic process.

Recently, Cui and others (2020) described four representative ferromanganese samples from a single dredge from the 7th Chinese National Arctic Research Expedition in 2016 to the Chukchi Sea, but they did not report whether the samples were morphologically more similar to ferromanganese crusts or to nodules. The dredge site is located on the Chukchi Shelf in U.S. waters at a depth of 153 m, and the authors noted that the ferromanganese samples in this region are sparsely populated at only about 0.04 kilograms per square meter (kg/m^2) (Cui and others, 2020). In comparison, the CCZ, a fracture zone in the central Pacific Ocean that approximately spans from Mexico to Hawaii and is the most well-studied region for manganese nodules of economic interest, exhibits a measured average abyssal plain nodule abundance of 5.6 kg/m^2 (ISA, 2010). These Chukchi Shelf deposits are more enriched in Ni, P, and Cu than CCZ nodules but have lower concentrations of Mn and Co (Cui and others, 2020; Kuhn and others, 2017). The composition of these Chukchi Shelf samples is similar to nearshore nodules studied by Baturin and Dubinchuk (2011) that were recovered from a single site in Russian waters of the Chukchi Sea at 79 m water depth during the expeditions coordinated by the Russia-US RUSALCA Program in 2009 (<https://oceanexplorer.noaa.gov/>

explorations/09arctic/welcome.html). However, when multiple nodule collection sites from both Russian and United States waters from the RUSALCA Program were investigated by Kolesnik and Kolesnik (2013), those nodules were found to have higher iron to manganese ratios and lower concentrations of phosphorus compared to the results of Baturin and Dubinchuk (2011).

The above compilation of crust and nodule occurrences confirms that ferromanganese oxide minerals have precipitated on and near the Chukchi Borderland. These data highlight that ferromanganese oxide precipitation is prevalent in the regions near the Chukchi Borderland, and especially highlight that ferromanganese oxides can form at very shallow depths in the Arctic Ocean, including as shallow as, or shallower than, the summits of the Chukchi Plateau. The areal extent of shallow ferromanganese deposits in the Alaska OCS remains unknown, as does the economic significance compared to abyssal plain nodules or ferromanganese crusts from the PCZ (fig. 3).

In contrast to the above studies with positive identification of ferromanganese oxides, several coring cruises have returned cores without identifying ferromanganese crust fragments or nodules. In 1992, the USGS sponsored the Arctic Summer West Scientific Party, an expedition to the eastern part of the Chukchi Borderland with USCG cutter *Polar Star*, cruise P192AR, with the goal of studying the geologic framework and tectonic origin of the borderland, sea ice transport of sediments, and paleoceanography (Grantz, 1993). Fifty-two piston cores and seventeen box cores were collected during the expedition with more sampling focused in the shallower and flatter regions of Northwind Ridge and Chukchi Plateau (minimum water depth 20 m and mean water depth 1,356 m), compared to *Healy* cruises in the 2000s where ferromanganese crusts were dredged from steep slopes at the margins of these edifices. Glacial dropstones were documented from these cores but not the presence of ferromanganese crusts or nodules (Grantz, 1993). These core findings, along with the data from Chinese expeditions showing only thin and plate-like ferromanganese oxides at shallow depths along the Chukchi Plateau, indicate that thick, metal-rich ferromanganese crusts are unlikely to be abundant in the Chukchi Borderland and may only occur in particular regions, such as steep slopes.

Abyssal Plain Nodules

Abyssal plain nodules, also called manganese, ferromanganese, or polymetallic nodules, occur on the flat abyssal plain regions of the Earth's oceans and are currently being considered for their mineral resource potential for manganese, nickel, cobalt, and copper by the international community, most prominently in the CCZ of the central Pacific Ocean (ISA, 2010). Abyssal plain nodules form by the precipitation of iron- and manganese-oxide particles around a small nucleus, creating spheroidal and ellipsoidal concretions of various sizes but not larger than a softball (typically <20 cm) (Hein and Koschinsky, 2014; Kuhn and others, 2017). Due to this slow accretionary growth mechanism, a

key parameter for the formation of nodules is that the rate of sedimentation of biological and detrital material to the seafloor is less than 10 mm/k.y. (Morgan, 2000). Nodules typically rest at the surface of sediments that cover abyssal plains, although nodules buried below the sediment surface have also been recovered (Hein and others, 2020; Heller and others, 2018; Usui and others, 1993). The occurrence of nodules at the sediment surface makes them of particular interest for potential mining. The persistence of nodules at the sediment surface also makes them an important substrate for the attachment of sessile benthic organisms (Gollner and others, 2017; Kuhn and others, 2020).

Abyssal plain nodules are dominantly composed of iron and manganese oxyhydroxide and oxide minerals in global oceans. However, the trace metal composition of nodules is variable and depends on the chemistry of the seawater from which they precipitate. When all metals precipitated in nodules are sourced from oxygenated seawater, they are called “hydrogenetic” and acquire elements such as Ti, REY, Zr, Nb, Ta, Hf, Co, Ce, and Te from seawater (Hein and others, 1997). On the other hand, if the metals incorporated into nodules are sourced from diagenetic reactions in the sediment pore waters, the nodules are referred to as “diagenetic” and are typically characterized by higher concentrations of Ni, Cu, Ba, Zn, Mo, Li, and Ga (Hein and others, 1997; Kuhn and others, 2017). The amount of diagenetic versus hydrogenetic input to a nodule depends largely on primary productivity in the surface ocean, which is reflected in sediment type and redox conditions at the seafloor and within the sediment column. Therefore, the compositions of nodules vary between different regions within the oceans (Wegorzewski and Kuhn, 2014).

Three of the most well-studied abyssal plain nodule fields in the global ocean represent the endmembers of nodule genesis: the Peru Basin where nodules are dominantly diagenetic, the Penrhyn Basin where nodules are dominantly hydrogenetic, and the CCZ where nodules are mixed hydrogenetic-diagenetic (Mizell and others, 2022). Primary productivity and detrital input in these regions are reflected within the sediment types, sedimentation rates, and material available for nuclei in these regions. The sediment type is also reflected in detrital sediment input to ferromanganese minerals. Investigation of these sedimentary and oceanographic factors within the poorly sampled Canada Basin can help determine if the region is prospective for abyssal plain nodules and indicate which genetic type and related metal enrichments might be expected.

In addition to abyssal plain nodules, which have generated economic interest (Lipton and others, 2016; Lipton and others, 2021), other types of nodules and nodule-like rocks occur in different geologic settings in the oceans. For example, iron- and (or) manganese-rich nodules also occur in shallow-water estuarine environments, including in the Arctic Ocean, such as in the Lena Valley of the Laptev Sea and in the Kara Sea, both offshore of Siberia (Holmes and Creager, 1974; Bogdanov and others, 1995). However, sedimentary redox conditions in these regions often facilitate high growth rates, resulting in nodules of vastly different composition—predominantly iron oxides. Thus, the presence of “seafloor

nodules” in a shallow-water region does not necessarily indicate that the nodules are comparable to abyssal plain nodules. In this section, we focus on the characteristics of, and probability of the occurrence of, nodules that form in conditions similar to abyssal plain nodules and, as a result, may contain similar enrichments. We do not include diagenetic nearshore iron-rich concretions, which are summarized by Kuhn and others (2017).

Canada Basin

Oceanographic and Geologic Setting

The Canada Basin (fig. 7) is a sedimentary basin located in the Arctic Ocean just north of Alaska. It is bounded to the west by the Chukchi Borderland, to the east by the Canadian Arctic Islands, and the northern extent gives way

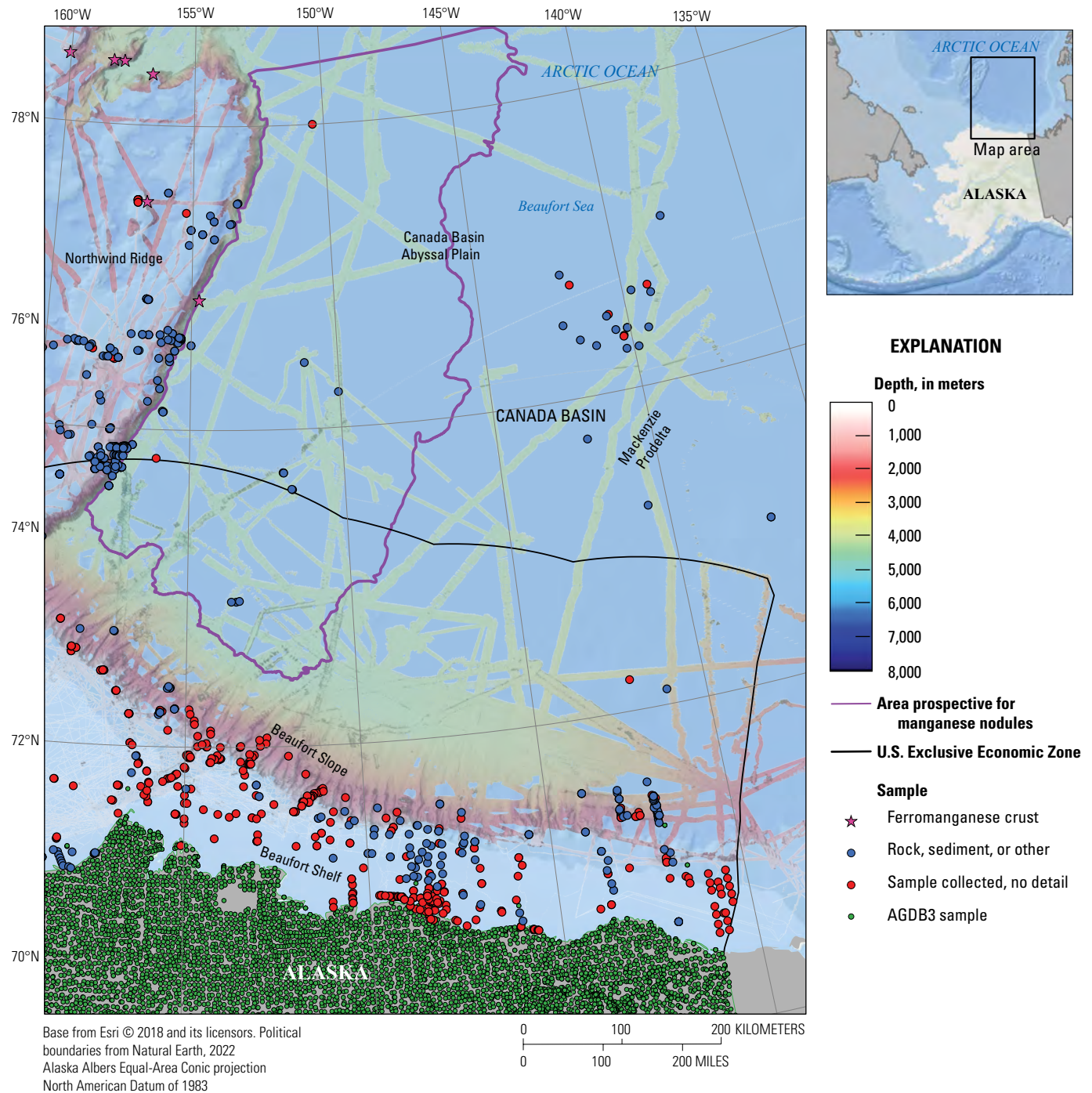


Figure 7. Map of the Canada Basin region. Areas prospective for manganese nodules are at water depths of 3,800 m or deeper, where the Canada Basin Abyssal Plain is deepest, flattest, and undergoes the lowest sedimentation rates. Geologic sample locations from the Index to Marine and Lacustrine Geological Samples IMLGS) (Curators of Marine and Lacustrine Geologic Sample Consortium, 1977) and the Alaska Geochemical Database, ver. 3.0 (AGDB3) (Granitto and others, 2019).

to the larger Amerasia Basin. The Canada Basin is more than 700,000 square kilometers (km²) and is filled with sediments derived mainly from the Mackenzie River drainage basin, but with significant contributions from the Chukotka area in Russia, Alaska, and northwest Canada (Grantz and Hart, 2012). The tectonic history of the Canada Basin remains enigmatic, and several models have been suggested regarding its formation. For example, researchers suggest that the basement of the Canada Basin may be oceanic crust created in the Mesozoic through multiple opening directions (Lawver and Scotese, 1990; Grantz and others, 2011; Døssing and others, 2013). Alternately, seafloor spreading may have caused the rotational separation of the Canadian Arctic Islands and northern Alaska, creating the Canada Basin (Embry, 1990; Gottlieb and others, 2014). However, evidence for thinned continental crust around the edges of the Canada Basin and asymmetrical distribution of oceanic crust at the margins suggest that more complex plate interactions are required than those provided by simple rotational models (Chian and others, 2016). The western part of the Canada Basin, which is within and to the north of the U.S. EEZ, is of particular interest to this study. It is thought this part of the basin was formed as the result of spreading during the late Early and Middle Jurassic (Grantz and Hart, 2012), which would allow ample time for the formation of manganese nodules in this part of the abyssal plain.

The deep waters (>2,600 m) of the Canada Basin that overlie areas of its abyssal plain with low sedimentation rates are uniform and have undergone little ventilation owing to strong stratification for at least the last 500 years (Timmermans and others, 2005). The lack of ventilation has resulted in oxygen drawdown and high nutrient concentrations in the deep waters of the Canada Basin (MacDonald and Carmack, 1991). The relatively low oxygen concentration may result in diagenesis near the surface of the sediment column. As discussed earlier, diagenetic inputs can influence nodule composition, size, and growth rates. Therefore, elements associated with high biological respiration (for example, Fe, Ni, Zn) (Boyd and others, 2017) may be incorporated into any nodules forming at the Canada Basin seafloor.

The sediments of the Canada Basin are mostly Early Jurassic through Holocene. Active sedimentation continues in the Canada Basin due to the numerous sediment sources at the margins (Grantz and Hart, 2012). The Canada Basin abyssal plain contains less sediment (6–7 km) than the Mackenzie Prodelta (9–14 km) and Beaufort Slope (8–12 km) at the margins of the Canada Basin; still, approximately 1 km of sediment has been deposited in the Canada Basin abyssal plain over the past ~48 m.y. (Grantz and Hart, 2012). This sedimentation rate is approximately 20 times faster than in the pelagic clay provinces of the North Pacific Ocean where typical and abundant ferromanganese nodules form (1 mm/k.y.) (Skornyakova and Andrushchenko, 1974). Nodules do form in places with similarly high sedimentation rates of up to 10 cm/k.y., including the biologically productive

Peru Basin (von Stackelberg, 2000); however, in some settings, high sedimentation rates inhibit nodule formation or cause them to be buried (Glasby and others, 1982).

Compared to Pacific abyssal plains, the Canada Basin abyssal plain is also unique owing to its persistent sea ice cover, which has implications both for mineral exploration and nodule formation. The Canada Basin has seen a marked decrease in sea ice over the past few decades (Comiso and others, 2008; Cavalieri and Parkinson, 2012), which has enabled exploration of the region for scientific and resource interests. Although currently declining, sea ice in the Arctic Ocean has been present since the last glaciation, which has contributed variable amounts of rafted sediments and dropstones to the seafloor below (Clark and others, 1980; St. John, 2008; Stein and others, 2012). Ice-rafted debris may serve two contrasting functions in the context of nodule formation: (1) it may contribute to the high sedimentation rates in the Canada Basin that potentially hinder nodule formation or bury nodules formed during periods of lower sedimentation and (2) sand to pebble-sized debris may encourage ferromanganese nodule formation by providing nuclei. It remains to be determined how the unique oceanography of the Canada Basin may influence the formation of any ferromanganese minerals in the region.

Marine Mineral Occurrences

To date, no full-sized (macro; larger than approximately one centimeter diameter) nodules have been recovered from the Canada Basin. However, microneodules were found in cores collected from the central Canada Basin during the T–3 sea ice island studies from 1963 to 1973 (Clark and others, 1980). Microneodules are often found concomitant with macroneodules in other regions of the global ocean. However, their chemical compositions can differ, and the lack of intermediate-sized nodules between the two endmembers suggests that microneodules are not precursors to macroneodules and that the two may have different formation processes (Addy, 1978, 1979; Pattan 1993; Duliu and others, 2009). Microneodules and manganese microparticles have not been considered to have economic potential, but they do provide key information about oxide formation in deep-ocean sediments (Uramoto and others, 2019). Canada Basin microneodules in the T–3 cores were most abundant in the sand-sized fraction from the oldest section of the cores (~6–5 Ma), but microneodules were found throughout the cores and were more abundant in some sedimentary units than others (Clark and others, 1980). Microneodules are not plentiful (<2 percent of mass) in the top layer of sediment at the surface of the cores (Clark and others, 1980), suggesting conditions may not have been favorable for oxide formation in the recent history of the Canada Basin. The increase of ferromanganese microneodules with age in sediment cores in the Arctic Ocean was corroborated by Hunkins (1971), Herman (1970), and Herman and others (1971); however, one study found that a core from the Canada Basin abyssal plain

showed an irregular but general decrease in ferromanganese particles in the sediment from the top to the bottom of the core (Li and others, 1969). The micronodules are mostly angular and irregular-shaped particles, and do not have the spherical shapes or laminated microtextures that are typical of abyssal plain nodules (Clark and others, 1980).

In addition to micronodules, many pebbles and foraminifera in sedimentary units from central Canada Basin cores were also coated with ferromanganese oxide (Clark and others, 1980). Furthermore, gravels from nearshore (within 60 nautical miles [nmi]) Alaskan regions of the Beaufort Sea are coated with ferromanganese oxides (Naidu, 1974). The micronodules, coatings, and encrustations indicate that sediment conditions were oxygenated, metal-rich, and favorable to ferromanganese oxide precipitation and suggest that macronodules could also have formed in locations where all oceanographic and geographic conditions are favorable. If nodules are present in the unsampled portions of the central Canada Basin, they may be similar in composition to nodules from the Peru Basin, due to analogous sediment compositions that are rich in foraminifera (Marchig and Reyss, 1984; Clark and others, 1980). This sediment composition is significantly different from that in the CCZ in which nodules are largest and most abundant in regions where the seafloor is close to the carbonate compensation depth and the sediment is mostly siliceous ooze (Kuhn and others, 2017).

Mineral relevant information within the Canada Basin is also provided by studies intended to discover and characterize benthic biology at the bottom of the ice-covered Canada Basin. At least two recent biological studies were carried out that included box core sampling and ROV footage along the margins of the Canada Basin and at the base of the Northwind Ridge. One study took place using Canadian Coast Guard Ship icebreaker *Louis S. St.-Laurent* in 2002 and another aboard *Healy* (cruise HLY-05-01) in 2005. Bluhm and others (2005) reported that for box cores collected in 2002, the surface layer was composed of mostly very fine, silty sediment over a thick clay layer, and that small pebbles and cobbles only occurred in stations near the base of Northwind Ridge. The rock type in these box cores was not identified and could be debris from the ridge or dropstones. MacDonald and others (2010) reported the results from the 2005 cruise, including a photograph from a station in the Canada Basin abyssal plain (3,843 m), which contains uniformly fine-grained pale gray silt with no nodules or rocks. Descriptions of three additional box core samples from the abyssal plain did not include either manganese nodules or dropstones (MacDonald and others, 2010).

In summary, the limited geological and biological investigations of the Canada Basin have returned no nodule samples; thus, there is currently no evidence that any full-sized (macro) nodules have formed in the Canada Basin. However, in support of the potential for nodule formation in the many unsampled areas, ferromanganese oxide mineralization in other forms has occurred throughout the Canada Basin and Beaufort

Sea. The presence of ferromanganese oxides indicates that the oxygenation and concentrations of iron and manganese in bottom waters and sediments has been sufficient for the precipitation of ferromanganese oxides to varying degrees throughout the past ~6 m.y. However, there is no evidence that any full-sized nodules occur in the Canada Basin.

Hydrothermal Minerals

Among potential marine hydrothermal mineral systems, interest to date has largely been restricted to SMS deposits, analogous to terrestrial VMS deposits. In the modern oceans, active hydrothermal vents are known to occur in every ocean basin, along mid ocean ridges, back-arc basins, arcs, and hotspots. Hydrothermal minerals are most typically associated with active hydrothermal vents, which contain fluids that may range in temperature from just above ambient to greater than 400 °C (Koschinsky and others, 2008). Hydrothermal sulfide minerals form predominantly from crustal and thermogenic sulfide, as well as magmatic sulfur dioxide disproportionation; biogenic sulfate reduction occurs widely (Frank and others, 2015) but is quantitatively less important for SMS deposit formation (McDermott and others, 2015). In addition to hydrothermal sulfide minerals, other hydrothermal minerals include sulfates (for example, barite), oxides, and silicates, which occur both within the high-temperature sulfide-dominant mineral assemblages, via low-temperature hydrothermal precipitation (Hein and others, 2008), and as more distal hydrothermal alteration products (Mills and Elderfield, 1995). Metal sulfide minerals dispersed throughout adjacent sediments may also be of hydrothermal origin and in some cases are suggested to be more extensive than the associated chimneys and chimney rubble; however, in modern seafloor systems the extent of these metalliferous sediments is rarely constrained (Murton and others, 2019).

Active hydrothermal vent systems are associated with high-biomass macrofaunal communities that vary between regions and make use of abundant and diverse chemosynthetic symbioses (Beinart and others, 2015; Mitchell and others, 2020). In part owing to these dense biological communities, some researchers have suggested that mineral exploration and exploitation activities should be limited at active hydrothermal systems (Van Dover and others, 2018). This issue reveals an important knowledge gap, as currently nearly all known occurrences of seafloor hydrothermal minerals occur at active hydrothermal systems, and little is known about the distribution of hydrothermal mineral deposits that are no longer associated with venting hydrothermal fluids (in other words, inactive hydrothermal deposits) (Jamieson and Gartman, 2020; Van Dover and others, 2020). Abundant hydrothermal minerals likely exist that are not associated with areas of active venting; however, knowledge of such systems is limited by exploration techniques and scientific research motivations (Jamieson and Gartman, 2020; Van Dover and others, 2020). The proximal to distal footprint of hydrothermal

systems is rarely constrained, even in well-studied, active systems. This knowledge gap compounds difficulties regarding exploration and research into inactive seafloor hydrothermal systems, where subsequent alteration and burial should be expected. In one deposit, a threshold of approximately 6 m of post-mineral cover has been proposed as an economic cutoff for development of an SMS deposit; this cutoff is for part of an active SMS deposit (Lipton and others, 2018). Typical burial depths for inactive deposits are unconstrained (Jamieson and Gartman, 2020).

These SMS deposits are considered analogous to terrestrial VMS, which are currently major sources of Cu, Pb, Zn, Au, and Ag, with variably significant enrichment and potential byproduct production of Be, Bi, Cd, Co, Cr, Ga, Ge, Hg, In, Mn, Mo, Ni, Se, Sn, Te, and PGE (Koski and Mosier, 2012; Galley and others, 2007; Hofstra and Kreiner, 2020). Therefore, in addition to the study of SMS deposits for their own resource potential, SMS deposits are of interest for their ability to inform VMS metallogenesis. Developing a stronger understanding of where, how, and why critical minerals are enriched in VMS deposits and methods for predicting which deposits may contain significant critical mineral enrichments are areas of current interest.

More than 1,000 VMS deposits are known globally and most contain between 106 and 1,010 metric tons (t) of ore, with copper, zinc, and lead summing to between 1 and 10 percent of the deposit by weight (Koski and Mosier, 2012; Mosier and others, 2009). In contrast, SMS deposits may be as large as 106 t, but few identified SMS deposits are estimated to occur at that scale (Hannington and others, 2010). For most hydrothermal occurrences, there is little information about commodity or grade (see “Introduction” section; Hannington and others, 2010). Metal grades for at least one proposed SMS deposit project (Solwara 1) (fig. 3) plots in the same range as VMS deposits (Lipton and others, 2018). Most VMS deposits are inferred to have formed in arc related settings and many economic deposits are suggested to have formed in submarine calderas (Ohmoto, 1978). The bias toward arc-related, rather than mid-ocean-ridge-related, settings for VMS deposits in the geologic record is likely an artifact of preservation (Huston and others, 2010). It is also worth noting that VMS deposits are not uniformly distributed throughout the geologic record (Huston and others, 2010), but instead coincide with periods of continent building and reflect contemporaneous ocean chemistry. This association suggests that modern SMS deposits may not completely mirror ancient VMS deposits.

Along arcs, hydrothermal venting may include influence from both magmatic and evolved seawater hydrothermal fluids, and it has been suggested that the influence of magmatic-hydrothermal fluids may be greater (de Ronde and others, 2003). Even small injections of magmatic fluids can significantly increase the metal budget in VMS deposits (Franklin and others, 2005). On average, arc-related hydrothermal activity typically occurs at shallower ocean depths than hydrothermal activity at mid-ocean

ridges, resulting in lower potential fluid temperatures for boiling (Monecke and others, 2014). Although the shallower depths often result in phase separation, which aids in metal deposition, the lower temperatures at which phase separation occurs as a function of depth also decreases the ability of fluids and vapors to transport metals. Shallow venting on arc volcanos may result in mineralization that is compositionally more similar to epithermal (Au-Ag) deposits and therefore commonly referred to as “epithermal-like” (Hannington and others, 2005; John and others, 2010).

Aleutian Arc

Oceanographic and Geologic Setting

The Aleutian Arc extends from the Gulf of Alaska to the Kamchatka Peninsula in the Russian Far East and separates the Pacific Ocean from the Bering Sea (fig. 8). The arc may be as old as 55 m.y. (Scholl and others, 1986), is volcanically active, and contains over 90 major Holocene volcanic centers (Tibaldi and Bonali, 2017). These volcanoes are monitored by the Alaska Volcano Observatory (<https://avo.alaska.edu/>) and include 56 known locations of subaerial hydrothermal activity (Motyka and others, 1993; Bergfeld and others, 2015). Seismicity in the Aleutian Arc is lower in the western than in the central and eastern sections (Glasby and others, 2006), and volcanism transitions from more felsic in the east, on the Alaska Peninsula, to more mafic in the west, with the transition occurring somewhere between Peulik and Ukinrek Maars (on the Alaska Peninsula, to the east of fig. 8) (Buurman and others, 2014). The continental influence in the eastern arc is also apparent in sedimentation, which decreases moving westward, and is reflected in thinning sedimentation loads in the marine basins (Marlow and others, 1973). The eastern intra-arc basins, Amlia and Amukta (fig. 8), include 2–5 km of sediment fill of both marine and terrestrial origin (Scholl and others, 1975; Geist and others, 1987) whereas fresh volcanic cones are apparent in the recently mapped western basins. Vallier and others (1994) placed the main division in the Aleutian Arc at Unimak Pass (fig. 9), dividing the Alaska Peninsula from islands and submarine components westward. In this section we are exclusively concerned with the western part of the arc, owing to its potential to host submarine hydrothermal systems, and we discuss the eastern section in the following “Coastal Marine Minerals” section.

Aleutian Arc volcanism transitions from subaerial to submarine west of Buldir Island, with some of the submerged cones as large as the eastern subaerial volcanoes (fig. 8) (Yogodzinski and others, 2015). In addition to the arc, active volcanism also occurs in the Aleutian back arc. Tibaldi and Bonali (2017) noted six back-arc volcanoes, of which Bogoslof and Saint Paul Islands are located in the Bering Sea (figs. 8, 9); both are emergent and basaltic. The heavy sedimentation of the back arc has led to descriptions of it as “virtually featureless” (Marlow and others, 1976), although it does include the extensional Saint George and Bristol Bay

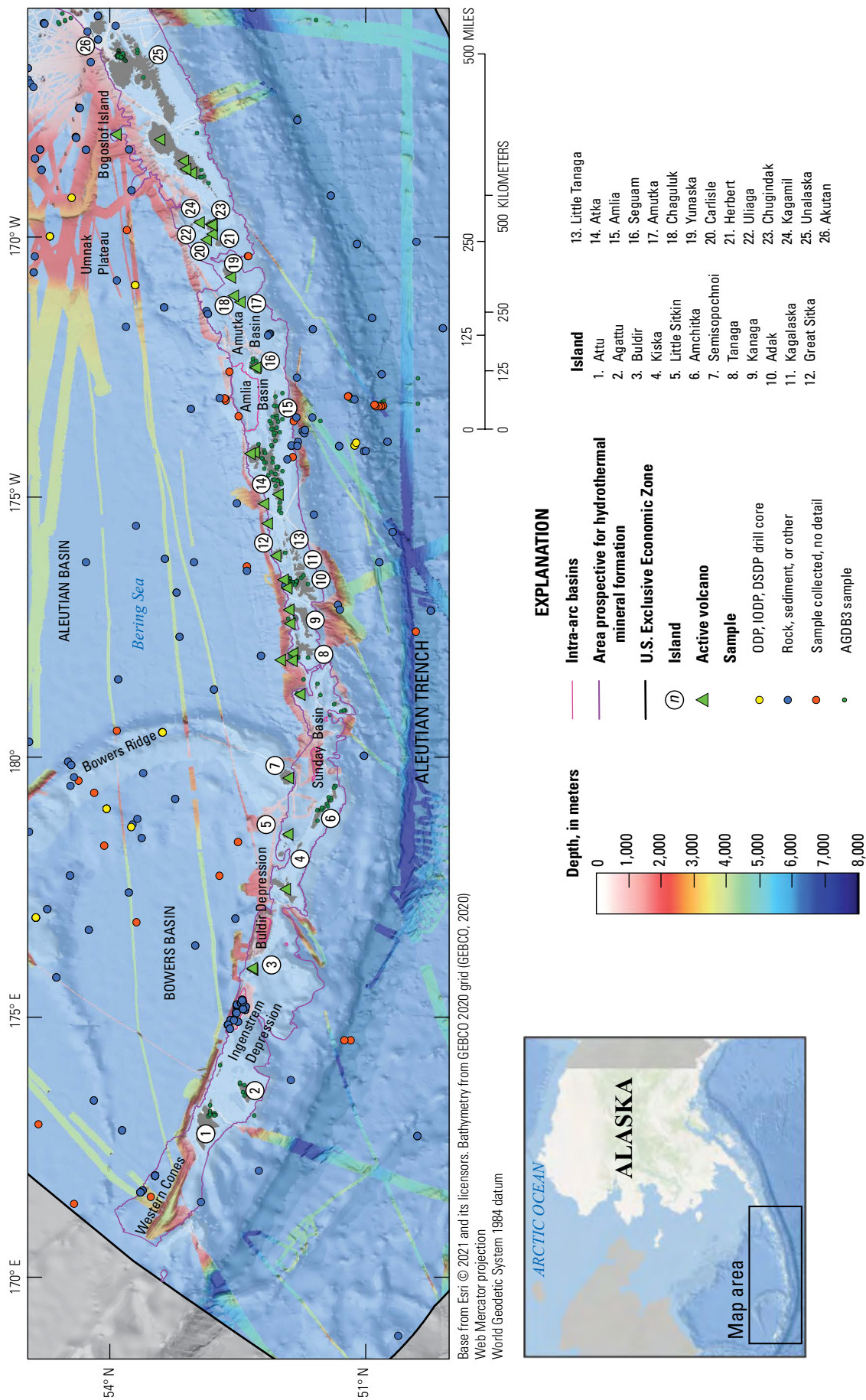
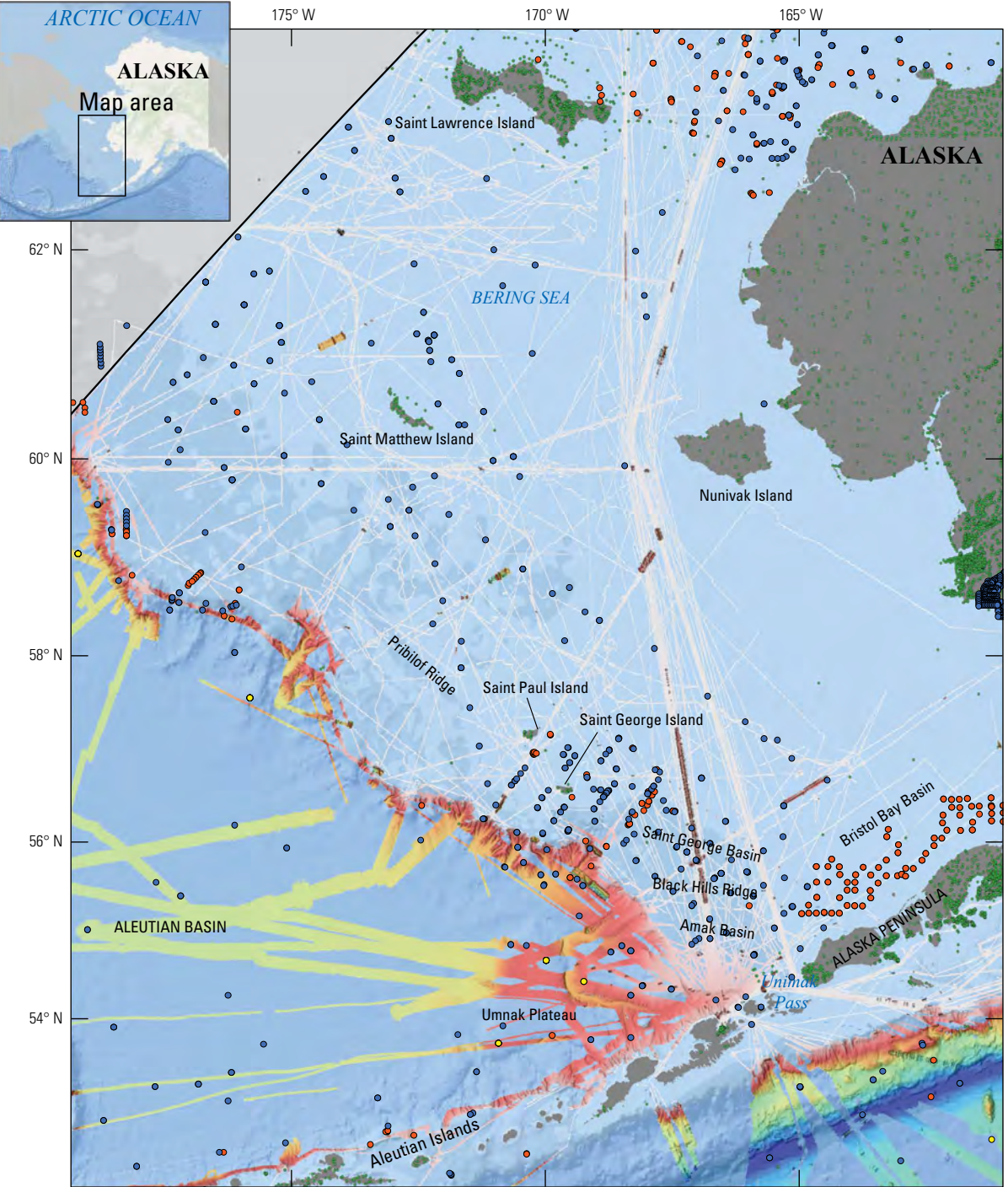


Figure 8. Map of the Aleutian Arc, Alaska, showing active volcanoes along the arc and back arc (continued in figure 9). Unimak Pass, the beginning of the offshore section of the Aleutian Arc, is at the easternmost end of the map. Seafloor is shown in gray outside of the U.S. Exclusive Economic Zone (EEZ). The arc and arc islands are prospective for hydrothermal mineral formation. Geologic sample locations from the Index to Marine and Lacustrine Geological Samples (IMLGS) (Curators of Marine and Lacustrine Geologic Sample Consortium, 1977), Yagodinski and others (2015), and the Alaska Geochemical Database, ver. 3.0 (AGDB3) (Granitto and others, 2019). ODP, Ocean Drilling Program; IODP, Integrated Ocean Drilling Program; DSDP, Deep Sea Drilling Project.



Base from Esri © 2021 and its licensors. Bathymetry from GEBCO 2020 grid (GEBCO, 2020), Web Mercator projection World Geodetic System 1984 datum

0 250 500 MILES
0 250 500 KILOMETERS

EXPLANATION

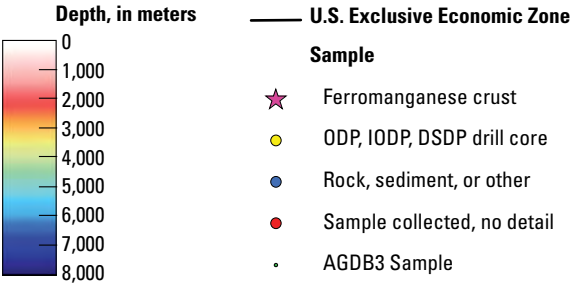


Figure 9. Map of the Bering Sea and Aleutian back arc, as well as part of the Alaska Peninsula. Seafloor is shown in gray outside of the U.S. Exclusive Economic Zone (EEZ). Basins and ridges were determined by seismic work in Marlow and others (1994). Geologic sample locations from the Index to Marine and Lacustrine Geological Samples (IMLGS) (Curators of Marine and Lacustrine Geologic Sample Consortium, 1977) and the Alaska Geochemical Database, ver. 3.0 (AGDB3) (Granitto and others, 2019). ODP, Ocean Drilling Program; IODP, Integrated Ocean Drilling Program; DSDP, Deep Sea Drilling Project.

Basins, filled with more than 10 km of sediment (Marlow and others, 1994), as well as the extinct margins of the Pribilof and Black Hills Ridges (Marlow and others, 1994).

The Aleutian Arc separates the North Pacific Ocean abyssal plain from the shallow Bering Sea in the east and the Aleutian Basin, surrounding Bowers Ridge and Bowers Basin, in the west. The major currents in the region are the Alaska North Slope Current, which flows east along the north side of the arc, and the Alaskan Stream, which flows west along the south side (Uchida, 2013). Seawater crosses the arc from south to north at Amukta Pass, Amchitka Pass, Buldir Pass, and Near Strait (west of Attu Island), which reaches 2,000 m depth. Seawater crosses from north to south at Amukta Pass, Amchitka Pass, and Kamchatka Strait (Uchida, 2013). In recent times, seasonal ice has not reached the western Aleutian Islands, even in cold years (2001–2010) (Van Pelt and others, 2015). The semi-enclosed nature of the Bering Sea is reflected in its high nutrient load and productivity, which in turn supports fisheries of significance to both local communities and the U.S. economy as a whole (Van Pelt, 2015).

Marine Mineral Occurrences

The Aleutian Arc is prospective for hydrothermal minerals, as active volcanic arcs host hydrothermal activity and associated mineralization throughout the global ocean. A survey of submarine arc volcanoes throughout the oceans noted that volcanoes are spaced 22–32 km apart on average, and hydrothermal venting has been observed at volcano summits and along volcano flanks and in calderas (de Ronde, 2003). There are many volcanic cones over the 600-km length of the western Aleutian Islands. The potential for hydrothermal activity and associated active seafloor mineralization in the Aleutian Arc is hypothesized to be associated with the extensional intra-arc/summit basins that occur between emergent volcanic islands, with basins forming as grabens associated with block rotation (Geist and others, 1988). Modern bathymetry within some of these basins was collected using RV *Thomas G. Thompson* during the 2005 Western Aleutian Volcano Expedition (cruise TN182) and the joint German–Russian KALMAR project 2009 RV *Sonne* cruise (SO201–1b). The resultant maps and co-collected dredges revealed recent volcanism of basalts, dacites, and rhyodacites dated from tens to thousands of years using $^{40}\text{Ar}/^{39}\text{Ar}$ analysis (Yogodzinski and others, 2015). No hydrothermal minerals were reported in association with any of these dredges. The bathymetric survey revealed numerous volcanic cones throughout the Buldir Basin and Ingenstrom Depression (fig. 10), and a region named Western Cones (fig. 8) (Yogodzinski and others, 2015). A water column survey would reveal if any of these areas include active hydrothermal emissions, and additional geophysical exploration may help constrain regions of interest for inactive hydrothermal mineral deposits, which formed from, but do not currently exhibit, venting fluids.

The only known submarine hydrothermal activity in the Aleutian Arc is Piip Volcano (lat 55°23' N., long 167°15' E.),

which falls within the Russian EEZ (Torokhov and Taran, 1994). Hydrothermal activity occurs at both Piip Volcano summit cones—depths of emission range from 380 to 650 m. Mineralogy of Piip Volcano samples includes hydrothermal manganese and iron oxides, anhydrite, barite, pyrite, and calcium carbonate. Pyrite is the only iron sulfide observed, and is enriched in arsenic, antimony, and mercury, consistent with shallow hydrothermal systems that result in enrichment of vapor-mobile elements. The InterRidge hydrothermal vents database (InterRidge, 2020) includes one additional hydrothermal occurrence in the Aleutian Islands, on Kagamil Island (lat 52°59' N., long 169°43' E., fig. 8); however, the only published reference at this site refers to subaerial (beach) activity (Kawai and others, 2008). InterRidge refers to the location's depth as 5 m and references a fall 2008 University of Alaska Fairbanks Aurora Magazine article (<https://www.uaf.edu/aurora/archives/>). There is also one location of deep-sea drilling relevant to the Aleutian Arc, Deep Sea Drilling Project (DSDP) site 183, which occurred south of the Aleutian Trench (Scholl and Creager, 1973). This drill core recovered a thin basal unit of hydrothermal ferruginous clay and ironstone, located below 500 m of pelagic sediments and turbidites (Natland, 1977). While the existence of additional active hydrothermal activity in the western Aleutian Islands is likely, the composition and extent of any associated minerals is speculative.

There is also the possibility of hydrothermal minerals that are not associated with active hydrothermal vents in this setting. However, current exploration activity typically begins with an active hydrothermal signal and may expand outward, as there are no current means to efficiently explore for inactive seafloor massive sulfides (Jamieson and Gartman, 2020). The propensity for explosive eruptions, collapse, and debris flows observed among Aleutian Island volcanoes (Hein and others, 1978; Coombs and others, 2007) does not contradict the long-term sustained conditions of hydrothermal venting that would be needed for seafloor-surface preservation of large SMS deposits, as explosive eruptions are known to occur in other locations with significant sulfide deposition (for example, Clague and others, 2009).

The potential for other types of hydrothermal mineral deposits may be expanded by considering the eastern Aleutian Arc above sea level. In addition to active geothermal activity (Motyka and others, 1993), islands of the eastern Aleutian Arc host the Alaska–Apollo and Shumagin epithermal deposits, located in Eocene to Pleistocene rocks, as well as broadly coeval porphyry mineralization at occurrences such as Pyramid Mine (Wilson and Cox, 1983). However, to date, there have been no porphyry prospects discovered in the deep ocean. Furthermore, any porphyry Cu would be both much more extensive and much lower grade (average terrestrial grade in 2008, 0.44 percent Cu; John and others, 2010) than typical SMS deposits. However, shallow marine hydrothermal deposits are well known and commonly resemble epithermal mineralization. In contrast to SMS/VMS deposits and epithermal mineralization, which form at or just below the seafloor in the oceans, any porphyry mineralization would be deeper, within

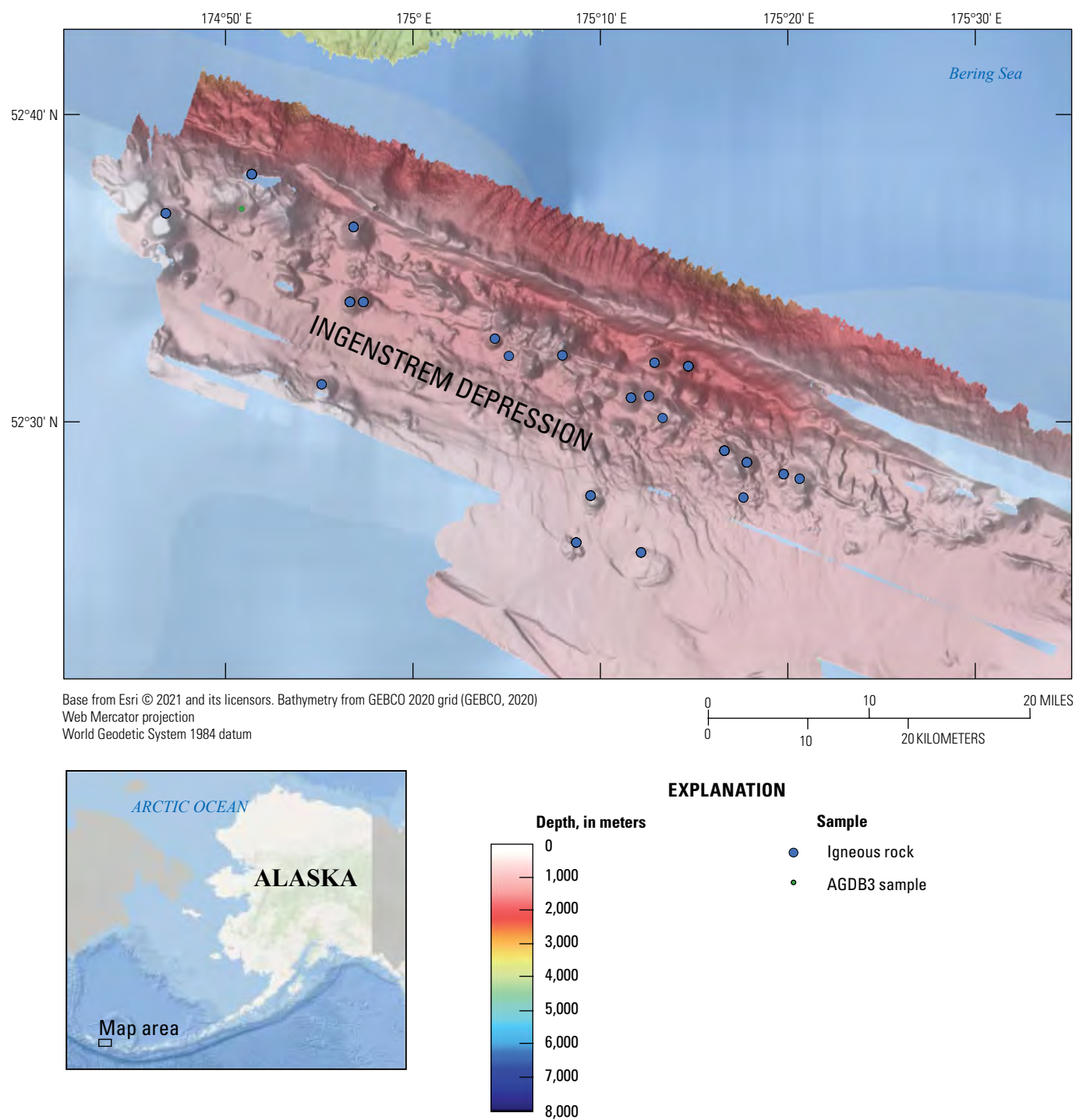


Figure 10. Map of the Ingenstrem Depression, Aleutian Arc, Alaska, which has numerous submarine volcanic cones. All rock samples collected by dredge from this region are lavas, which exhibit a range of compositions (Yogodzinski and others, 2015). Geological sample locations from Yogodzinski and others (2015) and the Alaska Geochemical Database, ver. 3.0 (AGDB3) (Granitto and others, 2019).

the upper oceanic crust (typically less than 5–10 km depth; John and others, 2010), unless seafloor exhumation occurred, bringing porphyry mineralization to the seafloor.

Coastal Marine Minerals

Coastal marine mineral occurrences in Alaska are widespread. Geologically, these deposits have typically formed during earlier events that are now preserved in the nearshore environment and are genetically and (or) temporally distinct from deep-ocean minerals. Additionally, redistribution of metals and economic minerals has occurred in some coastal locations, resulting in marine placer deposits, some of which are actively forming in response to modern climatic, coastal, and fluvial processes. Paleoplacers also exist (Jones and others, 2017; Van Gosen and others, 2017). Research, exploration, and development of near-shore mineral deposits rely largely on the understanding of nearby terrestrial deposits that may project offshore or directly supply minerals to near-shore environments through physical and chemical erosion. In contrast, deposits in the deep ocean require significantly greater resources to investigate and are generally not as well characterized owing to costs and access limitations.

Placer deposits are the most economically important nearshore deposits in Alaska, and nearshore placers in Norton Sound have produced more than 30 percent of total placer gold in Alaska (Cobb, 1973). Placer deposits form by erosion of lode deposits that have been preserved in the terrestrial environment and exposed at the modern surface and subject to erosion. In the nearshore setting, fluvial, glacial, and shallow marine processes transport metal-bearing sediments into a deltaic environment, where additional marine processes, including currents, concentrate the sediments into economic resources. Placer deposits in the coastal environment occur on ancient or modern beaches, in seafloor depressions, and in buried river valleys. Elements enriched in placer deposits are typically heavy or occur in minerals resistant to chemical breakdown and include gold, platinum (in ferroplatinum), tin (in cassiterite), chromium (in chromite), titanium (in ilmenite and rutile), tungsten (in scheelite), zirconium and hafnium (in zircon), and REE (in monazite and xenotime) (Scott, 2011; Schulz and others, 2014). Placer gold is mined terrestrially throughout Alaska, mainly in streams and rivers, as well as in the coastal zone. Additionally, these deposits are known to occur offshore. Similar to aggregate deposits, offshore placers are not stable and migrate seasonally, over time, and with storms. Offshore placers can also become buried by more recent erosion and deposition; as a result, it has been noted that most economic placers are Pleistocene or younger (Minter and Craw, 1999).

Historically there has been less hard rock mining of minerals contained in bedrock in nearshore regions, although that may be changing (Hannington and others, 2017). The offshore extension of continental crust along continental shelves and slopes, including the large continental shelf of the

Bering Strait, may contain mineral deposits similar to those discovered or suspected to occur above sea level; although, in the case of the Bering Sea, they may be buried under hundreds of meters of sediment (for example, Aiello and Ravelo, 2012) as a result of high sediment inputs from major rivers and formation of deltas (for example, the Yukon and Kuskokwim Rivers). Concealment beneath the water and subsequent burial beneath seafloor sediments make exploration difficult and costly. As a result, although the coastal regions of Alaska are by far more comprehensively sampled than the deep-ocean regions, most of these samples are surficial. What follows is a review of nearshore mineral settings and occurrences by region from north to south.

Seward Peninsula

Oceanographic and Geologic Setting

The Seward Peninsula (fig. 11) extends westward from mainland Alaska into the Bering Sea and is flanked on the south by Norton Sound. Water depth remains very shallow well offshore of much of the Seward Peninsula, although bathymetry coverage is not extensive (NOAA Office of Coast Survey, [undated]). Norton Sound is <30 m deep at its deepest location. Currents flow northward, out of the Bering Strait into the Arctic Ocean, with peak water flow occurring in summer (Wood and others, 2015) and annual water transport increasing since 1990 (Woodgate, 2018). Sediment transport is also generally northward, out of Yukon Delta and north into the Bering Strait (Drake and others, 1980). Historically, seasonal ice extended past Seward Peninsula through spring, even in warm years (Frey and others, 2015), although recent work suggests that seasonal ice extension past Seward Peninsula may not be the case in the future (Huntington and others, 2020).

The Yukon River, the longest and greatest volume river in Alaska (Inman and Nordstrom, 1971), discharges into the Bering Sea, just southwest of Norton Sound. Discharge from the sediment-laden Yukon River into the shallow coastal environment of the Bering Strait and Norton Sound is heavily influenced by fluvially transported detritus. The seafloor of Norton Sound is a mix of Yukon River sediment and relict sands, and the sediment texture is generally coarser along the shoreline (McManus and others, 1977). Sediment ridges resulting from coastal transport were oriented north-south as measured in the late 1970s (Field and others, 1981). A CO₂ seep, releasing thermogenic hydrocarbons, exists just off Cape Nome (Kvenvolden and others, 1979) and pockmarks (1–10 m diameter) and gas-rich sediment occur throughout Norton Sound, as well as some nearshore to the west in the Chirikov Basin (Nelson and others, 1979).

The majority of Seward Peninsula is underlain by rocks of the Paleozoic Arctic Alaska–Chukotka superterrane. The major rock types on the peninsula include limestone, slates, and schists (Mulligan, 1966) that have undergone varying, but generally intense, metamorphism (Till and others, 2011).

The metamorphic package was intruded by calc-alkaline to alkaline Cretaceous igneous rocks across the peninsula (Miller, 1989; Till and others, 2011). Important terrestrial minerals on Seward Peninsula include gold, tin, and base metals. Gold and tin have been identified in lode sources and nearby placers. Gold has been identified in predominantly small quartz vein-dominant systems developed in the

metamorphic rocks of the Nome Complex, which comprises most of the peninsula. Gold bearing veins are most abundant in the vicinity of Nome and along the southern coast of the Seward Peninsula. Tin occurs in middle Cretaceous granites, which intrude into the variably metamorphosed York terrane, in the northwest of the Seward Peninsula (Goldfarb and others, 2016, Till and others, 2011).

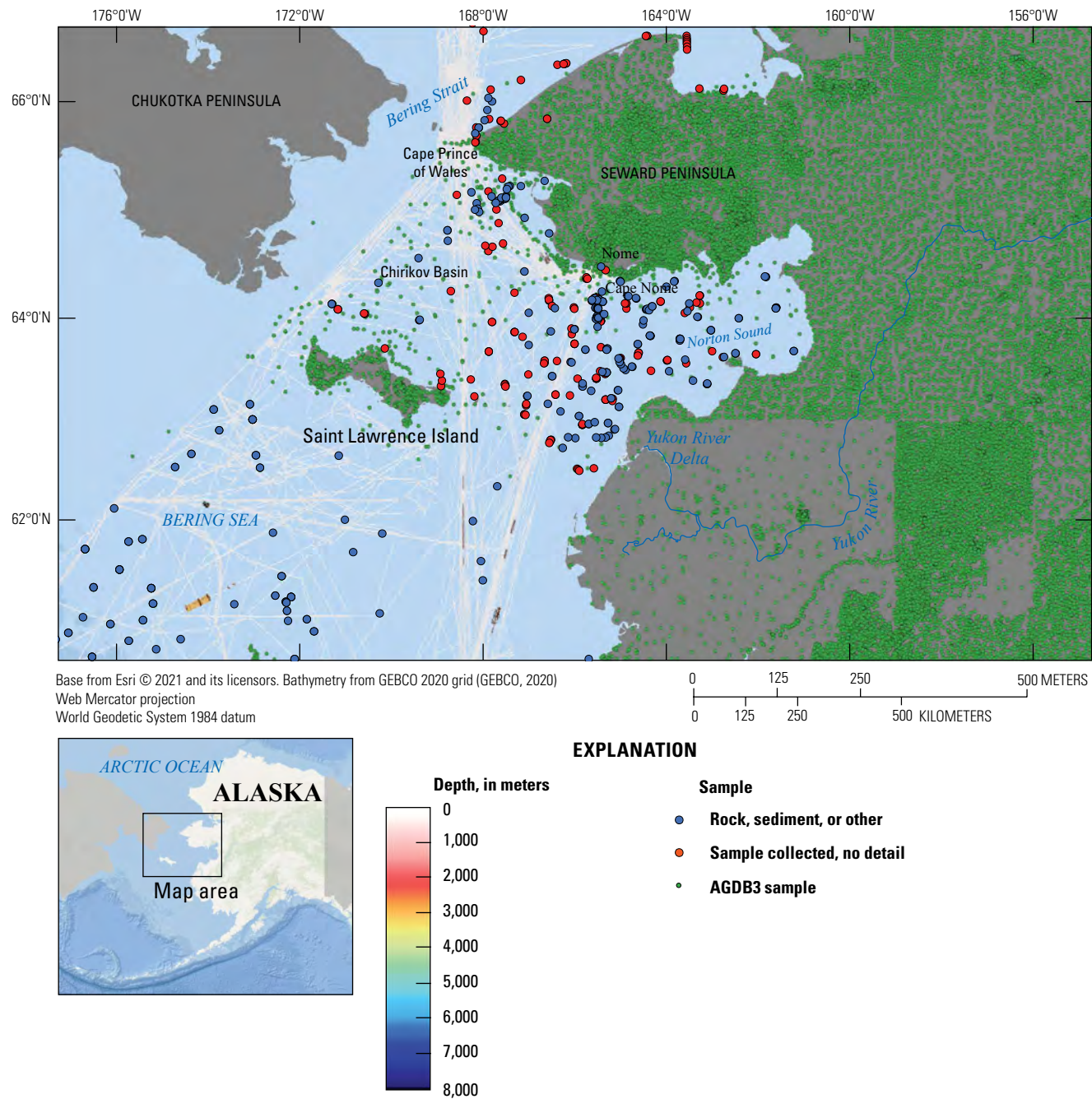


Figure 11. Map of Seward Peninsula, including Norton Sound and Saint Lawrence Island, Alaska, and the Chukotka Peninsula in Russia. Geologic sample locations from the Index to Marine and Lacustrine Geological Samples (IMLGS) (Curators of Marine and Lacustrine Geologic Sample Consortium, 1977), Nelson and Hopkins (1972), and the Alaska Geochemical Database, ver. 3.0 (AGDB3) (Granitto, 2019).

Marine Mineral Occurrences

Seward Peninsula contains abundant coastal mineral occurrences and has undergone extensive exploration and research, most recently in the 1980s (for example, Nelson and Hopkins, 1972; Moore and Welkie, 1976; Larsen and others, 1980). The Seward Peninsula remains prospective for more than 11 distinct types of mineral systems, many of which carry enrichments for critical minerals (Kreiner and Jones, 2020; Hofstra and Kreiner, 2020). Locally, these systems overlap in space, with some regions containing evidence for as many as eight mineral systems (Kreiner and Jones, 2020). Many of these mineral systems occur within proximity of the modern coastline, and some geologic belts containing prospective regions for mineral deposits demonstrably extend offshore and can be linked to Saint Lawrence Island in the Bering Sea (fig. 11). This includes a belt of middle Cretaceous alkaline magmatism that has associated porphyry Mo-W occurrences on the Seward Peninsula and Saint Lawrence Island, and per-alkaline REE mineral occurrences on the Seward Peninsula. The most significant nearshore placer opportunities are provided by the REE-metal bearing granite systems containing significant Sn and fluorospar resources in northwestern Seward Peninsula (Puchner, 1986), and the gold-bearing quartz veins in the southern portion of the Seward Peninsula (Goldfarb and others, 2016). The possibility of offshore Sn placers was suggested as early as 1980 in work published by Larsen and others (1980), which included analyzing sediments from 180 sampling stations for a variety of metals, finding the greatest concentration of Zn, Cr, Ce, Ti, Mn, La, Sc, Y, Yb, and Nd to co-occur approximately 30 km south of Cape Prince of Wales (Larsen and others, 1980). Tin, mainly as cassiterite, occurs in bench, stream, river, and beach placers onshore, as well as in bottom sediments offshore (Warner, 1985) where streams and rivers drain areas of known lode tin resources.

Abundant gold placers occur offshore of the southern margin of the Seward Peninsula, where most gold occurs near the coast within the coarser sediments. Gold is transported into Norton Sound via a network of fluvial drainages eroding lode gold vein deposits. Once gold is deposited into the Sound, longshore currents locally redistribute the gold, predominantly transporting the gold-rich sediments to the east and into the nearshore environment. Despite nearly 5 million troy ounces of total gold production from the Nome beach placers (Szumigala and others, 2011), very few lode-gold sources have been identified. Gold placer mining has occurred since 1960 offshore of Nome by a number of purveyors using various methods, predominantly dredging. In 2014, Alaska reported 43 operators working in Norton Sound (10 of which were considered recreational) (Freeman and others, 2015). Further details on the history of gold mining offshore of Nome, as well as remaining prospects are publicly available through the USGS Mineral Resources Online Spatial Data (https://mrdata.usgs.gov/ardf/show-ardf.php?ardf_num=NM253) and are not reproduced here.

Goodnews Bay

Oceanographic and Geologic Setting

The Goodnews Bay region (fig. 12) includes the greater Kuskokwim Bay, which leads into the semi-enclosed bodies of Carter, Goodnews, and Chagvan Bays, from north to south. The whole region is shallow, less than 30 m as far as 100 km offshore, and is typically ice-covered during winter months. The terrestrial district surrounding this area is also known as Goodnews Bay and sits inside the Togiak National Wildlife Refuge, with Cape Newenham State Game Refuge forming the southern boundary of the region.

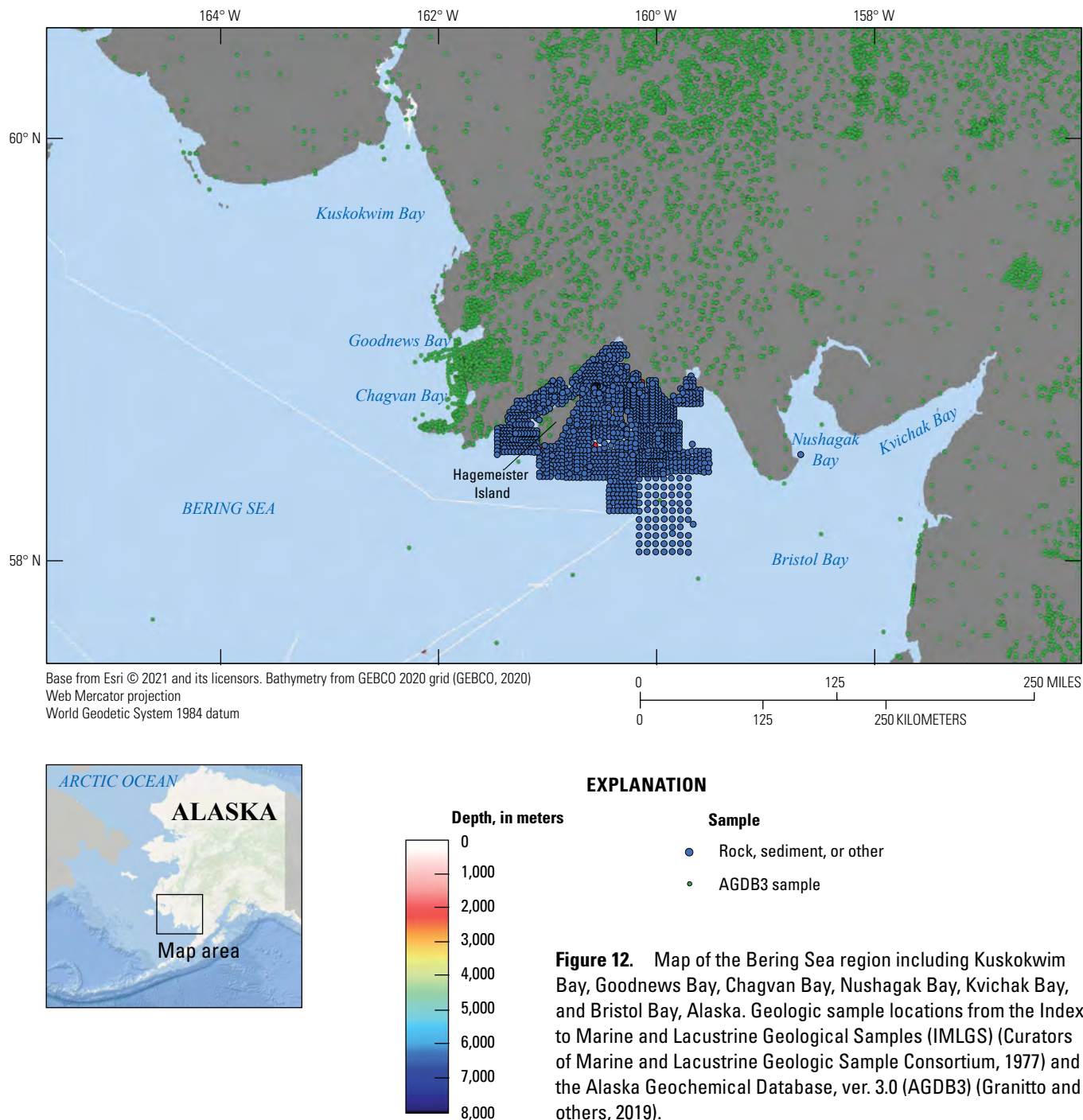
Onshore, the terrain is variably metamorphosed and underlain by rocks of the Goodnews Bay subduction complex (Carter to Goodnews Bays) and the Jurassic Togiak volcanic arc (around Chagvan Bay) (Plafker and Berg, 1994); the Goodnews Bay terrain is generally older. The larger Goodnews Bay region produced an estimated 555 thousand troy ounces of refined PGE (Ru, Rh, Pd, Os, Ir, and Pt) as platinum-bearing metal alloy inclusions within chromite (Bird and Clark, 1976) between 1934 and 1976 from terrestrial placers. It has been suggested that significant resources remain, including offshore (Szumigala and others, 2010). The main exposure of the Goodnews Bay Complex occurs at Red Mountain as an ultramafic body that is partially serpentinized dunite constituting structurally preserved slivers of ocean crust (Mertie, 1969).

Marine Mineral Occurrences

The Goodnews Bay region is prospective for mafic-ultramafic and orthomagmatic mineral deposits (Kreiner and Jones, 2020). It contains exposures of ancient oceanic crust preserved through subsequent tectonic events that resulted in the ophiolite sequence being overthrust during subduction and (or) accretionary episodes. The mafic-ultramafic sequence exposed at Red Mountain is prospective for chromite and PGE. The PGE minerals are typically found as ferroplatinum and are also associated with chromite and sulfide minerals including pyrrhotite, pentlandite, and chalcopyrite (Foley and others, 1997). Exploration for metal-rich sediments has occurred at least since 1969, by both academic and commercial entities, including a lease which was never exploited (Moore and Welkie, 1976; lease was to Inlet Oil). Most sampling has been focused on PGE (dominantly platinum) placers, most recently in 2005 (Oommen and others, 2008). That study, which integrated sampling from 2005 with earlier sampling, noted that much of the platinum is <100 micrometers (μm) in size, and that platinum concentration is higher within Goodnews Bay than outside of it. Mineralogically, the platinum commonly separates with the magnetic fraction and has been reported to occur both as inclusions in magnetite and in discrete grains, mainly as Pt-Fe, with common sperrylite (PtAs_2) and minor element associations that include iridium and rhodium (Rosenblum

and others, 1986). It is suggested that the offshore platinum originates from Red Mountain and is transported to the coast by the Salmon River (Moore and Welkie, 1976; Cronan, 1992). Deposits farther offshore likely originated during periods of prior glaciations. Detailed analysis of onshore placers suggest that the offshore placers would also be composed of majority isoferroplatinum (Pt₃Fe) with irasite (IrAsS), platarsite (PtAsS), osarsite ((Os,Ru)AsS), erlichmanite (OsS₂), and sperrylite (PtAs₂) (Tolstikh and others, 2002); these minerals are consistent with the elements identified in offshore sediment samples. In addition, geophysical indicators suggest that the

ultramafic body itself extends offshore, at depths of 12 to 15 m below sea level (Barker and Lamal, 1989; Oommen and others, 2008), although it has not been drilled. Nearly 17,000kg of PGE was produced from Goodnews Bay deposits from 1937 to 1975 using a bucket-line dredge (Zelenka, 1988). There is also one report of native mercury and cinnabar within Goodnews Bay (Hoare and Cobb, 1977). The mercury association likely represents a younger event superimposed onto the fault-dissected subduction complex and arc roots as mercury mineralization is not characteristic of mafic-ultramafic mineral systems.

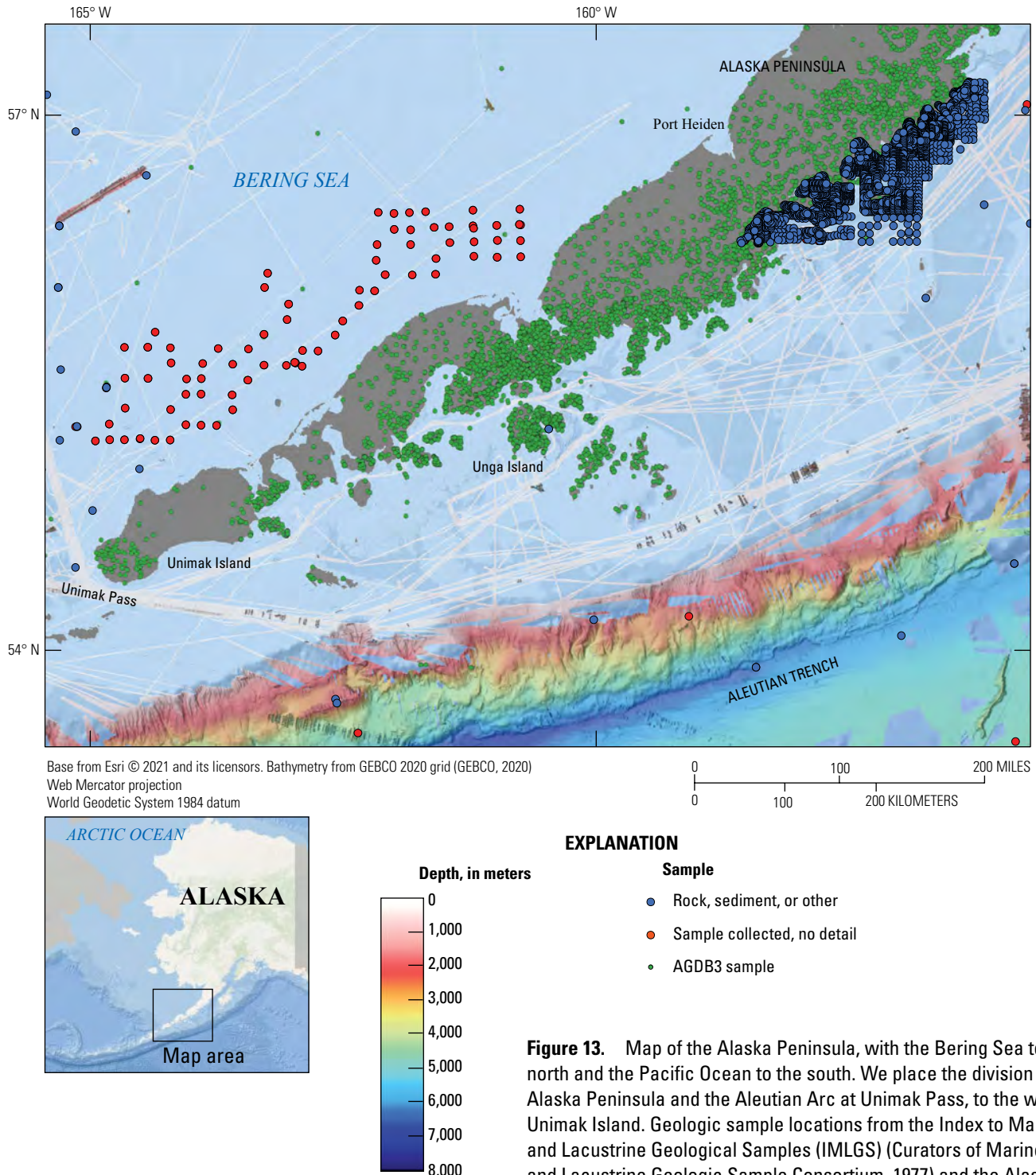


Bristol Bay and Alaska Peninsula

Oceanographic and Geologic Setting

The Alaska Peninsula (fig. 13) encompasses the eastern half of the Aleutian magmatic arc and includes regions of active subaerial volcanism. Bristol Bay is an embayment

of the Bering Sea that borders the north coast of the Alaska Peninsula. The Pacific Ocean is to the south, with inlets and small coastal bays along the shore (for example, Chignik, Castle, Devils, Kuiukta, Mitrofanía, Ivanof, and Pavlof Bays). Alongshore currents on the north side of the peninsula flow northeast and circulate into Bristol Bay. Sediments in Bristol Bay decrease in size with distance from shore (Sharma and



others, 1972). From 2003 to 2011, Bristol Bay had winter ice coverage reaching south to approximately Port Heiden. On the south coast of the Peninsula, the Alaskan Stream moves alongshore currents southwest; coastal islands and shallow shelf extend about 120 km from shore (Zimmerman and others, 2019).

Geologically, most of the Alaska Peninsula is underlain by Mesozoic turbiditic sedimentary rocks, as well as other volcanic and sedimentary rocks ranging from the Cretaceous to Quaternary (Vallier and others, 1994). Portions of the peninsula are underlain by the Paleozoic and early Mesozoic oceanic arc terranes of the Peninsular–Alexander Wrangellia (PAW) superterrane (Graham and others, 2013). The PAW superterrane has been intruded by a series of magmatic arcs ranging from the Jurassic through the modern Aleutian Arc. On the north side of the active arc, Mesozoic sedimentary rocks of the Kuskokwim–Kahiltna basin mark the boundary of the accreted terranes (Graham and others, 2013). The region has seen active uplift and volcanic activity over the past ~200 m.y. and currently is subjected to substantial alpine glaciation. This environment exposes a wide variety of mineralizing systems and structural levels to modern erosion close to the modern coastline.

Marine Mineral Occurrences

The Alaska Peninsula and Bristol Bay area are highly prospective for porphyry Cu–Mo–Au, epithermal, volcanogenic seafloor, and reduced intrusion-related gold mineral systems (Kreiner and Jones, 2020). The Bristol Bay region contains the Pebble porphyry deposit, which is one of the largest, unmined porphyry Cu–Mo–Au deposits in the world (Olson and others, 2020; Kelley and others, 2013; Goldfarb and others, 2013). Other porphyry systems in the region are as young as a few million years old and formed during magmatic-hydrothermal activity related to the Aleutian magmatic arc (Kreiner and others, 2021). In addition, the region contains volcanogenic seafloor systems (for example, Johnson Tract) and epithermal vein systems rich in precious and base metals (for example, Apollo) (Kreiner and Jones, 2020). Formation of porphyry deposits into the Holocene suggests the potential for active magmatic hydrothermal vents and the active formation of sulfide-bearing mineral deposits offshore.

A reconnaissance survey of sediments in Bristol Bay, collected using auger borings and shovels, noted small amounts of titaniferous magnetite, as well as “traces of flour gold” on Egegik beach (Berryhill, 1963; Mason and Arndt, 1996). Along the Alaska Peninsula, there are abundant records of offshore gold especially along the southern coasts and Kodiak Island (Mason and Arndt, 1996) although at most locations known mineralization is not of economic grades or tonnages. In the coastal zone, there is historical reference to mining gold in 1904 and 1905 from the beaches of Popof Island, and titaniferous magnetite and ilmenite is reported

at several points on the north shore, from Moffett Point (on Adak Island, [fig. 8](#)) to Port Heiden ([fig. 13](#)) (Cobb, 1973). Unga Island is adjacent to Popof Island ([fig. 14](#)) and contains the Apollo–Sitka and Shumagin epithermal gold deposits and related porphyry-style mineralization. These mines produced mainly Au and Ag and minor Cu, Pb, and Zn; the deposit formed as a result of hydrothermal circulation through andesite and dacite and has recently generated renewed work (Gustin and Weiss, 2018). Vein systems associated with the Unga and Apollo systems extend offshore (Gustin and Weiss, 2018), suggesting potential for the continuation into the marine environment. Cape Kubugakli, which is currently within Katmai National Park, also produced gold, lead, molybdenum, and antimony from placers. This entire region contains evidence of Mesozoic and Cenozoic arc magmatism, with known porphyry and epithermal style mineralization associated with the igneous arc rocks (Kreiner and others, 2021). Porphyry deposits are exposed close to tidewater at the Bee Creek prospect, Pyramid mine, and Warner Bay. Porphyry and associated epithermal mineralization are as young as 1.5 Ma (Kreiner and others, 2021) and exposures in some of the systems are in cliffs immediately on the coast, suggesting the potential for mineralization extending below sea level. In addition, the relatively young ages suggest that magmatic-hydrothermal systems continue to form in this active arc segment. Therefore, potential for systems having formed, or currently forming below sea level may be high.

Southern and Southeastern Alaska

Oceanographic and Geologic Setting

In the southern and southeastern Alaska region, we include coastal points from Kodiak Island and Prince William Sound through southeast Alaska ([figs. 15–17](#)). The region includes near coastal bodies north of the Gulf of Alaska, including Shelikof Strait and Cook Inlet. This entire region contains many narrow coastal waterways. The distance from land’s edge to the shelf break ranges from about 15 to 90 km; beyond the shelf break is the Gulf of Alaska. The Alaska Current and the Alaskan Stream transport surface water north and west along the coast and landward from the Alaskan Gyre. Along the eastern boundary of the Alaska Current, eddies occur that may result in temperature inversions and mix high productivity coastal waters with the high-nutrient, low-chlorophyll waters of the central Gulf of Alaska (Ladd and others, 2009). Climatically, the region is characterized by a temperate rain forest, with glaciation and high relief on the mountains along the Alaska–British Columbia, Canada, border, facilitating mineral transport.

Southeast Alaska and neighboring British Columbia are composed of a collage of terranes that have been accreted onto the western margin of North America. The Alaskan terranes include the Chugach, Wrangellia, Gravina, Admiralty, Craig,

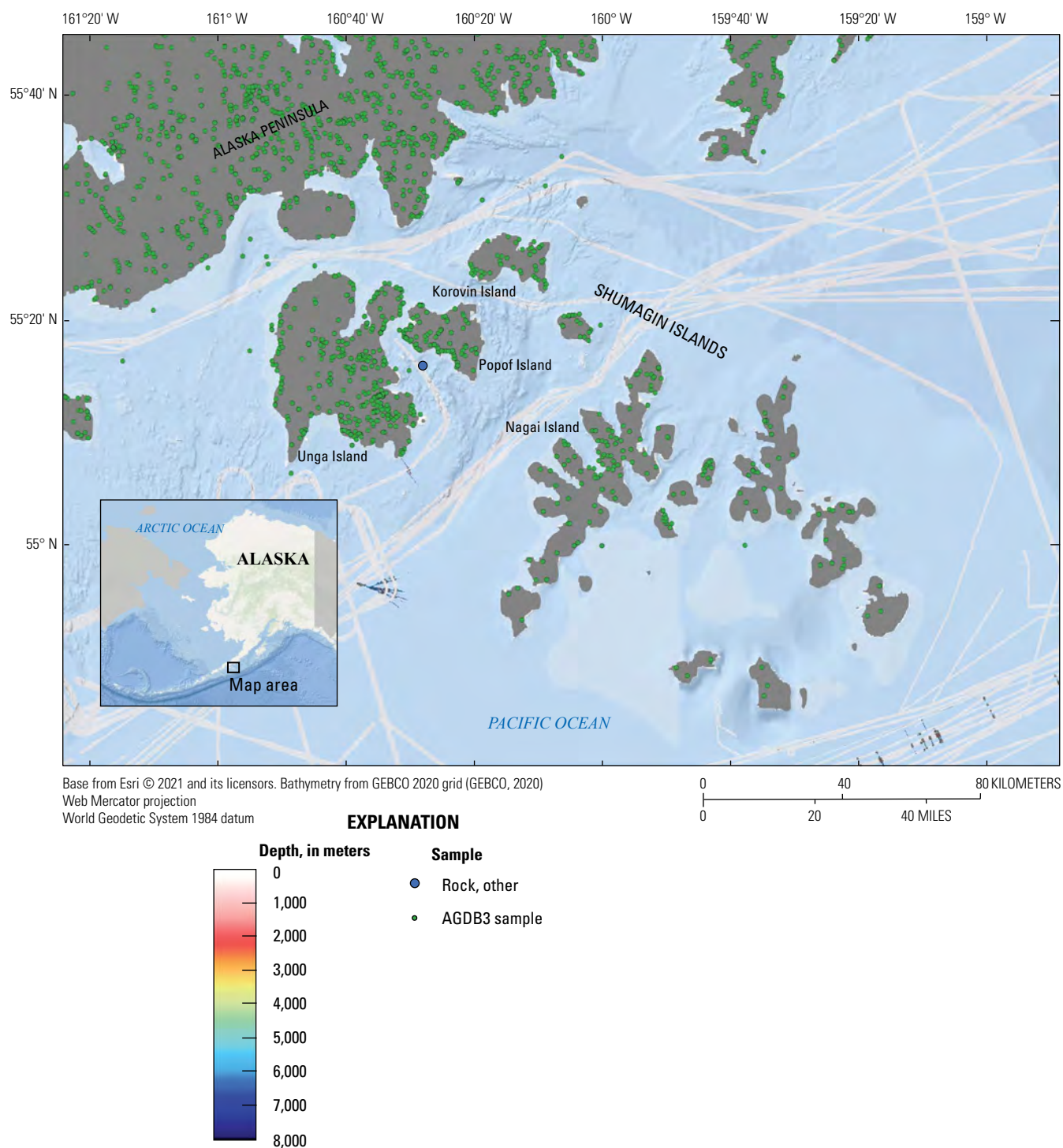


Figure 14. Map of Unga Island and some surrounding islands, off the southern coast of the Alaska Peninsula. Geologic sample locations from the Index to Marine and Lacustrine Geological Samples (IMLGS) (Curators of Marine and Lacustrine Geologic Sample Consortium, 1977) and the Alaska Geochemical Database, ver. 3.0 (AGDB3) (Granitto and others, 2019).

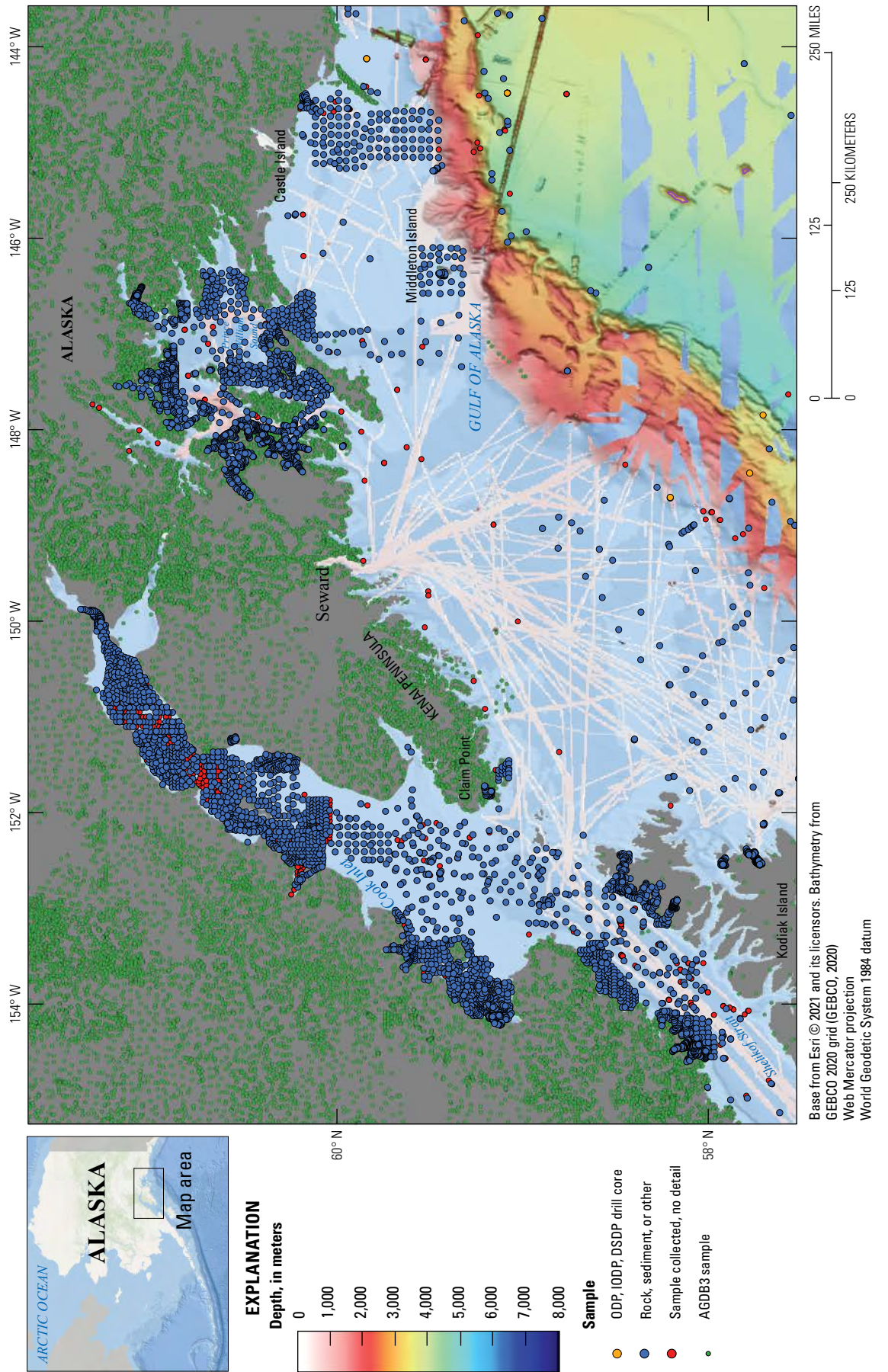


Figure 15. Map of Prince William Sound and Cook Inlet, Alaska. Geologic sample locations from the Index to Marine and Lacustrine Geological Samples (IMLGS) (Curators of Marine and Lacustrine Geologic Sample Consortium, 1977) and the Alaska Geochemical Database, ver. 3.0 (AGDB3) (Granitto and others, 2019). ODP, Ocean Drilling Program; IODP, Integrated Ocean Drilling Program; DSDP, Deep Sea Drilling Project.

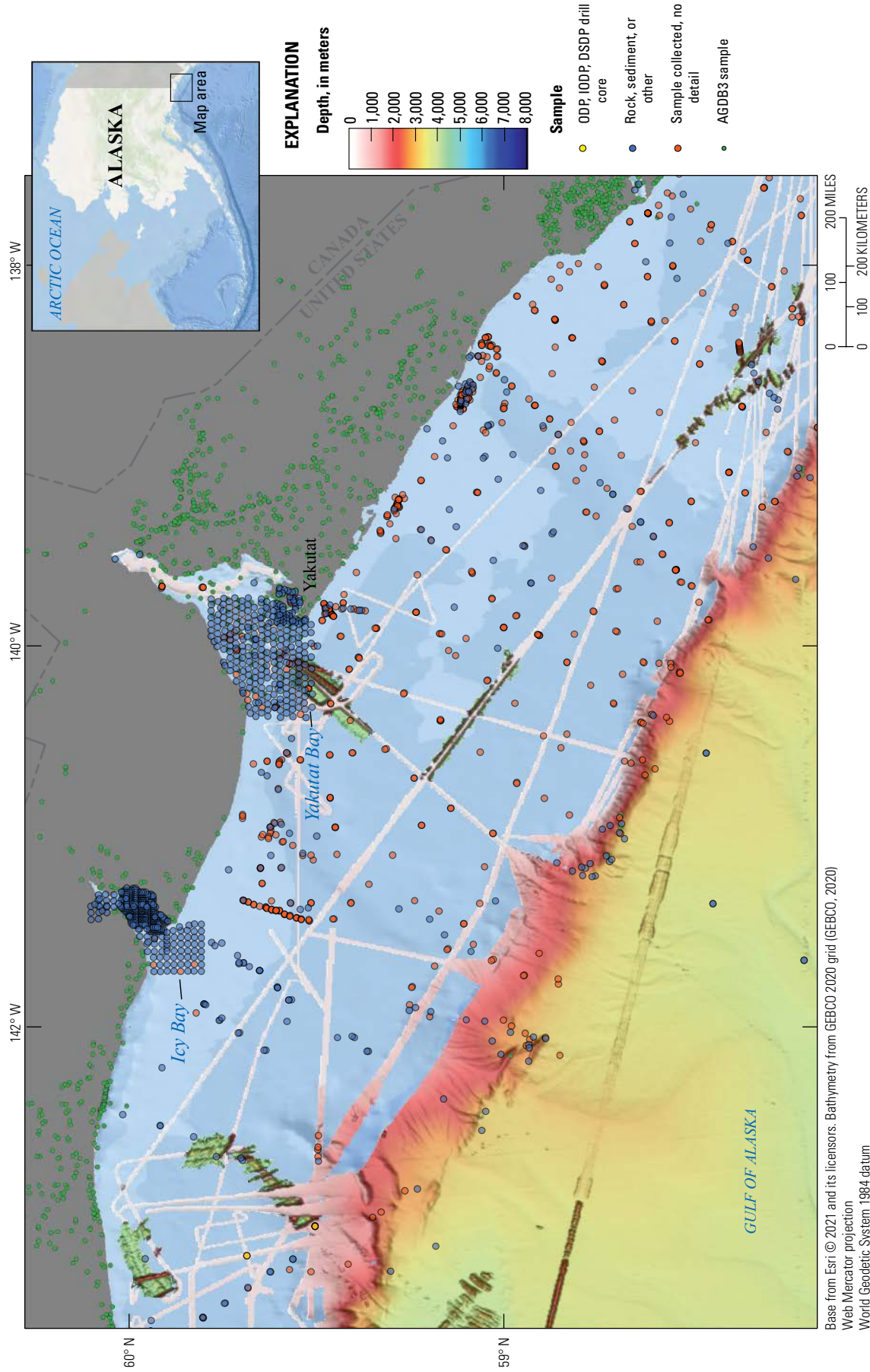


Figure 16. Map of Icy and Yakutat Bays, southeastern Alaska. Geologic sample locations from the Index to Marine and Lacustrine Geological Samples (IMLGS) (Curators of Marine and Lacustrine Geologic Sample Consortium, 1977) and the Alaska Geochemical Database, ver. 3.0 (AGDB3) (Granitto and others, 2019). ODP, Ocean Drilling Program; IODP, Integrated Ocean Drilling Program; DSDP, Deep Sea Drilling Project.

Yukon–Tanana/Taku, and Coast Mountains Batholith (Taylor and Johnson, 2010, [fig. 1](#); Goldfarb and others, 2016). The PAW superterrane oceanic arc, accreted during the Mesozoic, and the Chugach and Prince William forearc accretionary complex formed during the late Mesozoic (Graham and others, 2013); the terrains generally decrease in age moving seaward. In British Columbia, the predominant mineral deposits are Jurassic porphyry and related epithermal systems. Mineralization is largely Triassic and Jurassic and hosted in the Stikinia and Quesnellia terranes (Nelson and others, 2013). It is important to consider the mineral systems and potential in neighboring Canada, as transboundary watersheds transport eroded material from these systems across the international boundary. Therefore, deposits in Canada may be contributing components to possible placer occurrences along the coast of southeast Alaska.

Marine Mineral Occurrences

Because of the complex assemblage of disparate geologic terranes in southeast Alaska ([fig. 17](#)) and neighboring British Columbia, a variety of pre-, syn-, and post-accretionary mineral systems have been identified across the region. The most prominent are volcanogenic seafloor and orogenic gold mineral systems. These include the world-class volcanogenic deposits Greens Creek and Palmer, and orogenic gold systems in the Juneau gold belt (for example, Kensington). Several coastal or near coastal VMS deposits also occur in southern Alaska, including Midas, Threeman, Ellamar, Port Fidalgo, Rua Cove, and Beatson Leach (Shanks and Thurston, 2012), with metallic runoff from Threeman, Ellamar, and Beatson documented in Prince William Sound (Koski and others, 2008).

A very small gold beach placer was mined on Middleton Island ([fig. 15](#)) (Cobb, 1973). Claim Point on the Kenai Peninsula ([fig. 15](#); Foley and others, 1985) is one of only two deposits in Alaska from which chromite has been mined; the other is Red Mountain in the Goodnews Bay area. The Claim Point reef deposit is partially submerged, and further reserves are suggested to exist below sea level (Foley and others, 1985, [figs. 4, 5](#)).

In the Yakutat area of Alaska, a gold and heavy mineral deposit occurs in beach sands and historical coastal plains that are actively being eroded. The occurrence is termed the Icy Cape project and is owned and actively being explored by the Alaska Mental Health Trust ([fig. 16](#)). The deposit is hosted in a complex network of rivers draining the highlands into a deltaic environment on an inactive coastal plain. The

deposits occur within the finer sand layers deposited on the Yakataga Formation sandstones and siltstones and complexly interbedded with coarser cobbly sands with intercalated beach sands (Eden, 2018). In addition to gold, the sands contain heavy minerals consisting of zircon, ilmenite, garnet, and epidote-group minerals. Minor platinum-group metals have also been identified, but the extent and grades remain undetermined (Eden, 2018). The location of the deposits in the sands and deltaic environment at the tidal interface suggests the resource is likely extensive below the mean high tide line. Reworking of the modern deposits in the marine environment is also possible, which may result in additional concentrations below sea level.

Southeast Alaska has numerous mineral deposits, many of which are coastal as this area is composed of islands and shallow waterways. This region contains two of the five active hard rock mines in the State (Greens Creek, a VMS deposit, and Kensington, an orogenic gold deposit). In addition, two advanced stage exploration projects are also located in this part of the State. These prospects include the Palmer Cu-Pb-Zn VMS deposit within the Alexander Terrane near Haines and the Bokan Mountain peralkaline REE deposit near Ketchikan ([fig. 17](#)). Offshore mining of barite has occurred at Castle Island ([fig. 15](#)), and another high-grade barite lens is believed to exist offshore based on drilling results. This drilling indicated interbedded barite with schist and chert. This stratigraphic relationship suggests the lens was part of the Triassic Zarembo-Duncan Canal belt (Grybeck and others, 1984), with remaining offshore resources estimated to be 1 million metric tons (Mt) (Brew and others, 1991). Offshore mining occurred at water depths as great as 50 m (Grybeck and others, 1984), and total extraction was approximately 0.76 Mt, occurring between 1966 and 1980 (https://mrdata.usgs.gov/ardf/show-ardf.php?ardf_num=PE026).

Numerous small coastal porphyry molybdenum deposits occur, some of which may potentially extend offshore; such locations include Forrester Island (Clark and others, 1971), Baker Island, and Suemez Island ([fig. 17](#); Brew, 1991). This region contains extensive gold vein deposits that may also have enrichments of antimony, arsenic, and tungsten along the Juneau gold belt (Haeussler and others, 1995). These deposits occur near tidewater and additional resources may be located below sea level. The southeast Alaska region, in part due to the complex geology, is a metal-rich archipelago. As a result, significant potential exists for terrestrial resources to extend below sea level or for the occurrence of undiscovered deposits in the coastal environment.

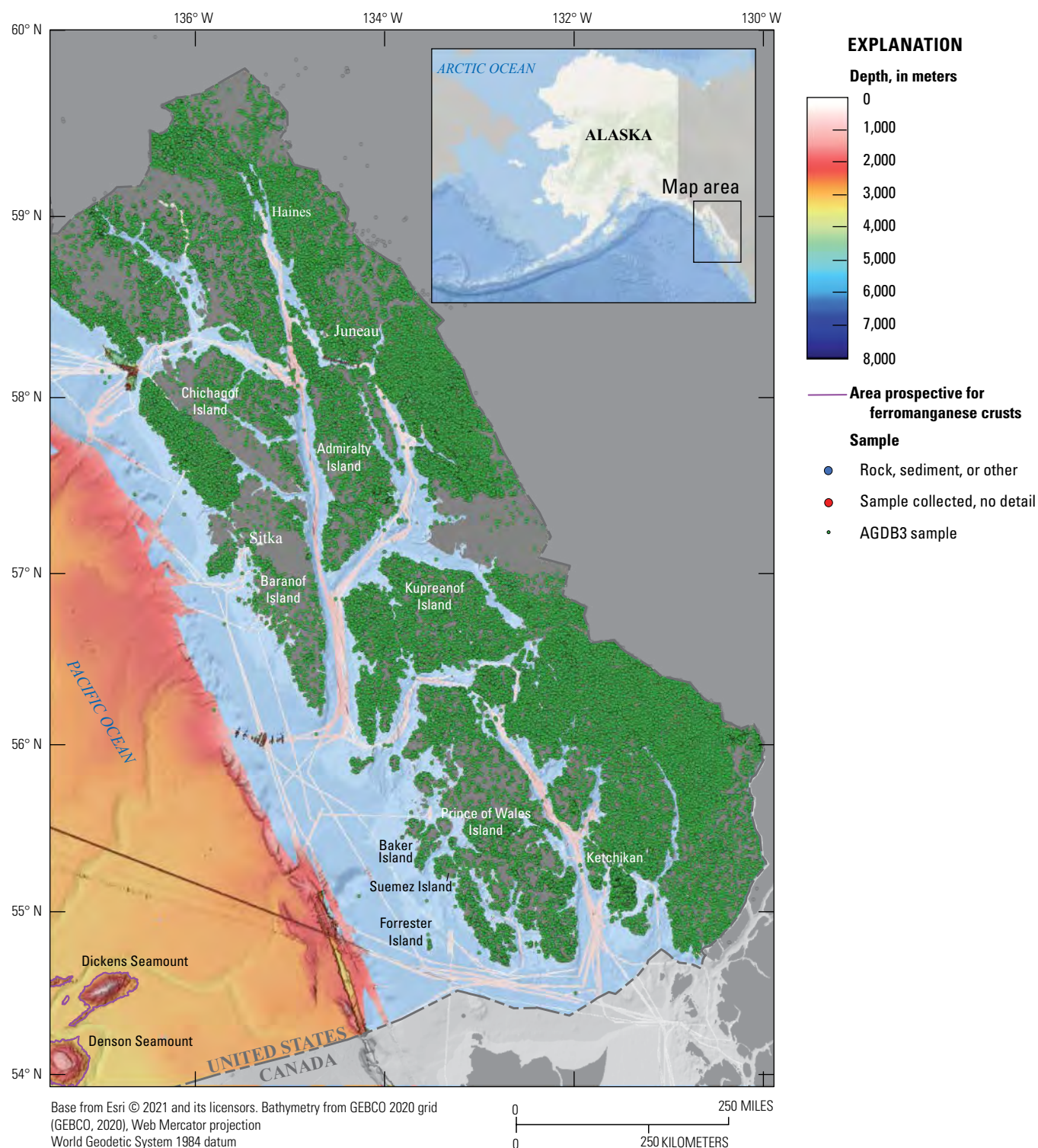


Figure 17. Map of southeast Alaska. Geologic sample locations from the Index to Marine and Lacustrine Geological Samples (IMLGS) (Curators of Marine and Lacustrine Geologic Sample Consortium, 1977) and the Alaska Geochemical Database, ver. 3.0 (AGDB3) (Granitto and others, 2019). The magenta regions in the southwestern corner of the map are seamounts prospective for ferromanganese crusts in the Gulf of Alaska region (fig. 4).

Summary

This data review of the Alaska coastal and ocean region, including the Outer Continental Shelf and adjacent deep-ocean regions, reveals marine mineral occurrences in a variety of settings. Ferromanganese crusts have been recovered from seamounts in the Gulf of Alaska in the North Pacific Ocean, as well as the Chukchi Borderland in the Arctic Ocean to the north of Alaska. The presence of ferromanganese crusts in these areas indicates that most seamounts, plateaus, and other seafloor edifices in these two regions are prospective for ferromanganese crusts. Manganese nodules have not been recovered from any of the Alaska offshore regions reviewed here, and oceanographic and geologic criteria suggest that the Canada Basin meets some, but not all, of the prospective criteria for the formation of abyssal-plain-type manganese nodules.

The Aleutian Arc is prospective for hydrothermal marine minerals as an active arc setting; however, no marine hydrothermal activity has been identified, nor have associated hydrothermal minerals been recovered along its extent within the U.S. EEZ. Volcanic cones have been identified in extensional basins within the Aleutian Arc, and sea going research could reveal whether any volcanic cones host active hydrothermal emissions or associated mineralization.

The well-studied nearshore regions of Alaska contain placer deposits, such as gold in Norton Sound sourced from the Seward Peninsula and chromite and platinum-group elements in Goodnews Bay sourced from the Red Mountain mafic-ultramafic sequence. Shoreline placer deposits are also being actively explored around Yakutat Bay. Porphyry-type mineralization also occurs in coastal and nearshore regions of Alaska, especially in Bristol Bay and southeast Alaska.

While tens of thousands of marine geologic samples were reviewed in this study, including hundreds of marine mineral samples, the enormous areas involved leave many data gaps in the deep-ocean regions. To ground truth and refine prospective regions and better understand the distribution of critical minerals within these occurrences, further samples and geochemical data are required. Additional ship-based geophysics could better define subseafloor structural geology. Further refinement of areas within prospective regions and comparison with available environmental datasets may also reveal additional data needs related to environmental characterization and mineral-associated ecosystems.

References Cited

- Addy, S.K., 1978, Distribution of Fe, Mn, Cu, Ni and Co in coexisting manganese nodules and micronodules: *Marine Geology*, v. 28, nos. 1–2, p. M9–M17, [https://doi.org/10.1016/0025-3227\(78\)90089-0](https://doi.org/10.1016/0025-3227(78)90089-0).
- Addy, S.K., 1979, Rare earth elements pattern in manganese nodules and micronodules from northwest Atlantic: *Geochimica et Cosmochimica Acta*, v. 43, no. 7, p. 1105–1115, [https://doi.org/10.1016/0016-7037\(79\)90097-8](https://doi.org/10.1016/0016-7037(79)90097-8).
- Aguilar-Islas, A.M., Rember, R., Nishino, S., Kikuchi, T., and Itoh, M., 2013, Partitioning and lateral transport of iron to the Canada Basin: *Polar Science*, v. 7, no. 2, p. 82–99, <https://doi.org/10.1016/j.polar.2012.11.001>.
- Aiello, I.W., and Ravelo, A.C., 2012, Evolution of marine sedimentation in the Bering Sea since the Pliocene: *Geosphere*, v. 8, no. 6, <https://doi.org/10.1130/GES00710.1>.
- Arrigoni, V., 2008, Origin and Evolution of the Chukchi Borderland: College Station, Tex., Texas A&M University, M.S. thesis, 64 p., <https://oaktrust.library.tamu.edu/bitstream/handle/1969.1/ETD-TAMU-2008-12-120/ARRIGONI-THESIS.pdf?sequence=2>.
- Baco, A.R., 2007, Exploration for Deep-Sea Corals on North Pacific Seamounts and Islands: *Oceanography*, v. 20, no. 4, p. 108–117, <https://www.jstor.org/stable/24860153>.
- Baker, E., Gaill, F., Karageorgis, A.P., Lamarche, G., Narayanaswamy, B., Parr, J., Raharimananirina, C., Santos, R., Sharma, R., Tuhumwire, J., 2016, Offshore Mining Industries, chap. 23 of United Nations (U.N.), The first global integrated marine assessment—World ocean assessment I: United Nations, Department of Economic and Social Affairs, 34 p. [Also available at <https://www.un.org/regulatoryprocess/content/first-world-ocean-assessment>.]
- Barker, J.C., and Lamal, K., 1989, Offshore extension of platiniferous bedrock and associated sedimentation of the Goodnews Bay ultramafic complex Alaska: *Marine Mining*, v. 8, p. 365–390.
- Baturin, G.N., and Dubinchuk, V.G., 2011, The composition of ferromanganese nodules of the Chukchi and East Siberian Seas: *Doklady Earth Sciences*, v. 440, p. 1258–64, <https://doi.org/10.1134/S1028334X11090029>.
- Beinart, R.A., Gartman, A., Sanders, J.G., Luther, G.W., and Girguis, P.R., 2015, The uptake and excretion of partially oxidized sulfur expands the repertoire of energy resources metabolized by hydrothermal vent symbioses, *Proceedings of the Royal Society B, Biological Sciences: The Royal Society*, v. 282, no. 1806, <http://dx.doi.org/10.1098/rspb.2014.2811>.
- Bergfeld, D., Neal, T., McGimsey, G., Werner, C., Waythomas, C., Lewicki, J., Lopez, T., Mangan, M., Miller, T., Diefenbach, A., Schaefer, J., Coombs, M., Wang, B., Nicolaysen, K., Izbekov, P., Maharrey, Z., Huebner, M., Hunt, A., Fitzpatrick, J., and Freeburg, G., 2015, Aleutian Arc geothermal fluids—Chemical analyses of waters and gases: U.S. Geological Survey Data Releases, <https://doi.org/10.5066/F74X55VB>.
- Berryhill, R.V., 1963, Reconnaissance of beach sands, Bristol Bay, Alaska: U.S. Bureau of Mines Report of Investigations 6214, 48 p. [Also available at <https://dggs.alaska.gov/webpubs/usbm/ri/text/ri6214.pdf>.]

- Bird, K.J., Charpentier, R.R., Gautier, D.L., Houseknecht, D.W., Klett, T.R., Pitman, J.K., Moore, T.E., Schenk, C.J., Tennyson, M.E., and Wandrey, C.R., 2008, Circum-arctic resource appraisal—Estimates of undiscovered oil and gas north of the Arctic Circle: U.S. Geological Survey Fact Sheet 2008–3049, 4 p., <https://doi.org/10.3133/fs20083049>.
- Bird, M.L., and Clark, A.L., 1976, Microprobe study of olivine chromitites of the Goodnews Bay ultramafic complex, Alaska, and the occurrence of platinum: U.S. Geological Survey Journal of Research, January–February 1976, v. 4, no. 1, p. 717–725.
- Björk, G., Jakobsson, M., Rudels, B., Swift, J.H., Anderson, L., Darby, D.A., Backman, J., Coakley, B., Winsor, P., Polyak, L., and Edwards, M., 2007, Bathymetry and deep-water exchange across the central Lomonosov Ridge at 88–89°N: Deep-Sea Research Part I, Oceanographic Research Papers, v. 54, no. 8, p. 1197–1208, <https://doi.org/10.1016/j.dsr.2007.05.010>.
- Bluhm, B.A., MacDonald, I.R., Debenham, C., and Iken, K., 2005, Macro- and megabenthic communities in the high Arctic Canada Basin—Initial findings: Polar Biology, v. 28, p. 218–231, <https://doi.org/10.1007/s00300-004-0675-4>.
- Bogdanov, Y.A., Gurvich, E.G., Bogdanova, O.Y., Ivanov, G.V., Isaeva, A.B., Murav'ev, K.G., Gorshkov, A.I., and Dubinina, G.I., 1995, Ferromanganese nodules of the Kara Sea: Oceanology, English Translation, v. 34, no. 5, p. 722–732, <https://epic.awi.de/id/eprint/39753/1/pap18.pdf>. [Translation from Russian.]
- Boyd, P.W., Ellwood, M.J., Tagliabue, A., and Twining, B.S., 2017, Biotic and abiotic retention, recycling and remineralization of metals in the ocean: Nature Geoscience, v. 10, p. 167–173, <https://doi.org/10.1038/ngeo2876>.
- Brew, D.A., Drew, L.J., Schmidt, L.M., Root, D.H., and Huber, D.F., 1991, Undiscovered locatable mineral resources of the Tongass National Forest and adjacent areas, southeastern Alaska: U.S. Geological Survey Open-File Report 91–10, 370 p., 12 pl., <https://doi.org/10.3133/ofr9110>.
- Brown, Z.W., Casciotti, K.L., Pickart, R.S., Swift, J.H., and Arrigo, K.R., 2015, Aspects of the marine nitrogen cycle of the Chukchi Sea shelf and Canada Basin—Deep Sea Research Part II: Topical Studies in Oceanography, v. 118, Part A, p. 73–87, <https://doi.org/10.1016/j.dsr2.2015.02.009>.
- Brumley, K., Miller, E.L., Konstantinou, A., Grove, M., Meisling, K.E., and Mayer, L.A., 2015, First bedrock samples dredged from submarine outcrops in the Chukchi Borderland, Arctic Ocean: Geosphere, v. 11, no. 1, p. 76–92, <https://doi.org/10.1130/GES01044.1>.
- Buurman, H., Nye, C.J., West, M.E., and Cameron, C., 2014, Regional controls on volcano seismicity along the Aleutian arc: Geochemistry, Geophysics, Geosystems, v. 15, no. 4, p. 1147–1163, <https://doi.org/10.1002/2013GC005101>.
- Canadian Institute of Mining, Metallurgy and Petroleum [CIM], 2011, NI 43–101 Standards of disclosure for mineral projects: Montréal, Canada, Canadian Institute of Mining, Metallurgy and Petroleum, <https://mrmr.cim.org/media/1017/national-instrument-43–101.pdf>.
- Carey, S., 1958, A tectonic approach to continental drift, in Continental Drift—A Symposium on the present status of the continental drift hypothesis, Geology Department of the University of Tasmania, March, 1956: Hobart, Tasmania, Australia, University of Tasmania, p. 177–355. [Available from the University of Tasmania Library, call no. QE 511.5 .C37.]
- Cavalieri, D.J., and Parkinson, C.L., 2012, Arctic sea ice variability and trends, 1979–2010: The Cryosphere, v. 6, no. 4, p. 881–889, <http://doi.org/10.5194/tc-6-881-2012>.
- Chaytor, J.D., Keller, R.A., Duncan, R.A., and Dziak, R.P., 2007, Seamount morphology in the Bowie and Cobb hot spot trails, Gulf of Alaska: Geochemistry, Geophysics, Geosystems, v. 8, no. 9, p. 1–26, <https://doi.org/10.1029/2007GC001712>.
- Chian, D., Jackson, H.R., Hutchinson, D.R., Shimeld, J.W., Oakey, G.N., Lebedeva-Ivanova, N., Li, Q., Saltus, R.W., and Mosher, D.C., 2016, Distribution of crustal types in Canada Basin, Arctic Ocean: Tectonophysics, v. 691, Part A, p. 8–30, <https://doi.org/10.1016/j.tecto.2016.01.038>.
- Clague, D.A., Paduan, J.B., and Davis, A.S., 2009, Widespread strombolian eruptions of mid-ocean ridge basalt: Journal of Volcanology and Geothermal Research, v. 180, no. 2–4, p. 171–188, <https://doi.org/10.1016/j.jvolgeores.2008.08.007>.
- Clark, D.L., Whitman, R.R., Morgan, K.A., and Mackey, S.D., 1980, Stratigraphy and glacial-marine sediments of the Amerasian Basin, central Arctic Ocean: Geological Society of America, Special Paper 181, 57 p., ISBN 0-8137-2181-4.
- Clark, A.L., Berg, H.C., Grybeck, D., and Ovenshine, A.T., 1971, Reconnaissance geology and geochemistry of Forrester Island National Wildlife Refuge, Alaska: U.S. Geological Survey Open File Report 71–67, 9 p., 1 sheet, scale 63:360, <https://doi.org/10.3133/ofr7167>.
- Coachman, L.K., and Aagaard, K., 1988, Transports through Bering Strait—Annual and interannual variability: Journal of Geophysical Research, v. 93 no. C12, p. 15535–15539, <https://doi.org/10.1029/JC093iC12p15535>.
- Cobb, E.H., 1973, Placer deposits of Alaska: U.S. Geological Survey Bulletin 1374, 213 p., 1 pl., <https://doi.org/10.3133/b1374>.

- Comiso, J.C., Parkinson, C.L., Gertson, R., and Stock, L., 2008, Accelerated decline in the Arctic sea ice cover: *Geophysical Research Letters*, v. 35, no. 1, <http://doi.org/10.1029/2007GL031972>.
- Conrad, T., Hein, J.R., Paytan, A., and Clague, D.A., 2017, Formation of Fe-Mn crusts within a continental margin environment: *Ore Geology Reviews*, v. 87, p. 25–40, <http://doi.org/10.1016/j.oregeorev.2016.09.010>.
- Coombs, M.L., White, S.M., and Scholl, D.W., 2007, Massive edifice failures at Aleutian arc volcanoes: *Earth and Planetary Science Letters*, v. 256, nos. 3–4, p. 403–418, <https://doi.org/10.1016/j.epsl.2007.01.030>.
- Cronan, D.S., 1992, *Marine minerals in Exclusive Economic Zones*: London, Chapman & Hall, 224 p.
- Cui, Y., Liu, X., Liu, C., Gao, J., Fang, X., Liu, Y., Wang, W., and Li, Y., 2020, Mineralogy and geochemistry of ferromanganese oxide deposits from the Chukchi Sea in the Arctic Ocean: *Arctic, Antarctic, and Alpine Research*, v. 52, no. 1, p. 120–129, <https://doi.org/10.1080/15230430.2020.1738824>.
- Curators of Marine and Lacustrine Geological Samples Consortium, 1977, *Index to Marine and Lacustrine Geological Samples (IMLGS)*: National Oceanic and Atmospheric Administration [NOAA], National Centers for Environmental Information, <https://doi.org/10.7289/V5H41PB8>.
- Dalrymple, G.B., Clague, D.A., Vallier, T.L., and Menard, H.W., 1987, $^{40}\text{Ar}/^{39}\text{Ar}$ age, petrology and tectonic significance of some seamounts in the Gulf of Alaska, in Keating, B.H., Fryer, P., Batiza, R., and Boehlert, G.W., eds., *Seamounts, islands, and atolls*: American Geophysical Union, *Geophysical Monograph Series*, v. 43, p. 297–315, <https://doi.org/10.1029/GM043p0297>.
- Danovaro, R., Fanelli, E., Aguzzi, J., Billett, D., Carugati, L., Corinaldesi, C., Dell’Anno, A., Gjerde, K., Jamieson, A.J., Kark, S. and McClain, C., 2020, Ecological variables for developing a global deep-ocean monitoring and conservation strategy: *Nature Ecology & Evolution*, v. 4, no. 2, p. 181–192, <https://doi.org/10.1038/s41559-019-1091-z>.
- de Forges, B.R., Koslow, J.A., and Poore, G.C.B., 2000, Diversity and endemism of the benthic seamount fauna in the southwest Pacific: *Nature*, v. 405, p. 944–946.
- de Ronde, C.E.J., Massoth, G.J., Baker, E.T., and Lupton, J.E., 2003, Submarine hydrothermal venting related to volcanic arcs, in Simmons, S.F., and Graham, I., eds., *Volcanic, geochemical, and ore-forming fluids—Rulers and witnesses of processes within the Earth*: Society of Economic Geologists Special Publication 10, p. 91–110, <https://doi.org/10.5382/SP.10.06>.
- Desonie, D.L., and Duncan, R.A., 1990, The Cobb-Eikelberg seamount chain—Hotspot volcanism with mid-ocean ridge basalt affinity: American Geophysical Union, *Journal of Geophysical Research, Solid Earth*, v. 95, no. B8, p. 12697–12711, <https://doi.org/10.1029/JB095iB08p12697>.
- Døssing, A., Jackson, H.R., Matzka, J., Einarsson, I., Rasmussen, T.M., Olesen, A.V., and Brozena, J.M., 2013, On the origin of the Amerasia Basin and the high Arctic large igneous province—Results of new magnetic data: *Earth and Planetary Science Letters*, v. 363, p. 219–230, <https://doi.org/10.1016/j.epsl.2012.12.013>.
- Douglas, D.C., 2010, Arctic sea ice decline—Projected changes in timing and extent of sea ice in the Bering and Chukchi Seas: U.S. Geological Survey Open-File Report 2010–1176, 32 p.
- Dove, D., Polyak, L., and Coakley, B., 2014, Widespread, multi-source glacial erosion on the Chukchi margin, Arctic Ocean, in Jakobsson, M., Ingólfsson, Ó., Long, A.J., and Spielhagen, R.F., eds., *APEX II—Arctic Palaeoclimate and its extremes*: *Quaternary Science Reviews*, v. 92, p. 112–122, <https://doi.org/10.1016/j.quascirev.2013.07.016>.
- Drake, D.E., Cacchione, D.A., Muench, R.D., and Nelson, C.H., 1980, Sediment transport in Norton Sound, Alaska: *Marine Geology*, v. 36, nos. 1–2, p. 97–126, [https://doi.org/10.1016/0025-3227\(80\)90043-2](https://doi.org/10.1016/0025-3227(80)90043-2).
- Duliu, O.G., Alexe, V., Moutte, J., and Szobotca, S.A., 2009, Major and trace element distributions in manganese nodules and microneodules as well as abyssal clay from the Clarion-Clipperton abyssal plain, Northeast Pacific: *Geo-Marine Letters*, v. 29, p. 71–83, <https://doi.org/10.1007/s00367-008-0123-5>.
- Eden, K., 2018, More dirt—More work, Ice Cape gold and industrial heavy minerals project update, Alaska Miners Association Fall 2018 Convention, Anchorage, Alaska, Nov. 6–8, 2018: Alaska Miners Association, accessed December 10, 2020, at https://www.dropbox.com/s/mcx4to8hrpun0r15_Eden_More%20dirt%20more%20work%20Karsten%20Eden.pdf?dl=0.
- Embry, A.F., 1990, Geological and geophysical evidence in support of anticlockwise rotation of Northern Alaska: *Marine Geology*, v. 93, p. 317–329, [https://doi.org/10.1016/0025-3227\(90\)90090-7](https://doi.org/10.1016/0025-3227(90)90090-7).
- Field, M.E., Nelson, C.H., Cacchione, D.A., and Drake, D.E., 1981, Sand waves on an epicontinental shelf—Northern Bering Sea, in Nittrouer, C.A., ed., *Sedimentary dynamics of continental shelves*: Amsterdam, Elsevier, v. 32, p. 233–258, [https://doi.org/10.1016/S0070-4571\(08\)70301-7](https://doi.org/10.1016/S0070-4571(08)70301-7). [Reprinted from *Marine Geology*, v. 42, no. 1/4.]

- Foley, J.Y., Light, T.V., Nelson, S.W., and Harris, R.A., 1997, Mineral occurrences associated with mafic-ultramafic and related alkaline complexes in Alaska, *in* Schroeter, T.G., ed., Mineral deposits of Alaska: Society of Economic Geologists, Economic Geology Monogram, v. 9, p. 396–449, <https://doi.org/10.5382/Mono.09.14>.
- Foley, J.Y., Barker, J.C., and Brown, L.L., 1985, Critical and strategic minerals investigations in Alaska—Chromium: U.S. Bureau of Mines, Open-File Report 97–85, 54p., 1 sheet. [Available at <https://dggs.alaska.gov/pubs/id/21472>.]
- Fortier, S.M., Nassar, N.T., Lederer, G.W., Brainard, J., Gambogi, J., and McCullough, E.A., 2018, Draft critical mineral list—Summary of methodology and background information—U.S. Geological Survey technical input document in response to Secretarial Order No. 3359: U.S. Geological Survey Open-File Report 2018–1021, 15 p., <https://doi.org/10.3133/ofr20181021>.
- Frank, K.L., Rogers, K.L., Rogers, D.R., Johnston, D.T., and Girguis, P.R., 2015, Key factors influencing rates of heterotrophic sulfate reduction in active seafloor hydrothermal massive sulfide deposits: *Frontiers in Microbiology*, v. 6, p. 1449, <https://doi.org/10.3389/fmicb.2015.01449>.
- Franklin, J.M., Gibson, H.L., Jonasson, I.R., Galley, A.G., 2005, Volcanogenic massive sulfide deposits, *in* Hedenquist, J.W., Thompson, J.F.H., Goldfarb, R.J., and Richards, J.P., eds., One hundredth anniversary volume, Ore deposit types: *Economic Geology*, <https://doi.org/10.5382/AV100.17>.
- Freeman, L.K., Athey, J.E., Lasley, P.S., and Van Oss, E.J., 2015, Alaska's mineral industry 2014: Alaska Division of Geological and Geophysical Surveys Special Report 70, 60 p., <http://doi.org/10.14509/29515>.
- Frey, K.E., Moore, G.W.K., Cooper, L.W., and Grebmeier, J.M., 2015, Divergent patterns of recent sea ice cover across the Bering, Chukchi, and Beaufort Seas of the Pacific Arctic Region, *in* Moore, S.E., and Stabeno, P.J., eds., Synthesis of Arctic research (SOAR): Progress in Oceanography, v. 136, p. 32–49, <https://doi.org/10.1016/j.pocean.2015.05.009>.
- Galley, A., Hannington, M., Jonasson, I., 2007, Volcanogenic massive sulphide deposits, *in* Goodfellow, W.D., ed., Mineral deposits of Canada—A synthesis of major deposit-types, district metallogeny, the evolution of geological provinces, and exploration methods: Geological Association of Canada, Mineral Deposits Division, Special Publication no. 5, p. 141–161, <https://silverspruceresources.com/site/assets/files/5585/vms-deposits-canada-review.pdf>.
- General Bathymetric Chart of the Oceans [GEBCO], 2020, GEBCO 2020 grid—A continuous terrain model of the global oceans and land: Liverpool, U.K., British Oceanographic Data Centre, National Oceanography Centre, NERC, <https://doi.org/10.5285/a29c5465-b138-234d-e053-6c86abc040b9>.
- Geist, E.L., Childs, J.R., and Scholl, D.W., 1987, The evolution and petroleum geology of Amlia and Amukta intra-arc basins Aleutian Ridge: *Marine and Petroleum Geology*, v. 4, no. 4, p. 334–352, [https://doi.org/10.1016/0264-8172\(87\)90011-0](https://doi.org/10.1016/0264-8172(87)90011-0).
- Geist, E.L., Childs, J.R., and Scholl, D.W., 1988, The origin of summit basins of the Aleutian Ridge—Implications for block rotation of an arc massif: *American Geophysical Union, Tectonics*, v. 7, no. 2, p. 327–341, <https://doi.org/10.1029/TC007i002p00327>.
- Gladenkov, A.Y., Oleinik, A.E., Marincovich, L., Jr., and Barinov, K.B., 2002, A refined age for the earliest opening of Bering Strait: *Palaeogeography, Palaeoclimatology, Palaeoecology*, v. 183, nos. 3–4, p. 321–328, [https://doi.org/10.1016/S0031-0182\(02\)00249-3](https://doi.org/10.1016/S0031-0182(02)00249-3).
- Glasby, G.P., Stoffers, P., Sioulas, A., Thijssen, T., and Friedrich, G., 1982, Manganese nodule formation in the Pacific Ocean—A general theory: *Geo-Marine Letters*, v. 2, no. 47, p. 47–53, <https://doi.org/10.1007/BF02462799>.
- Glasby, G.P., Cherkashov, G.A., Gavrilenko, G.M., Rashidov, V.A., and Slovtsov, I.B., 2006, Submarine hydrothermal activity and mineralization on the Kurile and western Aleutian island arcs, N.W. Pacific: *Marine Geology*, v. 231, nos. 1–4, p. 163–180, <https://doi.org/10.1016/j.margeo.2006.06.003>.
- Goldfarb, R.J., Anderson, E.D., and Hart, C.J.R., 2013, Tectonic setting of the Pebble and other copper-gold-molybdenum porphyry deposits within the evolving middle Cretaceous continental margin of northwestern North America: *Economic Geology*, v. 108, no. 3, p. 405–419, <https://doi.org/10.2113/econgeo.108.3.405>.
- Goldfarb, R.J., Meighan, C., Meinert, L., and Wilson, F.H., 2016, Mineral deposits and metallogeny, chap. 1 *of* Rognvald, B., Bjerkgård, T., Nordahl, B., and Schiellerup, H., eds., Mineral resources in the Arctic: Trondheim, Norway, Geological Survey of Norway Special Publication, 484 p. [Available at <https://www.ngu.no/en/publikasjon/mineral-resources-arctic>.]

- Gollner, S., Kaiser, S., Menzel, L., Jones, D.O.B., Brown, A., Mestre, N.C., van Oevelen, D., Menot, L., Colaço, A., Canals, M., Cuvelier, D., Durden, J.M., Gebruk, A., Eghe, G.A., Haeckel, M., Marcon, Y., Mevenkamp, L., Morato, T., Pham, C.K., Purser, A., Sanchez-Vidal, A., Vanreusel, A., Vink, A., and Martinez Arbizu, P., 2017, Resilience of benthic deep-sea fauna to mining activities: *Marine Environmental Research*, v. 129, p. 76–101, <https://doi.org/10.1016/j.marenvres.2017.04.010>.
- Gottlieb, E.S., Meisling, K.E., Miller, E.L., and Mull, C.G., 2014, Closing the Canada Basin—Detrital zircon geochronology relationships between the North Slope of Arctic Alaska and the Franklinian mobile belt of Arctic Canada: *Geosphere*, v. 10, no. 6, p. 1366–1384, <https://doi.org/10.1130/GES01027.1>.
- Graham, G.E., Goldfarb, R.J., Miller, M., Gibler, K., and Roberts, M., 2013, Tectonic evolution and cretaceous gold metallogenesis of southwestern Alaska, chap. 5 of Colpron, M., Bissig, T., Rusk, B.G., and Thompson, J.F.H., eds., *Tectonics, metallogeny, and discovery—The North American cordillera and similar accretionary settings*: Society of Economic Geologists Special Publication no. 17, p. 169–200, <https://doi.org/10.5382/SP.17.05>.
- Granitto, M., Wang, B., Shew, N.B., Karl, S.M., Labay, K.A., Weldon, M.B., Seitz, S.S., and Hoppe, J.E., 2019, Alaska geochemical database version 3.0 (AGDB3)—Including “best value” data compilations for rock, sediment, soil, mineral, and concentrate sample media: U.S. Geological Survey Data Series 1117, 33 p., <https://doi.org/10.3133/ds1117>.
- Grantz, A., 1993, Cruise to the Chukchi Borderland, Arctic Ocean, 1992 Arctic summer west scientific party: *Eos*, v. 74, no. 22, p. 249–254, <https://doi.org/10.1029/93EO00273>.
- Grantz, A., Clark, D.L., Phillips, R.L., Srivastava, S.P., Blome, C.D., Gray, L.B., Haga, H., Mamet, B.L., McIntyre, D.J., McNeil, D.H., Mickey, M.B., Mullen, M.W., Murchey, B.I., Ross, C.A., Stevens, C.H., Silberling, N.J., Wall, J.H., and Willard, D.A., 1998, Phanerozoic stratigraphy of Northwind Ridge, magnetic anomalies in the Canada basin, and the geometry and timing of rifting in the Amerasia basin, Arctic Ocean: *Geological Society of America Bulletin*, v. 110, no. 6, p. 801–820, [https://doi.org/10.1130/0016-7606\(1998\)110%3C0801:PSONRM%3E2.3.CO;2](https://doi.org/10.1130/0016-7606(1998)110%3C0801:PSONRM%3E2.3.CO;2).
- Grantz, A., Eittreim, S., and Dinter, D.A., 1979, Geology and tectonic development of the continental margin north of Alaska, in Keen, C.E., ed., *Crustal properties across passive margins: Tectonophysics*, v. 15, p. 263–291, <https://doi.org/10.1016/B978-0-444-41851-7.50019-4>.
- Grantz, A., and Hart, P.E., 2012, Petroleum prospectivity of the Canada Basin, Arctic Ocean: *Marine and Petroleum Geology*, v. 30, no. 1, p. 126–143, <https://doi.org/10.1016/j.marpetgeo.2011.11.001>.
- Grantz, A., Hart, P.E., and Childers, V.A., 2011, Geology and tectonic development of the Amerasia and Canada basins, Arctic Ocean, chap. 50 of Spencer, A.M., Embry, A.F., Gautier, D.L., Stoupakova, A.V., Sørensen, K., eds., *Arctic petroleum geology*: London, Geological Society Memoirs, v. 35, p. 771–799, <http://dx.doi.org/10.1144/M35.50>.
- Grantz, A., May, S.D., Taylor, P.T., and Lawver, L.A., 1990, Canada basin, in Grantz, A., Johnson, G.L., and Sweeney, J.F., eds., *The Arctic Ocean Region*, v. L of *The geology of North America*: Boulder, Colo., Geological Society of America, p. 379–402, <https://doi.org/10.1130/DNAG-GNA-L.379>.
- Grybeck, D.J., Berg, H.C., and Karl, S.M., 1984, Map and description of the mineral deposits in the Petersburg and eastern Port Alexander quadrangles, southeastern Alaska: U.S. Geological Survey Open-File Report 84–837, 87 p., 1 sheet, scale 1:250,000, <https://doi.org/10.3133/ofr84837>.
- Gustin, M.M., and Wiess, S.I., 2018, NI [Canadian National Instrument] 43–101 technical report on the Unga project, southwest Alaska, USA: Vancouver, B.C., Canada, Redstar Gold Corp. [now Heliostar Metals], prepared by Mine Development Associates, 151 p., http://www.mda.com/Portals/0/MDA/Reports/Unga_TechRpt_2018.pdf.
- Haeussler, P.J., Bradley, D., Goldfarb, R., Snee, L., Taylor, C., 1995, Link between ridge subduction and gold mineralization in southern Alaska: *Geology*, v. 23, p. 995–998, [https://doi.org/10.1130/0091-7613\(1995\)023%3C0995:LBRSA%3E2.3.CO;2](https://doi.org/10.1130/0091-7613(1995)023%3C0995:LBRSA%3E2.3.CO;2).
- Halgedahl, S., and Jarrard, R., 1987, Paleomagnetism of the Kupaaruk River formation from oriented drill core—Evidence for rotation of the arctic Alaska plate, in Tailleux, I., Weimer, P., eds., *Alaskan north slope geology: Pacific section*: Society for Sedimentary Geology (SEPM), p. 581–617, https://archives.datapages.com/data/pac_sepm/066/066001/pdfs/581.htm.
- Hamilton, E.L., 1967, Marine geology of abyssal plains in the Gulf of Alaska: *Journal of Geophysical Research*, v. 72, no. 16, p. 4189–4213, <https://doi.org/10.1029/JZ072i016p04189>.
- Hannington, M.D., de Ronde, C.E.J., and Petersen, S., 2005, Sea-floor tectonics and submarine hydrothermal systems, in Hedenquist, J.W., Thompson, J.F.H., Goldfarb, R.J., and Richards, J.P., eds., *One hundredth anniversary volume, Earth environments and processes*: Society of Economic Geologists, *Economic Geology*, p. 111–141, <https://doi.org/10.5382/AV100.06>.

- Hannington, M.D., Jamieson, J., Monecke, T., and Petersen, S., 2010, Modern sea-floor massive sulfides and base metal resources—Toward a global estimate of sea-floor massive sulfide potential, *in* Goldfarb, R.J., Marsh, E.E., and Monecke, T., eds., *The challenge of finding new mineral resources—Global metallogeny, innovative exploration, and new discoveries*, Volume 2—Zinc-lead, nickel-copper-PGE, and uranium: Society of Economic Geologists Special Publication, v. 15, p. 317–338, <http://oceanrep.geomar.de/id/eprint/9967>.
- Hannington, M.D., Petersen, S., and Krätschell, A., 2017, Sub-sea mining moves closer to shore: *Nature Geoscience*, v. 10, p. 158–159, <https://doi.org/10.1038/ngeo2897>.
- Hein, J.R., Clague, D.R., Koski, R.A., Embley, R.W., and Dunham, R.E., 2008, Metalliferous sediment and a silica-hematite deposit within the Blanco Fracture Zone, Northeast Pacific: *Marine Georesources and Geotechnology*, v. 26, no. 4, p. 317–339, <https://doi.org/10.1080/10641190802430986>.
- Hein, J.R., Conrad, T.A., and Dunham, R.E., 2009, Seamount characteristics and mine-site model applied to exploration- and mining-lease-block selection for cobalt-rich ferromanganese crusts: *Marine Georesources & Geotechnology*, v. 27, no. 2, p. 160–176, <https://doi.org/10.1080/10641190902852485>.
- Hein, J.R., Conrad, T., Mizell, K., Banakar, V.K., Frey, F.A., and Sager, W.W., 2016, Controls on ferromanganese crust composition and reconnaissance resource potential, Ninetyeast Ridge, Indian Ocean: *Deep Sea Research Part I—Oceanographic Research Papers*, v. 110, 19 p., <https://doi.org/10.1016/j.dsr.2015.11.006>.
- Hein, J.R., Konstantinova, N., Mikesell, M., Mizell, K., Fitzsimmons, J.N., Lam, P.J., Jensen, L.T., Xiang, Y., Gartman, A., Cherkashov, G., Hutchinson, D.R., and Till, C.P., 2017, Arctic deep water ferromanganese-oxide deposits reflect the unique characteristics of the Arctic Ocean: *Geochemistry, Geophysics, Geosystems*, v. 18, no. 11, p. 3771–3800, <https://doi.org/10.1002/2017GC007186>.
- Hein, J.R., and Koschinsky, A., 2014, Deep-ocean ferromanganese crusts and nodules, *in* Scott, S.D., ed., *Treatise on geochemistry*, Volume 13—Geochemistry of mineral deposits (2d ed.): Amsterdam, v Elsevier, v. 13, p. 273–291, <https://doi.org/10.1016/B978-0-08-095975-7.01111-6>.
- Hein, J.R., Koschinsky, A., Bau, M., Manheim, F.T., Kang, J.-K., and Roberts, L., 2000, Cobalt-rich ferromanganese crusts in the Pacific, chap. 9 *of* Cronan, D.S., ed., *Handbook of marine mineral deposits*: Boca Raton, Fla., CRC Press, p. 239–279, <https://doi.org/10.1201/9780203752760>.
- Hein, J.R., Koschinsky, A., Halbach, P., Manheim, F.T., Bau, M., Kang, J.K., and Lubick, N., 1997, Iron and manganese oxide mineralization in the Pacific: London, Geological Society of London, Special Publication, v. 119, no. 1, p. 123–138.
- Hein, J.R., Koschinsky, A., and Kuhn, T., 2020, Deep-ocean polymetallic nodules as a resource for critical materials: *Nature Reviews Earth and Environment*, v. 1, p. 158–169, <https://doi.org/10.1038/s43017-020-0027-0>.
- Hein, J.R., Madureira, P., Bebianno, M.J., Colaço, A., Pinheiro, L.M., Roth, R., Singh, P., Strati, A., and Tuhumwire, J.T., 2021, Changes in seabed mining, chap. 18 *of* United Nations (U.N.), *The second world ocean assessment—World Ocean assessment II: United Nations, Department of Economic and Social Affairs*, v. II, p. 257–277 [Also available at <https://sdgs.un.org/publications/launch-second-world-ocean-assessment-woa-ii-volume-ii-32885>.]
- Hein, J.R., Scholl, D.W., and Miller, J., 1978, Episodes of Aleutian Ridge explosive volcanism: *Science*, v. 199, no. 4325, p. 137–141, <https://doi.org/10.1126/science.199.4325.137>.
- Hegewald, A., and Jokat, W., 2013, Tectonic and sedimentary structures in the northern Chukchi region, Arctic Ocean: *Journal of Geophysical Research, Solid Earth*, v. 118, p. 3285–3296, <https://doi.org/10.1002/jgrb.50282>.
- Heller, C., Kuhn, T., Versteegh, G.J.M., Wegorzewski, A.V., and Kasten, S., 2018, The geochemical behavior of metals during early diagenetic alteration of buried manganese nodules: *Deep Sea Research Part I, Oceanographic Research Papers*, v. 142, p. 16–33, <https://doi.org/10.1016/j.dsr.2018.09.008>.
- Herman, Y., 1970, Arctic paleo-oceanography in late Cenozoic time: *Science*, v. 169, no. 3944, p. 474–477, <https://doi.org/10.1126/science.169.3944.474>.
- Herman, Y., Grazzini, C.V., and Hooper, C., 1971, Arctic paleotemperatures in late Cenozoic time: *Nature*, v. 232., p. 466–469, <https://doi.org/10.1038/232466a0>.
- Hill, V., and Cota, G., 2005, Spatial patterns of primary production on the shelf, slope and basin of the Western Arctic in 2002: *Deep Sea Research Part II, Topical Studies in Oceanography*, v. 52, no. 24–26, p. 3344–3354, <https://doi.org/10.1016/j.dsr2.2005.10.001>.
- Hoare, J.M., and Cobb, E.H., 1977, Mineral occurrences (other than mineral fuels and construction materials) in the Bethel, Goodnews, and Russian Mission quadrangles, Alaska: U.S. Geological Survey Open-File Report 77–156, 98 p., <https://doi.org/10.3133/ofr77156>.

- Hofstra, A.H., and Kreiner, D.C., 2020, Systems-deposits-commodities-critical minerals table for the Earth Mapping Resources Initiative (ver. 1.1, May 2021): U.S. Geological Survey Open-File Report 2020–1042, 26 p., <https://doi.org/10.3133/ofr20201042>.
- Holmes, M.L., and Creager, J.S., 1974, Holocene history of the Laptev Sea continental shelf, chap. 9 of Herman, Y., ed., Marine geology and oceanography of the Arctic Seas: New York, Springer-Verlag, https://doi.org/10.1007/978-3-642-87411-6_9.
- Hunkins, K.L., and others, 1971, The late Cenozoic history of the Arctic Ocean, in Turekian, K.K., ed., The Late Cenozoic glacial ages: New Haven, Conn., Yale University Press, p. 215–237.
- Huntington, H.P., Danielson, S.L., Wiese, F.K., Baker, M., Boveng, P., Citta, J.J., de Robertis, A., Dickson, D.M.S., Farley, E., George, J.C., Iken, K., Kimmel, D.G., Kuletz, K., Ladd, C., Levine, R., Quakenbush, L., Stabeno, P., Stafford, K.M., Stockwell, D., and Wilson, C., 2020, Evidence suggests potential transformation of the Pacific Arctic ecosystem is underway: Nature Climate Change, v. 10, p. 342–348, <https://doi.org/10.1038/s41558-020-0695-2>.
- Huston, D.L., Pehrsson, S., Eglington, B.M., and Zaw, K., 2010, The geology and metallogeny of volcanic-hosted massive sulfide deposits—Variations through geologic time and with tectonic setting: Economic Geology, v. 105, no. 3, p. 571–591, <https://doi.org/10.2113/gsecongeo.105.3.571>.
- Hutchinson, D.R., Jackson, H.R., Houseknecht, D.W., Li, Q., Shimeld, J.W., Mosher, D., Chian, D., Saltus, R.W., Oakey, G.N., 2017, Significance of northeast-trending features in Canada basin, Arctic Ocean: Geochemistry, Geophysics, Geosystems, v. 18, no. 11, p. 4156–4178, <https://doi.org/10.1002/2017GC007099>.
- Ilhan, I., and Coakley, B.J., 2018, Meso–Cenozoic evolution of the southwestern Chukchi Borderland, Arctic Ocean: Marine and Petroleum Geology, v. 95, p. 100–109, <https://doi.org/10.1016/j.marpetgeo.2018.04.014>.
- Inman, D.L., and Nordstrom, C.E., 1971, On the tectonic and morphologic classification of coasts: The Journal of Geology, v. 79, no. 1, p. 1–21, <https://www.journals.uchicago.edu/doi/pdf/10.1086/627583>.
- International Seabed Authority [ISA], 2010, A geological model of polymetallic nodule deposits in the Clarion-Clipperton fracture zone: Kingston, Jamaica, International Seabed Authority, 105 p.
- InterRidge, 2020, InterRidge vents database, ver. 3.4—Kagamil Island: Seoul, Korea [rotating chair], InterRidge, International Cooperation in Ocean Floor Studies, accessed March 2020, at <https://vents-data.interridge.org/ventfield/kagamil-island>.
- Jakobsson, M., 2002, Hypsometry and volume of the Arctic Ocean and its constituent seas: Geochemistry, Geophysics, Geosystems, v. 3, no. 5, <https://doi.org/10.1029/2001GC000302>.
- Jakobsson, M., Backman, J., Rudels, B., Nycander, J., Frank, M., Mayer, L., Jokat, W., Sangiorgi, F., O'Regan, M., Brinkhuis, H., and Moran, K., 2007, The early Miocene onset of a ventilated circulation regime in the Arctic Ocean: Nature, v. 447, p. 986–990, <https://doi.org/10.1038/nature05924>.
- Jakobsson, M., Cherkis, N.Z., Woodward, J., Macnab, R., and Coakley, B., 2000, A new grid of Arctic bathymetry aids scientists and mapmakers: Eos, Transactions, v. 81, no. 9, p. 89, 93, 96 <https://doi.org/10.1029/00EO00059>.
- Jakobsson, M., Gardner, J.V., Vogt, P.R., Mayer, L.A., Armstrong, A., Backman, J., Brennan, R., Calder, B., Hall, J.K., and Kraft, B., 2005, Multibeam bathymetric and sediment profiler evidence for ice grounding on the Chukchi Borderland, Arctic Ocean: Quaternary Research, v. 63, p. 150–160, <https://doi.org/10.1016/j.yqres.2004.12.004>.
- Jamieson, J., and Gartman, A., 2020, Defining active, inactive, and extinct seafloor massive sulfide deposits: Marine Policy, v. 117, <https://doi.org/10.1016/j.marpol.2020.103926>.
- John, D.A., Ayuso, R.A., Barton, M.D., Blakely, R.J., Bodnar, R.J., Dilles, J.H., Gray, F., Graybeal, F.T., Mars, J.C., McPhee, D.K., Seal, R.R., Taylor, R.D., and Vikre, P.G., 2010, Porphyry copper deposit model, chap. B of Mineral deposit models for resource assessment: U.S. Geological Survey Scientific Investigations Report 2010–5070-B, 169 p., <https://doi.org/10.3133/sir20105070B>.
- Jones, E.P., Rudels, B., and Anderson, L.G., 1995, Deep waters of the Arctic Ocean—Origins and circulation: Deep-Sea Research Part I, Oceanographic Research Papers, v. 42, no. 5, p. 737–760, [https://doi.org/10.1016/0967-0637\(95\)00013-V](https://doi.org/10.1016/0967-0637(95)00013-V).
- Jones, J.V., III, Piatak, N.M., and Bedinger, G.M., 2017, Zirconium and hafnium, chap. V of Schulz, K.J., DeYoung, J.H., Jr., Seal, R.R., II, and Bradley, D.C., eds., Critical mineral resources of the United States—Economic and environmental geology and prospects for future supply: U.S. Geological Survey Professional Paper 1802, p. V1–V26, <https://doi.org/10.3133/pp1802V>.
- Kalinenko, V.V., Pavlidis, Y. A., 1982, Ferruginous nodules of the Chukchi Sea, in Problems of shelf geomorphology, lithology, and lithodynamics: Moscow, Nauka, p. 115–129. [In Russian.]
- Kamilli, R.J., Kimball, B.E., and Carlin, J.F., Jr., 2017, Tin, chap. S of Schulz, K.J., DeYoung, J.H., Jr., Seal, R.R., II, and Bradley, D.C., eds., Critical mineral resources of the United States—Economic and environmental geology and prospects for future supply: U.S. Geological Survey Professional Paper 1802, p. S1–S53, <https://doi.org/10.3133/pp1802S>.

- Kawai, H., Hanyuda, T., Lindeberg, M., and Lindstrom, S. C., 2008, morphology and molecular phylogeny of *Aureo-phycus aleuticus* gen. et sp. nov. (Laminariales, Phaeophyceae) from the Aleutian Islands: *Journal of Phycology*, v. 44, no. 4, p. 1013–1021.
- Keller, R.A., Fisk, M.R., Duncan, R.A., and White, W.M., 1997, 16 m.y. of hotspot and nonhotspot volcanism on the Patton-Murray seamount platform, Gulf of Alaska: *Geology*, v. 25, no. 6, p. 511–514, [https://doi.org/10.1130/0091-7613\(1997\)025%3C0511:MYOHAN%3E2.3.CO;2](https://doi.org/10.1130/0091-7613(1997)025%3C0511:MYOHAN%3E2.3.CO;2).
- Kelley, K.D., Lang, J.R., and Eppinger, R.G., 2013, The giant Pebble Cu-Au-Mo deposit and surrounding region, southwest Alaska—Introduction: *Economic Geology*, v. 108, no. 3, p. 397–404.
- Knauss, J.A., 1962, On some aspects of the deep circulation of the Pacific: *Journal of Geophysical Research*, v. 67, no. 10, p. 3943–3954, <https://doi.org/10.1029/JZ067i010p03943>.
- Kolesnik, O.N., and Kolesnik, A.N., 2013, Specific chemical and mineral composition of ferromanganese nodules from the Chukchi Sea: *Russian Geology and Geophysics*, v. 54, no. 7, p. 653–663, <https://doi.org/10.1016/j.rgg.2013.06.001>.
- Kondo, Y., Obata, H., Hioki, N., Ooki, A., Nishino, S., Kikuchi, T., and Kuma, K., 2016, Transport of trace metals (Mn, Fe, Ni, Zn and Cd) in the western Arctic Ocean (Chukchi Sea and Canada Basin) in late summer 2012: *Deep Sea Research I, Oceanographic Research Papers*, v. 116, p. 236–252, <https://doi.org/10.1016/j.dsr.2016.08.010>.
- Koschinsky, A., Garbe-Schönberg, D., Sander, S., Schmidt, K., Gennerich, H.-H., and Strauss, H., 2008, Hydrothermal venting at pressure-temperature conditions above the critical point of seawater, 5° S on the Mid-Atlantic Ridge: *Geology*, v. 36, p. 615–618, <https://doi.org/10.1130/G24726A.1>.
- Koski, R.A., 1988, Ferromanganese deposits from the Gulf of Alaska Seamount Province—mineralogy, chemistry, and origin: *Canadian Journal of Earth Sciences*, v. 25, no. 1, p. 116–133, <https://doi.org/10.1139/e88-012>.
- Koski, R.A., and Mosier, D.L., 2012, Deposit type and associated commodities, chap. 2 of Shanks, W.C.P., III, and Thurston, Roland, eds., *Volcanogenic massive sulfide occurrence model: U.S. Geological Survey Scientific Investigations Report 2010–5070–C*, p. 10–21.
- Koski, R.A., Munk, L., Foster, A.L., Shanks, W.C., III, and Stillings, L.L., 2008, Sulfide oxidation and distribution of metals near abandoned copper mines in coastal environments, Prince William Sound, Alaska, USA, in Seal, R.R., and Shanks, W.C., eds., *Sulfide oxidation—Sulfide Oxidation, Insights from experimental, theoretical, stable isotope, and predictive studies in the field and laboratory: Applied Geochemistry Special Issue*, v. 23, no. 2, p. 227–254, <https://doi.org/10.1016/j.apgeochem.2007.10.007>.
- Kreiner, D.C., and Jones, J.V., III, 2020, Focus areas for data acquisition for potential domestic resources of 11 critical minerals in Alaska—Aluminum, cobalt, graphite, lithium, niobium, platinum group elements, rare earth elements, tantalum, tin, titanium, and tungsten, chap. C of U.S. Geological Survey, *Focus areas for data acquisition for potential domestic sources of critical minerals: U.S. Geological Survey Open-File Report 2019–1023*, 20 p., <https://doi.org/10.3133/ofr20191023C>.
- Kreiner, D.C., Jones, J.V., III, Kelley, K.D., and Graham, G.E., 2021, Tectonic and magmatic controls on the metallogenesis of porphyry deposits in Alaska, in Sharman, E.R., Lang, J.R., and Chapman, J.B., eds., *Porphyry deposits of the northwestern cordillera of North America—A 25-year update, Section I—Cordillera in Context: Montreal, Quebec, Canadian Institute of Mining, Metallurgy and Petroleum Special Volume 57*, p. 134–175.
- Kuhn, T., Uhlenkott, K., Vink, A., Rühlemann, C., and Martinez Arbizu, P., 2020, Manganese nodule fields from the Northeast Pacific as benthic habitats, chap. 58 of Harris, P.T., Baker, E., eds., *Seafloor geomorphology as benthic habitat* (2d ed.): Amsterdam, Elsevier, p. 933–947, <https://doi.org/10.1016/B978-0-12-814960-7.00058-0>.
- Kuhn, T., Wegorzewski, A., Rühlemann, C., Vink, A., 2017, Composition, formation, and occurrence of polymetallic nodules, in Sharma, R., ed., *Deep-sea mining: Springer, Cham.*, p. 23–63, https://doi.org/10.1007/978-3-319-52557-0_2.
- Kvenvolden, K.A., Weliky, K., Nelson, C.H., DesMarais, D.J., 1979, Submarine seep of carbon dioxide in Norton Sound, Alaska: *Science*, v. 205, no. 4412, p. 1264–1266, <https://doi.org/10.1126/science.205.4412.1264>.
- Ladd, C., Crawford, W.R., Harpold, C.E., Johnson, W.K., Kachel, N.B., Stabeno, P.J., and Whitney, F., 2009, A synoptic survey of young mesoscale eddies in the eastern Gulf of Alaska: *Deep Sea Research, Part II, Topical Studies in Oceanography*, v. 56, no. 24, p. 2460–2473, <https://doi.org/10.1016/j.dsr2.2009.02.007>.
- Larsen, B.R., Nelson, C.H., Heropoulos, C., and Patry, S.S., 1980, Distribution of trace elements in bottom sediments of northern Bering Sea: U.S. Geological Survey Open File Report 80–399–A, 40 p., <https://doi.org/10.3133/ofr80399A>.
- Lawver, L.A., Scotese, C.R., 1990, A review of tectonic models for the evolution of Canada Basin, in Grantz, A., Johnson, L., and Sweeney, J.F., eds., *The Arctic Ocean region, v. L of The Geology of North America: Boulder, Colo., Geological Society of America*, p. 593–618, <https://doi.org/10.1130/DNAG-GNA-L.593>.
- Li, Y.-H., Bischoff, J., and Mathieu, G., 1969, The migration of manganese in the Arctic Basin sediment: *Earth and Planetary Science Letters*, v. 7, no. 3, p. 265–270, [https://doi.org/10.1016/0012-821X\(69\)90063-6](https://doi.org/10.1016/0012-821X(69)90063-6).

- Lipton, I. T., Nimmo, M. J. and Parianos, J. M., 2016, Clarion Clipperton Zone project, Pacific Ocean: Nautilus Minerals, Tonga Offshore Mining Limited, Technical report NI 43-101, accessed July 1, 2020 at http://www.nautilusminerals.com/irm/PDF/1813_0/TOML.
- Lipton, I., Gleeson, E., and Munru, P., 2018, NI [Canadian National Instrument] 43–101 technical report—Preliminary economic assessment of the Solwara Project Bismarck Sea PNG: Toronto, Nautilus Minerals Niugini Ltd., prepared by AMC Consultants Pty, Ltd., 260 p., 2 appendixes. [Available at <https://www.sedar.com/GetFile.do?lang=EN&docClass=24&issuerNo=00005833&issuerType=03&projectNo=02734259&docId=4265015>.]
- Lipton, I., Nimmo, M., and Stevenson, I., 2021, NI [Canadian National Instrument] 43–101 technical report—NORI Area D Clarion Clipperton Zone mineral resource estimate: Vancouver, B.C., DeepGreen Metals Inc., prepared by AMC Consultants Pty., Ltd., 189 p. [Available at <https://www.sedar.com/GetFile.do?lang=EN&docClass=24&issuerNo=00044394&issuerType=03&projectNo=03163672&docId=4873987>.]
- MacDonald, I.R., Bluhm, B.A., Iken, K., Gagaev, S., and Strong, S., 2010, Benthic macrofauna and megafauna assemblages in the Arctic deep-sea Canada Basin: Deep-Sea Research II, Topical Studies in Oceanography, v. 57, p. nos. 1–2, 136–152, <https://doi.org/10.1016/j.dsr2.2009.08.012>.
- MacDonald, R.W., and Carmack, E.C., 1991, Age of Canada Basin deep waters—A way to estimate primary production for the Arctic Ocean: Science, v. 29, p. 1348–1350, <https://doi.org/10.1126/science.254.5036.1348>.
- Maloney, N.E., 2004, Sablefish, *Anoplopoma fimbria*, populations on Gulf of Alaska seamounts: Marine Fisheries Review, v. 66, no. 3, p. 1–12, <https://spo.nmfs.noaa.gov/sites/default/files/pdf-content/MFR/mfr663/mfr6631.pdf>.
- Marchig, V., and Reyss, J.L., 1984, Diagenetic mobilization of manganese in the Peru Basin sediments: Geochimica et Cosmochimica Acta, v. 48, no. 6, p. 1349–1352, [https://doi.org/10.1016/0016-7037\(84\)90068-1](https://doi.org/10.1016/0016-7037(84)90068-1).
- Marlow, M.S., Cooper, A.K., Fisher, M.A., 1994, Geology of the eastern Bering Sea continental shelf, in Plafker, G., and Berg, H.C., eds., The geology of Alaska, v. G–1 of The Geology of North America: Boulder, Colo., Geological Society of America, p. 271–284, <https://doi.org/10.1130/DNAG-GNA-G1.271>.
- Marlow, M.S., Scholl, D.W., Buffington, E.C., and Alpha, T.R., 1973, Tectonic history of the western Aleutian arc: Boulder, Colo., The Geological Society of America Bulletin, v. 84, no. 5, p. 1555–1574, [https://doi.org/10.1130/0016-7606\(1973\)84%3C1555:THOTCA%3E2.0.CO;2](https://doi.org/10.1130/0016-7606(1973)84%3C1555:THOTCA%3E2.0.CO;2).
- Marlow, M.S., Scholl, D.W., Cooper, A.K., Buffington, E.C., 1976, Structure and evolution of Bering Sea shelf south of St. Lawrence Island: American Association of Petroleum Geologists Bulletin, v. 60, no. 2, p. 161–183, <https://doi.org/10.1306/83D92299-16C7-11D7-8645000102C1865D>.
- Mason, G.T., and Arndt, R.E., 1996, Mineral Resources Data System (MRDS): U.S. Geological Survey Data Series 20, <https://doi.org/10.3133/ds20>.
- McDermott, J.M., Ono, S., Tivey, M.K., Seewald, J.S., Shanks, W.C., III, and Solow, A.R., 2015, Identification of sulfur sources and isotopic equilibria in submarine hot-springs using multiple sulfur isotopes: Geochimica Cosmochimica Acta, v. 160, p. 169–187, <https://doi.org/10.1016/j.gca.2015.02.016>.
- McGarry, L., Langlands, J.G., and Dowrick, T., 2014, NI [Canadian National Instrument] 43–101 updated and amended technical report—Review of historic resource estimates and new resource estimate for the Atlantis II deep copper, zinc, silver and manganese deposit, Red Sea: Vancouver, B.C., Diamond Fields International, Ltd., prepared by ACA Howe International Ltd., 67 p. [Available at <https://www.sedar.com/GetFile.do?lang=EN&docClass=24&issuerNo=00009000&issuerType=03&projectNo=01794594&docId=3608951>.]
- McManus, D.A., Kolla, V., Hopkins, D.M., and Nelson, C.H., 1977, Distribution of bottom sediments on the continental shelf, northern Bering Sea. U.S. Geological Survey Professional Paper 759–C, 31 p., <https://doi.org/10.3133/pp759C>.
- Mertie, J.B., Jr., 1969, Economic geology of the platinum metals: U.S. Geological Survey, Professional Paper 630, 120 p., <https://doi.org/10.3133/pp630>.
- Miller, T.P., 1989, Contrasting plutonic rock suites of the Yukon-Koyukuk basin and the Ruby geanticline, Alaska: Journal of Geophysical Research, v. 94, no. B11, p. 15969–15987.
- Mills, R.A., and Elderfield, H., 1995, Hydrothermal activity and the geochemistry of metalliferous sediment: American Geophysical Union, Geophysical Monograph 91, p. 392–392.
- Minter, W.E.L., and Craw, D., 1999, A special issue on placer deposits, preface: Economic Geology, v. 94, no.5, p. 603–604, <https://doi.org/10.2113/gsecongeo.94.5.603>.
- Mitchell, J.H., Leonard, J.M., Delaney, J., Girguis, P.R., and Scott, K.M., 2020, Hydrogen does not appear to be a major electron donor for symbiosis with the deep-sea hydrothermal vent tubeworm *Riftia pachyptila*: Applied Environmental Microbiology, v. 86, no. 1, <https://doi.org/10.1128/AEM.01522-19>.

- Mizell, K., and Hein, J. R., 2020, Ocean floor manganese deposits, in Alderton, D., and Elias, S.A., eds., *Encyclopedia of Geology* (2d ed.), Volume 5, Resources of the future: Amsterdam, Elsevier, p. 993–1001, <https://doi.org/10.1016/B978-0-08-102908-4.00030-8>.
- Mizell, K., Hein, J.R., Lam, P.J., Koppers, A.A.P., and Staudigel, H., 2020, Geographic and oceanographic influences on ferromanganese crust composition along a Pacific Ocean meridional transect, 14N to 14S: *Geochemistry, Geophysics, Geosystems*, v. 21, no. 2, <https://doi.org/10.1029/2019GC008716>.
- Mizell, K., Hein, J.R., Au, M., Gartman, A., 2022, Estimates of metals contained in abyssal manganese nodules and ferromanganese crusts in the global ocean based on regional variations and genetic types of nodules, in Sharma, R., ed., *Perspectives on deep-sea mining*: Springer, Cham, p. 53–80, https://doi.org/10.1007/978-3-030-87982-2_3.
- Monecke, T., Petersen, S., and Hannington, M. D., 2014, Constraints on water depth of massive sulfide formation—Evidence from modern seafloor hydrothermal systems in arc-related settings: *Economic Geology*, v. 109, no. 8, p. 2079–2101.
- Moore, J.R., and Welkie, C.J., 1976, Metal-bearing sediments of economic interest, coastal Bering Sea, in Miller, T.P., ed., *Proceedings of the symposium on recent and ancient sedimentary environments in Alaska*, Anchorage, 1976: Alaska Geological Society, p. K1–K17. [Available as a CD at <https://www.alaskageology.org/publications1.html>.]
- Morgan, J.W., 1972, Deep mantle convective plumes and plate motions: *American Association of Petroleum Geologists Bulletin*, v. 56, no. 2, p. 201–213, <https://doi.org/10.1306/819A3E50-16C5-11D7-8645000102C1865D>.
- Morgan, C., 2000, Resource estimates of the Clarion-Clipperton manganese nodule deposits. In: Cronan DS (ed) *Handbook of Marine Mineral Deposits*, CRC Press, p. 145–170.
- Mosier, D.L., Berger, V.I., and Singer, D.A., 2009, Volcanogenic massive sulfide deposits of the world—Database and grade and tonnage models: U.S. Geological Survey Open-File Report 2009–1034, <https://doi.org/10.3133/ofr20091034>.
- Motyka, R.J., Liss, S.A., Nye, C.J., and Moorman, M.A., 1993, Geothermal resources of the Aleutian Arc: Alaska Division of Geological & Geophysical Surveys Professional Report 114, 17 p., 4 sheets, scale 1:1,000,000, <https://doi.org/10.14509/2314>.
- Mulligan, J.J., 1966, Tin-lode Investigation, Cape Mountain area, Seward Peninsula, Alaska (with section on petrography by W.L. Gnagy): U.S. Bureau of Mines Report of Investigations 6737. [Available at <https://dggs.alaska.gov/pubs/id/21217>.]
- Murton, B.J., Lehrmann, B., Dutrieux, A.M., Martins, S., de la Iglesia, A.G., Stobbs, I.J., Barriga, F.J.A.S., Bialas, J., Dannowski, A., Vardy, M.E., North, L.J., Yeo, I.A.L.M., Lusty, P.A.J., and Petersen, S., 2019, Geological fate of seafloor massive sulphides at the TAG hydrothermal field (Mid-Atlantic Ridge): *Ore Geology Reviews*, v. 107, p. 903–925, <https://doi.org/10.1016/j.oregeorev.2019.03.005>.
- Musgrave, D.L., Weingartner, T.J., and Royer, T.C., 1992, Circulation and hydrography in the northwestern Gulf of Alaska: Deep Sea Research Part A, *Oceanographic Research Papers*, v. 39, no. 9, p. 1499–1519, [https://doi.org/10.1016/0198-0149\(92\)90044-T](https://doi.org/10.1016/0198-0149(92)90044-T).
- Naidu, A.S., 1974, Sedimentation in the Beaufort Sea—A synthesis, chap. 7 of Herman, Y., ed., *Marine geology and oceanography of the Arctic seas*: New York, Springer-Verlag, p. 173–190, <https://doi.org/10.1007/978-3-642-87411-6>.
- Natland, J.H., 1977, Basal ferromanganoan sediments at DSDP site 183, Aleutian abyssal plain and site 192, Meiji guyot, Northwest Pacific, Leg 19, chap. 15 of Volume XIX, covering Leg 19 of the cruises of the Drilling Vessel *Glomar Challenger*, Kodiak, Alaska to Yokohama, Japan, July–September 1971—Part III, Shore laboratory studies: Initial reports of the Deep Sea Drilling Project, v. 19, p. 629–641, <https://doi.org/10.2973/dsdp.proc.19.115.1973>.
- Nelson, J.L., Colpron, M., and Israel, S., 2013, The cordillera of British Columbia, Yukon, and Alaska—Tectonics and metallogeny, in Colpron, M., Bissig, T., Rusk, B.G., and Thompson, J.F.H., eds., *Tectonics, metallogeny and discovery—The North American Cordillera and similar accretionary settings*: Society of Economic Geologists Special Publication 17, p. 53–103, <https://doi.org/10.5382/SP.17.03>.
- Nelson, C.H., and Hopkins, D.M., 1972, Sedimentary processes and distribution of particulate gold in the northern Bering Sea: U.S. Geological Survey Professional Paper 689, 27 p., 1 sheet, scale 1:1,000,000, <https://doi.org/10.3133/pp689>.
- Nelson, C.H., Thor, D.R., Sandstrom, M.W., and Kvenvolden, K.A., 1979, Modern biogenic gas-generated craters (seafloor “pockmarks”) on the Bering Shelf, Alaska: *Geological Society of America Bulletin*, v. 90, no. 12, p. 1144–1152, [https://doi.org/10.1130/0016-7606\(1979\)90%3C1144:MBGCSP%3E2.0.CO;2](https://doi.org/10.1130/0016-7606(1979)90%3C1144:MBGCSP%3E2.0.CO;2).
- Ness, G.E., 1972, The structure and sediments of Surveyor Deep-Sea Channel: Corvallis, Oregon State University, M.S. thesis, 77 p., https://ir.library.oregonstate.edu/concern/graduate_thesis_or_dissertations/wd375z35r.
- Nielsen, S.G., Mar-Gerrison, S., Gannoun, A., LaRowe, D., Klemm, V., Halliday, A.N., Burton, K.W., and Hein, J.R., 2009, Thallium isotope evidence for a permanent increase in marine organic carbon export in the early Eocene: *Earth and Planetary Science Letters*, v. 278, nos. 3–4, p. 297–307, <https://doi.org/10.1016/j.epsl.2008.12.010>.

- National Oceanic and Atmospheric Administration [NOAA] Office of Coast Survey, [undated], National Ocean Service (NOS) Bathymetric Maps: National Oceanic and Atmospheric Administration, National Centers for Environmental Information.
- North Pacific Fishery Management Council, 2005, EFH final action NPFMC February 10, 2005, Council Motion: Anchorage, Alaska, North Pacific Fishery Management Council, 3 p., 5 pl., https://www.npfmc.org/wp-content/PDFdocuments/conservation_issues/HAPC/HAPCMotion205.pdf.
- O'Brien, T.M., Miller, E.L., Benowitz, J.P., Meisling, K.E., and Dumitru, T.A., 2016, Dredge samples from the Chukchi Borderland—Implications for paleogeographic reconstruction and tectonic evolution of the Amerasia Basin of the Arctic: *American Journal of Science*, v. 316, no. 9, p. 873–924, <https://doi.org/10.2475/09.2016.03>.
- Ohmoto, H., 1978, Submarine calderas—A key to the formation of volcanogenic massive sulfide deposits?: *Mine Geology*, v. 28, no. 150, p. 219–231, <https://doi.org/10.11456/shigenchishitsu1951.28.219>.
- Olson, N.H., Lang, J.R., and Dilles, J.H., 2020, The Pebble porphyry Cu-Au-Mo deposit, southwestern Alaska, in Sharman, E.R., Lang, J.R., Chapman, J.R., eds., *Porphyry deposits of the northwestern Cordillera of North America—A 25-year update: Canadian Institute of Mining, Metallurgy and Petroleum Special Volume 57*, p. 287–307.
- Oommen, T., Prakash, A., Misra, D., Naidu, S., Kelley, J.J., and Bandopadhyay, S., 2008, GIS based marine platinum exploration, Goodnews Bay Region, Southwest Alaska: *Marine Georesources and Geotechnology*, v. 26, no. 1, p. 1–18, <https://doi.org/10.1080/10641190701706270>.
- Pattan, J.N., 1993, Manganese micronodules—A possible indicator of sedimentary environments: *Marine Geology*, v. 113, nos. 3–4, p. 331–344, [https://doi.org/10.1016/0025-3227\(93\)90026-R](https://doi.org/10.1016/0025-3227(93)90026-R).
- Paulmier, A., and Ruiz-Pino, D., 2009, Oxygen minimum zones (OMZs) in the modern ocean: Progress in Oceanography: v. 80, nos. 3–4, p. 113–128, <https://doi.org/10.1016/j.pocean.2008.08.001>.
- Pavlidis, Y.A., 1982, Sedimentation environments in the Chukchi Sea and sedimentary- facies zones of its shelf, in *Problems of Shelf Geomorphology, Lithology, and Lithodynamics: Nauka, Moscow*, p. 47–76. [In Russian.]
- Plafker, G., and Berg, H.C., eds., 1994, *The Geology of Alaska*, v. G–1 of *The Geology of North America: Boulder, Colo., Geological Society of America*, 1068 p., <https://doi.org/10.1130/DNAG-GNA-G1>.
- Puchner, C.C., 1986, Geology, alteration, and mineralization of the Kougark Sn deposit, Seward Peninsula, Alaska: *Economic Geology*, v. 81, no. 7, p. 1775–1794, <https://doi.org/10.2113/gsecongeo.81.7.1775>.
- Raymore, P.A., Jr., 1982, Photographic investigations on Three Seamounts in the Gulf of Alaska: University of Hawaii Press, Pacific Science, v. 36, no. 1, p. 15–34.
- Rona, P.A., 2008, The changing vision of marine minerals: *Ore Geology Reviews*, v. 33, nos. 3–4, p. 618–666, <https://doi.org/10.1016/j.oregeorev.2007.03.006>.
- Rosenblum, S., Carlson, R.R., Nishi, J.M., and Overstreet, W.C., 1986, Platinum-group elements in magnetic concentrates from the Goodnews Bay District, Alaska: *U.S. Geological Survey Bulletin*, v. 1660, 38 p., <https://doi.org/10.3133/b1660>.
- Scholl, D.W., and Creager, J.S., 1973, Geologic synthesis of Leg 19 (DSDP) results; far North Pacific, and Aleutian Ridge, and Bering Sea, chap. 37 of *Volume XIX, covering Leg 19 of the cruises of the Drilling Vessel Glomar Challenger*, Kodiak, Alaska to Yokohama, Japan, July–September 1971—Part IV, Cruise Synthesis: Initial reports of the Deep Sea Drilling Project, v. 19, p. 897–911, <https://doi.org/10.2973/dsdp.proc.19.137.1973>.
- Scholl, D.W., Marlow, M.S., and Buffinton, E.C., 1975, Summit basins of Aleutian Ridge, North Pacific: The American Association of Petroleum Geologists Bulletin, v. 59, no. 5, p. 799–816, <https://doi.org/10.1306/83D91D2B-16C7-11D7-8645000102C1865D>.
- Scholl, D.W., Vallier, T.L., and Stevenson, A.J., 1986, Terrane accretion production and continental growth—A perspective based on the origin and tectonic fate of the Aleutian- Bering Sea region: *Geology*, v. 14, no. 1, p. 43–47, [https://doi.org/10.1130/0091-7613\(1986\)14%3C43:TAPACG%3E2.0.CO;2](https://doi.org/10.1130/0091-7613(1986)14%3C43:TAPACG%3E2.0.CO;2).
- Schulz, K.J., Woodruff, L.G., Nicholson, S.W., Seal, R.R., II, Piatak, N.M., Chandler, V.W., and Mars, J.L., 2014, Occurrence model for magmatic sulfide-rich nickel-copper-(platinum-group element) deposits related to mafic and ultramafic dike-sill complexes: *U.S. Geological Survey Scientific Investigations Report 2010–5070–I*, 80 p., <https://doi.org/10.3133/sir20105070I>.
- Scott, S.D., 2011, Marine minerals—Their occurrences, exploration and exploitation, in *Oceans'11 MTS/IEEE Kona Joint Conference*, Sept. 19–22, 2011, Waikoloa, Hawaii: Marine Technology Society (MTS)/Institute of Electrical and Electronics Engineers (IEEE), p. 1–8, <https://doi.org/10.23919/OCEANS.2011.6107119>.
- Shanks, W.C.P., III, and Roland, T., eds., 2012, Volcanogenic massive sulfide occurrence model, chap. C of *Mineral deposit models for resource assessment: U.S. Geological Survey Scientific Investigations Report 2010–5070–C*, 345 p., <https://doi.org/10.3133/sir20105070C>.
- Sharma, G.D., Naidu, S.A., Hood, D.W., 1972, Bristol Bay—Model contemporary graded shelf: The American Association of Petroleum Geologists Bulletin, v. 56, no. 10, <https://doi.org/10.1306/819A41A6-16C5-11D7-8645000102C1865D>.

- Shnyukov, E.F., Ogorodnikov, V.I., Krasovskii, K.S., 1987, Ferromanganese nodules in seas of the USSR: *Geologicheskii Zhurnal*, v. 47, no. 1, p. 32–43.
- Skornyakova, N.S., and Andrushchenko, P.F., 1974, Iron-manganese concretions in the Pacific Ocean: *International Geology Review*, v. 16, no. 8, p. 863–919, <https://doi.org/10.1080/00206817409471786>.
- Stein, R., Fahl, K., and Müller, J., 2012, Proxy reconstruction of Cenozoic Arctic Ocean sea-ice history—From IRD to IP25: *Polarforschung*, v. 82, no. 1, p. 37–71, https://epic.awi.de/id/eprint/34914/2/Polarforschung_82-1_lowres.pdf#page=39.
- St. John, K., 2008, Cenozoic ice-rafting history of the central Arctic Ocean—Terrigenous sands on the Lomonosov Ridge, *in* *Cenozoic paleoceanography of the central Arctic Ocean: Paleoceanography and Paleoclimatology Special Issue*, v. 23, no. 1, <https://doi.org/10.1029/2007PA001483>.
- Szumigala, D.J., Harbo, L.A., and Adleman, J.N., 2011, Alaska's mineral industry 2010: Alaska Division of Geological and Geophysical Surveys Special Report 65, 83 p., <http://doi.org/10.14509/22822>.
- Szumigala, D.J., Harbo, L.A., and Hughes, R.A., 2010, Alaska's mineral industry 2009: Alaska Division of Geological and Geophysical Surveys Special Report 64, 81 p., <https://doi.org/10.14509/21881>.
- Talley, L.D., Pickard, G.L., Emery, W.J., Swift, J.H., 2011, Pacific Ocean, chap. 10 *of* Talley, L.D., Pickard, G.L., Emery, W.J., and Swift, J.H., eds., *Descriptive physical oceanography* (6th ed.): Academic Press, p. 303–362, <https://doi.org/10.1016/B978-0-7506-4552-2.10010-1>.
- Taylor, C.D., and Johnson, C.A., 2010, Geology, geochemistry and genesis of the Greens Creek massive sulfide deposit, Admiralty Island, southeast Alaska: U.S. Geological Survey Professional Paper 1763, p. 429, 7 plates on CD, <https://doi.org/10.3133/pp1763>.
- Tibaldi, A., and Bonali, F.L., 2017, Intra-arc and back-arc volcano-tectonics—Magma pathways at Holocene Alaska-Aleutian volcanoes: *Earth-Science Reviews*, v. 167, p. 1–26, <https://doi.org/10.1016/j.earscirev.2017.02.004>.
- Till, A.B., Dumoulin, J.A., Weldon, M.B., and Bleick, H.A., 2011, Bedrock geologic map of the Seward Peninsula, Alaska, and accompanying conodont data: U.S. Geological Survey Scientific Investigations Map 3131, 75 p., 2 sheets, scale 1:500,000, <https://doi.org/10.3133/sim3131>.
- Timmermans, M.-L., Winsor, P., and Whitehead, J.A., 2005, Deep-water flow over the Lomonosov Ridge in the Arctic Ocean: *Journal of Physical Oceanography*, v. 35, no. 8, p. 1489–1493, <https://doi.org/10.1175/JPO2765.1>.
- Tolstykh, N.D., Foley, J.Y., Sidorov, E.G., and Laajoki, K.V.O., 2002, Composition of the platinum-group minerals in the Salmon River placer deposit, Goodnews Bay, Alaska: *Canadian Mineralogist*, v. 40, no. 2, p. 463–471, <https://doi.org/10.2113/gscanmin.40.2.463>.
- Torokhov, P.A., and Taran, Y.A., 1994, Hydrothermal fields of the Piip sub-marine volcano, Komandorsky back-arc basin—Chemistry and origin of vent mineralization and bubbling gas: *Bulletin of the Geological Society of Denmark*, v. 41, p. 55–64, <https://doi.org/10.37570/bgdsd-1995-41-06>.
- Turner, D.L., Forbes, R.B., and Naeser, C.W., 1973, Radiometric ages of Kodiak seamount and Giacomini guyot, Gulf of Alaska—Implications for circum-Pacific tectonics: *Science*, v. 182, no. 4112, p. 579–581, <https://doi.org/10.1126/science.182.4112.579>.
- Turner, D.L., Jarrard, R.D., and Forbes, R.B., 1980, Geochronology and origin of the Pratt-Welker seamount chain, Gulf of Alaska—A new pole of rotation for the Pacific Plate: *Journal of Geophysical Research*, v. 85, p. 6547–6556.
- Uchida, R., Kuma, K., Omata, A., Ishikawa, S., Hioki, N., Ueno, H., Isoda, Y., Sakaoka, K., Kamei, Y., and Takagi, S., 2013, Water column iron dynamics in the subarctic North Pacific Ocean and the Bering Sea: *Journal of Geophysical Research Oceans*, v. 118, no. 9, <https://doi.org/10.1002/jgrc.20097>.
- Urabe, T., Ura, T., Tsujimoto, T., and Hotta, H., 2015, Next-generation technology for ocean resources exploration (Zipangu-in-the-Ocean) project in Japan, *in* *Oceans'15 MTS/IEEE Genova Joint Conference*, May. 18–21, 2015, Genova, Italy: Marine Technology Society (MTS)/Institute of Electrical and Electronics Engineers (IEEE) Oceans, p. 1–5, <https://doi.org/10.1109/OCEANS-Genova.2015.7271762>.
- Uramoto, G.I., Morono, Y., Tomioka, N., Wakaki, S., Nakada, R., Wagai, R., Uesugi, K., Takeuchi, A., Hoshino, M., Suzuki, Y., Shiraishi, F., Mitsunobu, S., Suga, H., Takeichi, Y., Takahashi, Y., Inagaki, F., 2019, Significant contribution of seafloor microparticles to the global manganese budget: *Nature Communications*, v. 10, no. 400, <https://doi.org/10.1038/s41467-019-08347-2>.
- Usui, A., Nishimura, A., and Mita, N., 1993, Composition and growth history of surficial and buried manganese nodules in the Penrhyn Basin, Southwestern Pacific: *Marine Geology*, v. 114, no. 1–2, p. 133–153, [https://doi.org/10.1016/0025-3227\(93\)90044-V](https://doi.org/10.1016/0025-3227(93)90044-V).
- Vallier, T.L., Scholl, D.W., Fisher, M.A., Bruns, T.R., Wilson, F.H., von Huene, Roland, and Stevenson, A.J., 1994, Geologic framework of the Aleutian arc, Alaska, *in* Plafker, G., and Berg, H.C., eds., *The geology of Alaska*, v. G–1 *of* *The Geology of North America*: Boulder, Colo., Geological Society of America, p. 367–388, <https://doi.org/10.1130/DNAG-GNA-G1.367>.
- van der Loeff, M.R., Cai, P., Stimac, I., Bauch, D., Hanfland, C., Roeske, T., and Moran, S. B., 2012, Shelf-basin exchange times of Arctic surface waters estimated from $^{228}\text{Th}/^{228}\text{Ra}$ disequilibrium: *Journal of Geophysical Research Oceans*, v. 117, <https://doi.org/10.1029/2011JC007478>.

- Van Dover, C., Arnaud-Haond, S., Gianni, M., Helmreich, S., Huber, J., Jaeckel, A., Metaxas, A., Pendleton, L.H., Petersen, S., Ramirez-Llodra, E., Steinberg, P.E., Tunnicliffe, V., and Yamamoto, H., 2018, Scientific rationale and international obligations for protection of active hydrothermal vent ecosystems from deep-sea mining: *Marine Policy*, v. 90, p. 20–28, <https://doi.org/10.1016/j.marpol.2018.01.020>.
- Van Dover, C.L., Colaço, A., Collins, P.C., Croot, P., Metaxas, A., Murton, B.J., Swaddling, A., Boschen-Rose, R.E., Carlsson, J., Cuyvers, L. and Fukushima, T., 2020. Research is needed to inform environmental management of hydrothermally inactive and extinct polymetallic sulfide (PMS) deposits: *Marine Policy*, v. 121, p.104183, <https://doi.org/10.1016/j.marpol.2020.104183>.
- Van Gosen, B.S., Verplanck, P.L., Seal, R.R., II, Long, K.R., and Gambogi, Joseph, 2017, Rare-earth elements, chap. O of Schulz, K.J., DeYoung, J.H., Jr., Seal, R.R., II, and Bradley, D.C., eds., *Critical mineral resources of the United States—Economic and environmental geology and prospects for future supply*: U.S. Geological Survey Professional Paper 1802, p. O1–O31, <https://doi.org/10.3133/pp1802O>.
- Van Pelt, T.I., ed., 2015, *The Bering Sea Project—Understanding ecosystem processes in the Bering Sea*: Alexandria, Va., National Science Foundation, Bering Ecosystem Study, North Pacific Research Board, <https://doi.org/10.13140/RG.2.1.1668.2482>.
- von Stackelberg, U., 2000, Manganese nodules of the Peru Basin, in Cronan, D.S., ed., *Handbook of marine mineral deposits*: Boca Raton, Fla., CRC Press, p. 197–238.
- Warner, J.D., 1985, Critical and strategic minerals in Alaska—Tin, Tantalum, and Columbium: U.S. Bureau of Mines Information Circular 9037, 19 p. 1 sheet. [Available at <https://dggs.alaska.gov/pubs/id/21284>.]
- Weeks, R.J., Roberts, A.P., Verosub, K.L., Okada, M., and Dubuisson, G.J., 1995, Magnetostratigraphy of upper Cenozoic sediments from Leg 145, North Pacific Ocean, in Rea, D.K., Basov, I.A., Scholl, D.W., and Allan, J.F., eds., *North Pacific transect—Covering leg 145 of the cruises of the drilling vessel Joides Resolution*, Yokohama, Japan, to Victoria, Canada, sites 881–887, 20 July 20–September 1992: *Proceedings of the Ocean Drilling Program, Scientific Results*, v. 145, p. 491–521, <https://doi.org/10.2973/odp.proc.sr.145.138.1995>.
- Wegorzewski, A., and Kuhn, T., 2014, The influence of suboxic diagenesis on the formation of manganese nodules in the Clarion Clipperton nodule belt of the Pacific Ocean: *Marine Geology*, v. 357, p. 123–138, <https://doi.org/10.1016/j.margeo.2014.07.004>.
- Wei, Z., Chen, H., Lei, R., Yu, X., Zhang, T., Lin, L., Tian, Z., Zhuang, T., Li, T., and Yuan, Z., 2019, Overview of the 9th Chinese national arctic research expedition: *Atmospheric and Oceanic Science Letters*, v. 13, no. 1, <https://doi.org/10.1080/16742834.2020.1675137>.
- Wilson, F.H., and Cox, D.P., 1983, Geochronology, geochemistry, and tectonic environment of porphyry mineralization in the central Alaska Peninsula: U.S. Geological Survey Open-File Report 83–783, 24 p., <https://doi.org/10.3133/ofr83783>.
- Wood, K.R., Bond, N.A., Danielson, S.L., Overland, J.E., Salo, S.A., Stabeno, P.J., and Whitefield, J., 2015, A decade of environmental change in the Pacific Arctic region: *Progress in Oceanography*, v. 136, p. 12–31, <https://doi.org/10.1016/j.pocean.2015.05.005>.
- Woodgate, R.A., 2018, Increases in the Pacific inflow to the Arctic from 1990 to 2015, and insights into seasonal trends and driving mechanisms from year-round Bering Strait mooring data: *Progress in Oceanography*, v. 160, p. 124–154, <https://doi.org/10.1016/j.pocean.2017.12.007>.
- Worthington, L.V., 1981, The water masses of the world ocean—Some results of a fine-scale census, in Warren, B.A., and Wunsch, C., eds., *Evolution of Physical Oceanography—Scientific surveys in honor of Henry Stommel*: Cambridge, Mass., MIT Press, p. 42–69.
- Yogodzinski, G.M., Brown, S.T., Kelemen, P.B., Vervoort, J.D., Portnyagin, M., Sims, K.W.W., Hoernle, K., Jicha, B.R., and Werner, R., 2015, The role of subducted basalt in the source of island arc magmas—Evidence from seafloor lavas of the western Aleutians: *Journal of Petrology*, v. 56, no. 3, p. 441–492, <https://doi.org/10.1093/petrology/egv006>.
- Zelenka, B.R., 1988, A review of favorable offshore and coastal depositional sites for platinum-group metals in the Goodnews Bay mining district, Alaska: U.S. Bureau of Mines Open-File Report 11–88, 25 p. [Available at <https://dggs.alaska.gov/pubs/id/21337>.]
- Zhao, H.J., Ma, F.S., Li, G.Q., Zhang, Y.M., and Guo, J., 2012, Study of the hydrogeological characteristics and permeability of the Xinli Seabed Gold Mine in Laizhou Bay, Jiaodong Peninsula, China: *Environmental Earth Sciences*, v. 65, p. 2003–2014, <https://doi.org/10.1007/s12665-011-1181-y>.
- Zimmermann, M., Prescott, M.M., and Haeussler, P.J., 2019, Bathymetry and geomorphology of Shelikof Strait and the Western Gulf of Alaska: *Geosciences, Geological Seafloor Mapping Special Issue*, v. 9, no. 10, p. 409, <https://doi.org/10.3390/geosciences9100409>.

